

1-1-2013

Feasibility of Residential Combined Cooling, Heating, and Power Generation System in Canada

Navid Ekrami
Ryerson University

Follow this and additional works at: <http://digitalcommons.ryerson.ca/dissertations>

 Part of the [Energy Systems Commons](#)

Recommended Citation

Ekrami, Navid, "Feasibility of Residential Combined Cooling, Heating, and Power Generation System in Canada" (2013). *Theses and dissertations*. Paper 2077.

This Thesis is brought to you for free and open access by Digital Commons @ Ryerson. It has been accepted for inclusion in Theses and dissertations by an authorized administrator of Digital Commons @ Ryerson. For more information, please contact bcameron@ryerson.ca.

FEASIBILITY OF RESIDENTIAL COMBINED COOLING, HEATING, AND
POWER GENERATION SYSTEM IN CANADA

By

Navid Ekrami

B.Sc. (Aerospace Engineering)

Azad Science and Research University, Tehran, Iran, 2007

A Thesis

Presented to Ryerson University

In Partial Fulfillment of the

Requirements for the degree of

MASTER OF APPLIED SCIENCE

In the program of

Mechanical Engineering

Toronto, Ontario, Canada, 2013

© Navid Ekrami, 2013

Author's Declaration

I hereby declare that I am the sole author of this thesis.

I authorize Ryerson University to lend this thesis to other institutions or purpose of scholarly research.

Navid Ekrami

I further authorize Ryerson University to reproduce this thesis by photocopying or by other means, in total or in part, at the request of other institutions or individuals for the purpose of scholarly research.

Navid Ekrami

FEASIBILITY OF RESIDENTIAL COMBINED COOLING, HEATING, AND POWER GENERATION SYSTEM IN CANADIAN CITIES

Navid Ekrami

Master of Applied Science

Program of Mechanical Engineering

Ryerson University, Toronto, Ontario, Canada, 2013

Abstract

In order to investigate the feasibility of a combined heating, cooling, and power generation system in the residential sector, an integrated system was designed and installed at the Archetype Sustainable House (ASH) of the Toronto and Region Conservation Authority (TRCA). A Stirling engine based cogeneration unit was used to produce the thermal energy for a thermally driven chiller. The engine supplies hot water up to 95°C. The overall efficiency of up to 90% is determined for the cogeneration system. A thermo-chemical accumulator provided by the ClimateWell AB, was installed and connected to the cogeneration unit. The experimental coefficient of performance (COP) of this chiller during the test period was less than 0.4. Since the ClimateWell chiller rejects heat during both charging and discharging processes, a heat recovery system using three cascade tanks and an outdoor fan coil was designed and installed to utilize the waste heat, for domestic hot water production. A complete TRNSYS model of the tri-generation system was used to verify the experimental results.

Acknowledgment

This thesis would not have been possible without the kind support of my supervisors Dr. Alan Fung, Dr. Seth Dworkin, and Dr. David Naylor. Their guidance and trust in my personal work and innovation enabled me to finish this great task and inspired my passion for the research beyond the university walls. Without their enthusiasm, motivation and their invaluable guidance, my academic perspective would not be this straightforward.

I would like to thank my fellow project partner Mr. Zannatul Moiet Hasib. I would also express my special thanks to Mr. John Overall, Mr. Lars Sjoberg, Mr. David Nixon, Mr. Dahai Zhang, and Mr. Pushan Lele for their guidance and support in completion of this thesis.

I would also like to acknowledge Union Gas Limited, Renteknik Group, Natural Science and Engineering Research Council (NSERC) of Canada, MITACS, ClimateWell and Toronto and Region Conservation Authority (TRCA) for their support in this project.

Last but not least, my immense appreciation, love and sincere thanks to my wife, Shaghayegh, and my parents, Mehri and Masoud, for their unconditional support, constant love, and encouragement during my study. To them, I dedicate this thesis.

Abbreviations

AC	Air Conditioning
ACAC	Condenser AC valve of Barrel-A
ACHS	Condenser Heat Sink valve of Barrel-A
AHU	Air Handling Unit
AFC	Alkaline Fuel Cells
ARHS	Reactor Heat Sink Valve of Barrel-A
ARSP	Reactor Solar Panel Valve of Barrel-A
ASME	American Society of Mechanical Engineers
ASHRAE	American Society of Heating, Refrigeration and Air- Conditioning Engineers
BCAC	Condenser AC Valve of Barrel-B
BILD	Building Industry and Land Development Association
BCHS	Condenser Heat Sink Valve of Barrel-B
BRHS	Reactor Heat Sink Valve of Barrel-B
BRSP	Reactor Solar Panel Valve of Barrel-B
BTU	British Thermal Unit
CCHT	Canadian Center for Housing Technology
CHCP	Combined Heating, Cooling and Power
CHP	Combined Heat and Power
CHS	Condenser Heat Sink (valve)
CAC	Condenser AC (valve)
COP	Coefficient of Performance

CSA	Canadian Standard Association
CW	ClimateWell [®]
DAQ	Data Acquisition System
DHWT	Domestic Hot Water Tank
DHW	Domestic Hot Water
EU	European Union
FC	Fuel Cell
GHG	Greenhouse Gas
GPM	Gallon per Minute
GSHP	Ground Source Heat Pump
HHV	Higher Heating Value
HS	Heat Sink
HVAC	Heating, Ventilation and Air conditioning
HX	Heat Exchanger
IC	Internal Combustion
kWh	Kilowatt Hour
LEED	Leadership in Energy and Environment Design
MCFC	Molten Carbonate Fuel Cells
MCHP	Micro Combined Heat and Power
NRCan	Natural Resources Canada
PAFC	Phosphoric Acid Fuel Cells
PEMFC	Polymer Electrolyte Membrane Fuel Cell
P&ID	Piping and Instrumentation Diagram

PG	Propylene Glycol
RHS	Reactor Heat Sink (valve)
RSP	Reactor Solar Panel (valve)
RTD	Resistance Temperature Detector
SEER	Seasonal Energy Efficiency Ratio
SOC	State of Charge
SOFC	Solid Oxide Fuel Cells
SOV	State of Valve
SQL	Structured Query Language
TCA	Thermo-chemical Accumulator
TDC	Thermally Driven Chillers
TOU	Time-of-Use
TRCA	Toronto and Regional Conservation Authority
VH	Valve in the Heat Rejection Circuit/Loop
XT	Expansion Tank

Nomenclature

C_p	Specific heat capacity of water (J/kg.K)
$E_{\text{Generation}}$	Electrical Energy Generation
F	Temperature (°F)
FL	Flow rate (l/min)
m	mass flow rate (kg/min)
Q	Thermal energy (kWh)
$Q_{\text{Electrical}}$	Electrical energy

\dot{Q}_{abs}	Rate of absorbed thermal energy
\dot{Q}_{rej}	Rate of rejected thermal energy
\dot{Q}_{gen}	Rate of generated thermal energy
T	Temperature (°C)
T_{a}	Ambient temperature
UA	Overall heat transfer coefficient (kW/°C)

Greek symbols

ρ	Density (kg/m ³)
\dot{V}	Volumetric flow rate (m ³ /s)
η	Efficiency

Table of Contents

Author's Declaration.....	ii
Abstract	iii
Acknowledgment	iv
Abbreviations	v
Nomenclature	vii
Greek symbols	viii
Chapter 1 - Introduction and Objectives	1
1.1 Introduction	1
1.2 Objective and Intent of Research	6
Chapter 2 - Literature Review	8
2.1 Cogeneration Systems	9
2.1.1 Reciprocating Internal Combustion Engine	9
2.1.1.1 Operation Principles of IC Engines	10
2.1.1.2 Performance Characteristics of IC Engines	11
2.1.2 Fuel Cells.....	12
2.1.2.1 Operation Principle of Fuel Cell	12
2.1.2.2 Different Types of Fuel Cells	14
2.1.2.3 Performance Characteristics of Fuel Cells	15
2.1.3 Stirling Engine.....	16
2.1.3.1 Operation Principle of the Stirling Engine	17
2.1.3.2 Stirling engine configuration	17
2.1.3.3 Performance Characteristics of Stirling engines.....	18
2.1.4 Prime Mover Studies	19
2.1.4.1 Cogeneration Test at CCHT House by NRCan	19

2.1.4.2 Cogeneration Test in Combustion Research Laboratory at University of Toronto	20
2.1.4.3 Cogeneration Test in Italy	22
2.1.5 WhisperGen Stirling Engine.....	23
2.2 Tri-generation.....	24
2.3 Heat Activated Cooling Systems	25
2.3.1 Absorption Systems.....	26
2.3.2 Adsorption Systems.....	27
2.3.3 Available Technologies in the Market	29
2.3.4 Climate-Well	30
2.3.4.1 Charging Process	32
2.3.4.2 Discharging Process.....	33
Chapter 3 - TRCA House	35
3.1 “House A & B” Descriptions	36
3.2 Mechanical Systems	38
3.2.1 House A	38
3.2.2 House B	38
Chapter 4 - Methodology	40
4.1 Description of the Tri-generation Project	41
4.2 Monitoring System.....	44
4.2.1 DAQ System.....	44
4.2.2 ClimateWell Database	45
4.2.3 Sensor Calibration	46
4.2.3.1 Temperature Sensors	46
4.2.3.2 Water Flow Meters	46
4.3 Working Fluid and Its Properties	47

4.4 Energy Consumption, Generation and Efficiency Equations of Equipment.....	48
4.4.1 WhisperGen Stirling Engine-Micro Combined Heat and Power (CHP) Unit.....	48
4.4.2 ClimateWell Chiller.....	49
4.4.3 Heat Rejection System.....	51
4.4.3 WhisperGen Stirling Engine Model in TRNSYS 17.....	52
Chapter 5 - Data Analysis	55
5.1 Preliminary Experimental Results of the Stirling Engine	55
5.1.1 Daily Breakdown of Thermal Energy Production of TRCA house	56
5.1.2 Thermal Efficiency of Stirling Engine	57
5.1.3 Electrical Output of the Stirling Engine, Daily Break Down and Efficiency	58
5.1.4 Cyclic Behaviour of Stirling Engine	60
5.1.5 Stirling Engine Performance with a Built in Auxiliary Burner	62
5.2 Feasibility Analysis	64
5.2.1 Heating and Cooling Demand and Production	64
5.2.2 Time of Running Stirling Engine and Gas Consumption.....	68
5.2.3 Extrapolating the Heating and Cooling Demands and Gas consumption	71
5.2.4 Prediction for Other Canadian Cities	73
5.2.5 Cost and GHG Emission in Toronto	74
5.3 Tri-generation System's Experiments.....	76
5.3.1 Charging Behavior of the ClimateWell.....	76
5.3.2 Discharging Behavior of the ClimateWell Chiller.....	85
5.4 TRNSYS Simulation for Charging and Discharging Optimization	88
5.4.1 Tri-generation Model.....	88
5.4.2 Charging and Discharging Simulation Result	89
5.4.3 Simulation Results of Different CHP and Heat Rejection Systems	92

Chapter 6 - Summary and Conclusion	95
6.1 Summary of Results	95
6.1.1 The Stirling Engine Performance	95
6.1.2 Feasibility Analysis	96
6.1.3 Cost and GHG Emission Analysis	96
6.1.4 The Tri-generation System Performance.....	96
6.1.5 TRNSYS Simulation	97
6.2 Author's Contribution	97
6.3. Recommendations and Future Works	98
Bibliography.....	100
Appendices:.....	106
Appendix A – Sensors List.....	106
Appendix B – PG-Water Solution Specifications	114
Appendix C – Cooling Demand Prediction Based on Different COPs	117
Appendix E – Valves Positions for the Heat Rejection Circuit.....	118
Appendix F – HOUSE B Pictures	119

List of Figures

Figure 1.1 - Residential Energy Consumption of Different Countries in 2006	1
Figure 1.2 - Energy Consumption by Sector in Canada	2
Figure 1.3 - GHG Emission by Different Sectors in Canada	2
Figure 1.4 - Energy Use by Type of Fuel in Canada	3
Figure 1.5 - Average Canadian Household Energy Use by Specific Source	4
Figure 1.6 - Distribution of Residential Energy Use in Canada	5
Figure 2.7 - Output of Different Systems	8
Figure 2.8 - General Schematic Working Principle of Internal Combustion Engine	10
Figure 2.9 - Simplified Schematic of IC Engine Cogeneration	11
Figure 2.10 - Basic Theoretical Fuel Cell Operation System	13
Figure 2.11 -Three-Cell Stack Schematic	14
Figure 2.12 - Stirling Engine Working Plan	17
Figure 2.13 - Whispergen Stirling Engine	23
Figure 2.14 - Absorption Process	26
Figure 2.15 - Adsorption Process First Stage	28
Figure 2.16 - Adsorption Process Second Stage	28
Figure 2.17 - Schematic of a single Barrel of ClimateWell.....	32
Figure 2.18 - Temperature of the Reactor and the Condenser of a Barrel During Charging and Discharging	34
Figure 2.19 - ClimateWell Machine	34
Figure 3.20 - Rear View of TRCA Houses – North Side	36
Figure 3.21 - Front View of TRCA Houses – South Side	36
Figure 4.22 - General Schematics of Tri-generation System.....	42
Figure 4.23 - Detail Schematic of the Tri-generation System	43
Figure 4.24 - Front Panel of LabVIEW Program at TRCA.....	45
Figure 4.25 - Micro CHP Unit - Sensor Locations	49
Figure 4.26 - ClimateWell Unit - Sensor Locations	51
Figure 4.27 - Heat Rejection/Recovery System - Sensors Locations	52
Figure 5.28 - Daily Thermal Energy Production of the Stirling Engine - March 2011	56
Figure 5.29 - Thermal Efficiency of Stirling Engine versus Supplied Temperature	58

Figure 5.30 - Daily Electrical Production of Stirling Engine-Winter 2011	59
Figure 5.31 - Stirling Engine Performance – February 20, 2011.....	61
Figure 5.32 - Typical Cyclic Behavior of the Stirling Engine	62
Figure 5.33 - Stirling Engine Performance with Auxiliary Burner - October 18, 2012	63
Figure 5.34 - Predicted Heating and Cooling Demands of House B by TRNSYS Software	65
Figure 5.35 – Experimental Thermal Energy Generated versus Daily Average Temperature	65
Figure 5.36 - Thermal Demand of House B Prediction by TRNSYS.....	66
Figure 5.37 - TRNSYS House B simulated model Predicted and Experimental Thermal Output vs Average Daily Outdoor Temperature	67
Figure 5.38 - Predicted Cooling Demand (TRNSYS) of House B and Required Thermal Load vs Average Daily Temperature.....	68
Figure 5.39 - TRNSYS Thermal Prediction & Required Time of Running & Gas Consumption	69
Figure 5.40 – TRNSYS Cooling Prediction & Required Co-gen Runtime & Gas Consumption	70
Figure 5.41 - Daily Demand of House B	71
Figure 5.42 - Cumulative Heating and Cooling Demand of the House.....	72
Figure 5.43 - Estimated Daily Gas Consumption VS Daily Average Outdoor Temperature.....	73
Figure 5.44 - Annual Demand & Corresponding Gas Consumption in Different Canadian Cities	74
Figure 5.45 - Supply and Return Temperature for both Ideal and Actual Conditions.....	78
Figure 5.46 - Temperature & Flow Rate of Different Sensors During Charging Process vs Time	79
Figure 5.47 - Heat Transfer Rate and Cumulative Energy Generation by the Stirling Engine	80
Figure 5.48 - Stored and Rejected Heat Transfer Rate	81
Figure 5.49 - Cumulative Stored, Generated, and Rejected Energy During Charging Period	81
Figure 5.50 - Temperature Variation of Working Fluid in the Heat Rejection Circuit	83
Figure 5.51 - Temperature Variation of Main Domestic Water in Heat Recovery Circuit	84
Figure 5.52 - Share of Each Component in the Heat Rejection Circuit.....	84
Figure 5.53 - Temperatures and Flow Rate of the AC Loop	86
Figure 5.54 - Discharge Rate and Total Discharged Energy	86
Figure 5.55 - Rejected Rate and Cumulative Rejected Energy	87
Figure 5.56 - Simulated Behavior of the Stirling Engine Based on the Experimental Result.....	89
Figure 5.57 – State of Charging of the ClimateWell Barrels for the Ideal Case & TRCA House .	91
Figure 5.58 - Simulated Chilled Water Supply at TRCA (T13)	92

Figure 5.59 - Simulated SOC of the ClimateWell Barrels with a Bigger CHP Unit at TRCA	93
Figure 5.60 - Simulated SOC of the ClimateWell Barrels at TRCA with Higher Heat Rejection Rate	93
Figure 5.61 - Simulated SOC of the ClimateWell Barrels at TRCA with Smaller CHP Unit and Higher Heat Rejection Rate	94
Figure B.1 - Density and Specific Heat Change of Water-PG Solution Versus Temperature ...	114
Figure B.2 - Error of Considering Average Values of Density and Specific Heat	114
Figure C1 - Predicted Cooling Demand & Required Thermal Load With Multiple COP	117
Figure F.1 - TRCA House B	119
Figure F.2 - Air Handling Unit	119
Figure F.3 - RTD Sensors	120
Figure F.4 - Stirling Engine Cogeneration Unit.....	120
Figure F.5 - Flow Meter and Pump.....	121
Figure F.6 - Heat Rejection Tanks	121
Figure F.7 - ClimateWell Chiller	122

List of Tables

Table 1.1 - Residential Energy Indicators in Canada	3
Table 2.2 - Energy and Exergy Efficiencies for Tested CHP Systems at U of T	21
Table 2.3 - WhisperGen DC System Performance	21
Table 2.4 - Performance of Micro CHP Systems	22
Table 2.5 - Whispergen Stirling Engine Technical Specification	24
Table 2.6 - CHP Range of Specification	29
Table 2.7 - TDC Range of Specification	30
Table 2.8 - Climate-Well Technical Specifications	31
Table 3.9- Structural Features of the Twin Houses	37
Table 3.10 - Detail Specifications of Equipment, and Manufacturer/Distributor.....	39
Table 4.11 - Constant Density & Specific Heat Values of Water-PG 35% Solution	48
Table 5.12- Daily Maximum, Minimum, & Average at House B – February and March 2011 ...	57
Table 5.13 - Efficiencies of the Stirling Engine – Winter 2012	59
Table 5.14 - Numeric Sample of Heating Season Demands.....	69
Table 5.15 - Numeric Sample of Cooling Season Demands	70
Table 5.16 - Cost and GHG Emission in Toronto	75
Table 5.17 - Cost and GHG Emission Comparison Between Tri-generation and Conventional Systems	76
Table 5.18 - Charging Process Results	82
Table 5.19 - Details of Ideal Simulated Case by ClimateWell and TRCA Conditions	90
Table B.20 - Densities of Water-PG Solutions (kg/m ³).....	115
Table B.21 - Specific Heat of Water-PG Solution (kJ/kg.K)	116

Chapter 1 - Introduction and Objectives

1.1 Introduction

A major portion of worldwide energy consumption is for heating and cooling of residential, commercial, and industrial buildings. The energy consumption is followed by greenhouse gas (GHG) emission while the cost of energy is another important factor. Energy consumption of industrial and commercial sectors, because of their similar structures, detailed defined regulations, willingness and expertise in lowering the energy consumption, are well studied and understood. On the other hand, although the major sources of residential end use groups are known which includes space heating, space cooling, domestic hot water, and appliances and lighting, residential energy consumption is not as clear and well defined in the literature as it is in the industrial sector. Some of the important reasons are as follow: diversity of size, structure, and thermal envelopes, and also variation of home owners and occupants' behaviors. However, the share of energy consumption by each end use group relies on climate, system efficiencies, and building structure [1]. Therefore, average energy consumption of residential buildings in different countries, as shown in Figure 1.1, varies between 16% and 50% of total energy consumption [2].

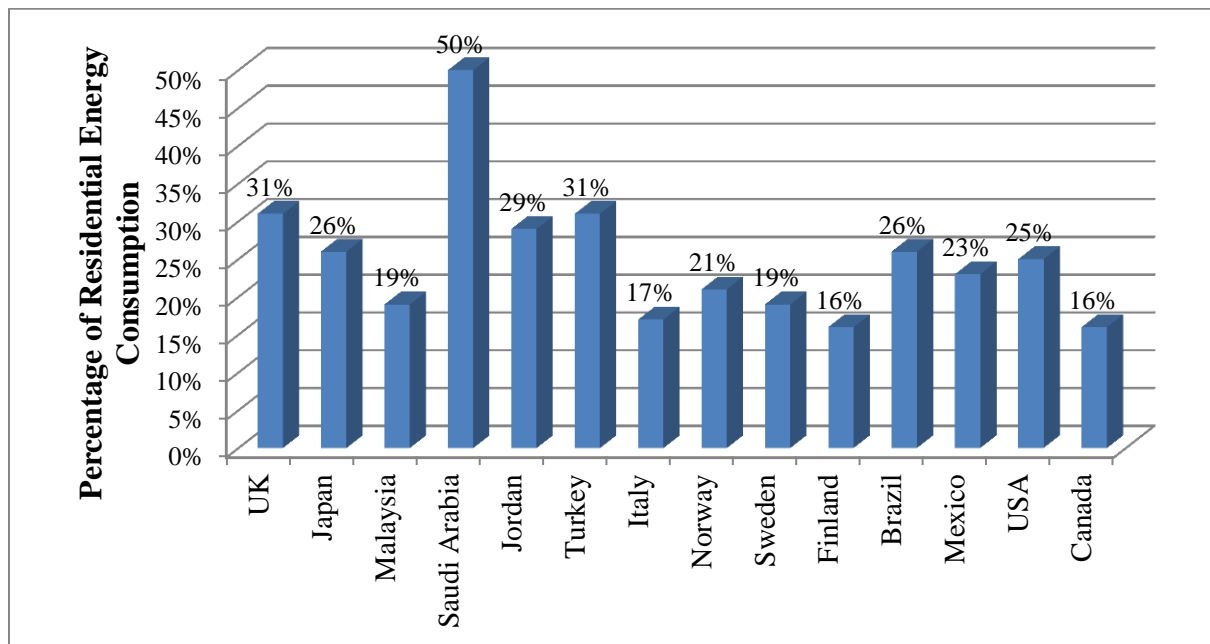


Figure 1.1 - Residential Energy Consumption of Different Countries in 2006 [2]

In Canada, as shown in Figure 1.2, the share of residential sector energy consumption is 16% of the total energy used by all sectors such as industrial, transportation, agricultural, and commercial. Canadians spent over \$28 billion for residential energy consumption. Although the industrial sector uses the largest portion of energy, the GHG emission produced by the transportation sector ranks highest among the other sectors (Figure 1.3) with 36% of GHG emissions [3].

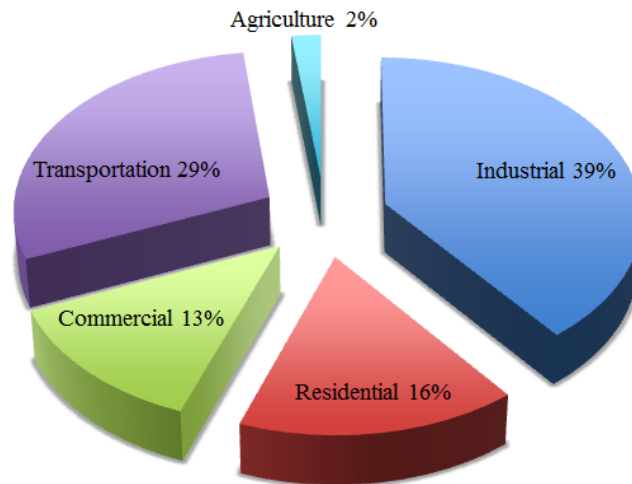


Figure 1.2 - Energy Consumption by Sector in Canada [3]

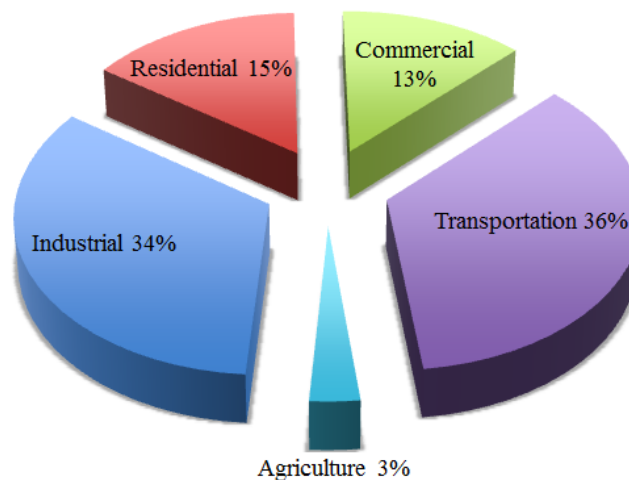


Figure 1.3 - GHG Emission by Different Sectors in Canada [3]

In addition to the 19% population growth in Canada for the last 20 years, the average living space per person increased 10% in total since 1990 (see Table 1.1). An aging population

which tends to stay home longer, single household occupancy by lots of young people, and an increase in the number of devices at home such as computers, televisions, and microwaves caused 13% growth of energy consumption in the residential sector since 1990, while in the industrial sector it also rapidly grew by 28% [3].

Table 1.1 – Residential Energy Indicators in Canada [3]

Year	1990	2007
People Per Household	2.8	2.5
Living Space per Household	116 m ²	128 m ²
Number of Households	9.9 million	13 million
Number of Appliances per House	15	21
Percent of Occupied Floor Space Cooled	23	43

As Figure 1.4 shows, electricity and natural gas are used for almost half of the required energy in Canada. Due to lower price than oil and a rise in availability, these two sources play important roles in the residential sectors as well.

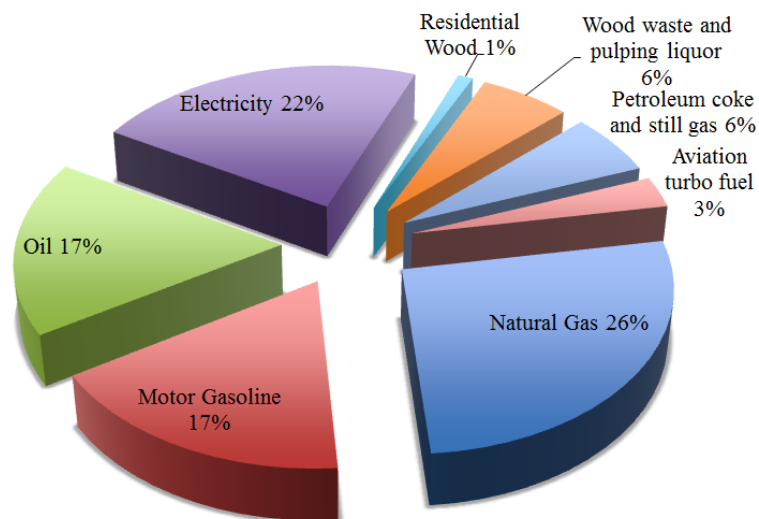


Figure 1.4 - Energy Use by Type of Fuel in Canada [3]

Although natural gas and electricity are widely used in Canada, different provinces based on their climate, buildings structure, occupant behavior, and heating/cooling equipment have

different average energy usage [4]. Figure 1.5 shows the electricity and natural gas consumption for an average household in Ontario, British Columbia, Manitoba, and Saskatchewan. Saskatchewan ranks highest in natural gas consumption per household and Manitoba ranks the highest in electricity consumption per household.

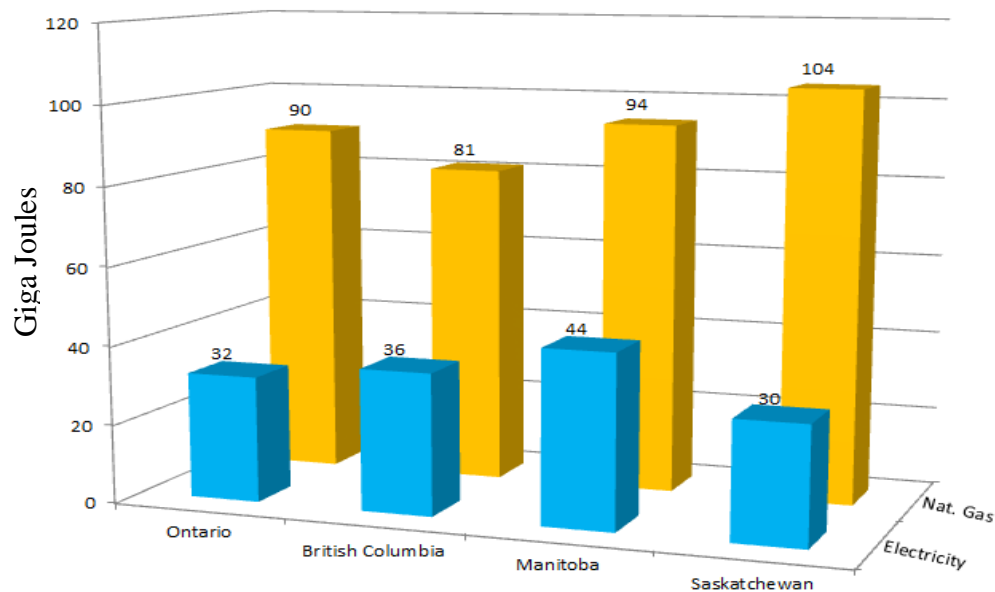


Figure 1.5 - Average Canadian Household Energy Use by Specific Source [4]

Figure 1.6 illustrates the distribution of energy use in the residential sector in Canada, which space heating has the biggest share with 63% and space cooling has the lowest with 2%.

To decrease energy consumption, and adhere to international environmental rules and regulations, one potential solution is cogeneration or tri-generation, which is simultaneous production of electricity and thermal energy and in case of tri-generation, cooling production is included [5]. Combined energy production systems will improve efficiency by using the waste heat. Traditional systems burn fossil fuels to produce electricity for the grid, and then use electricity for cooling in residential houses, or use electricity for cooling and burning more fossil fuel for heating purposes.

Applying small scale cogeneration technology for residential buildings will reduce the grid dependency of consumers by the production of electricity while recovering waste heat to meet the thermal demand of the building. However, by implementing a heat activated cooling

system in the building, the integrated system becomes a combined production of heating, cooling, and power (CHCP). Tri-generation systems have been used for industrial purposes for a while but it is not yet common to use micro tri-generation systems in the residential houses [6].

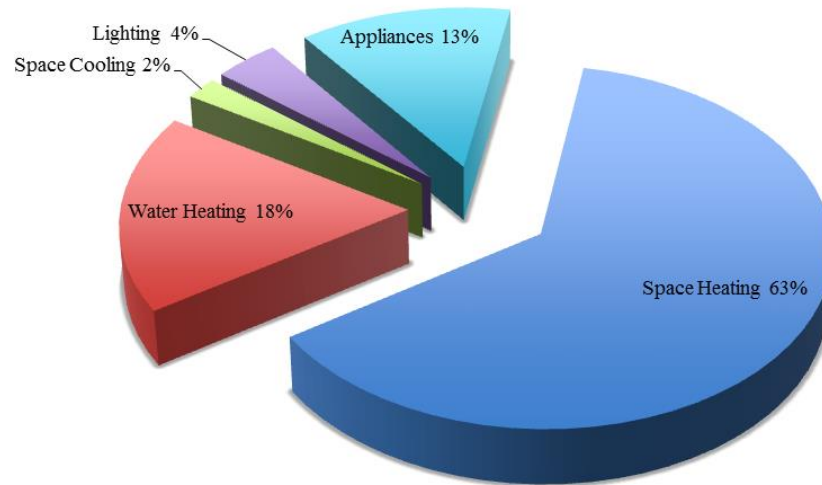


Figure 1.6 - Distribution of Residential Energy Use in Canada [3]

In an industrial scale tri-generation plant, waste heat from electricity production such as from a boiler or gas turbine is used for heating and also driving a cooling system. This heat usage will improve the overall efficiency and decrease the environmental impact. Industrial scale tri-generation systems must be used as decentralized plants since far end users would have no benefit due to cooling/heating losses [7].

This residential tri-generation project is designed to develop and assess the feasibility of micro tri-generation system in Canadian houses. The field test is at the Toronto and Region Conservation Authority (TRCA). In order to demonstrate and test sustainable housing technologies, TRCA along with Building Industry and Land Development (BILD) Association have built an Archetype Sustainable House (ASH) at the Living City Campus of Kortright Centre in Vaughan, Ontario, Canada [8]. The Archetype House includes two semi-detached houses equipped with over 300 installed sensors and with a long term monitoring infrastructure using a Data Acquisition System (DAQ) capable of recording data every 5 seconds. In addition, the control system at the house is able to simulate the required load under real life condition [9, 10].

A Stirling engine based cogeneration unit is used for the electrical and thermal production. This engine can produce up to 12 kW of thermal and 1 kW of electricity with a very low level of vibration and noise, which is suitable for residential applications. The engine burns natural gas and has been tested at different period of time, outdoor temperatures, and under different demand conditions. The data have been recorded and analyzed during the test and after. In addition, all types of heat activated cooling systems have been reviewed (see literature review – Chapter 2). Due to interests of Union Gas Ltd, a local natural gas distributor, and ClimateWell AB, a Swedish company that manufactured and patented the new Thermo Chemical Accumulator (TCA) system, a residential tri-generation project was planned. Feasibility study showed that the Stirling engine is well suit for this collaborated project. Accordingly, an integrated tri-generation system was designed and installed at House B of the ASH.

1.2 Objective and Intent of Research

In order to investigate the feasibility of residential tri-generation in Canadian houses, a major research project was conducted. The research started with the collaboration of Ryerson University, Union Gas Ltd, Climatewell, Renteknik Group, and TRCA to better understand the performance of the micro tri-generation system using natural gas for a typical single family home in Toronto. The detailed objectives of this thesis are given below:

1. Review of different types of cogeneration and tri-generation systems

A comprehensive literature review of different types of integrated systems was carried out to understand the most suitable match for Canadian weather considering the availability and price of different fuels.

2. Preliminary tests and feasibility analysis

Before design and installation of a tri-generation system, series of tests were conducted on the cogeneration system. The results were analyzed to investigate potential difficulties that could occur in running the system. Moreover, considering Toronto weather and predicted cooling and heating demands of the TRCA house, a feasibility analysis was conducted which showed a promising result.

3. Design and installation of a micro tri-generation system at the ASH

Based on the preliminary test results, a detailed strategy for the next level of tests including the whole integrated system was planned. Piping for charging, discharging, and heat rejection circuits was designed and installed in summer 2012. Also, required sensors such as flow meters, watt-nodes, and temperature sensors were installed and integrated into the existing DAQ system.

4. Investigation of energy efficiency, cost, and potential improvements

Recorded data via the data acquisition system were analyzed. Heating and cooling production of the integrated system were studied in detail. In addition, efficiency of different circuits along with potential problems and solutions are discussed. Moreover, an energy cost analysis was conducted.

5. Verification of experimental data using TRNSYS 17 energy modeling software

TRNSYS 17 was used to model the house including all conditioning equipment of the integrated system such as the cogeneration system, Climatewell, heat rejection system, and air handling unit. The annual performance of the system was simulated in Toronto and other Canadian regions.

Chapter 2 - Literature Review

A comprehensive literature review of the integrated energy production methods including cogeneration and tri-generation systems was carried out. Many studies in the literature have investigated industrial and large scale integrated systems. The focus of the other literature are mostly industrial power plants, which are recovering the waste heat for heating and cooling purposes for another industrial use close to the plants. In addition, a noticeable amount of small scale cogeneration systems have been studied around the world (see Section 2.1.4). Many research groups have performed detailed feasibility analysis of using micro cogeneration systems as prime movers for residential buildings. Although micro cogeneration systems help to save energy and reduce costs by recovering the waste heat, in hot seasons the heating demand is lower and recovering waste heat is not required. Therefore, adding a heat activated cooling system to a cogeneration unit would help to cover cooling demand in the summer time. Heat activated systems or Thermally Driven Chillers (TDC) are of different types such as absorption systems, adsorption systems, and thermo chemical accumulators. Figure 2.7 illustrates the difference between traditional power generation system, cogeneration system, and tri-generation systems. All related systems and components to cogeneration and tri-generation systems were studied in this chapter.

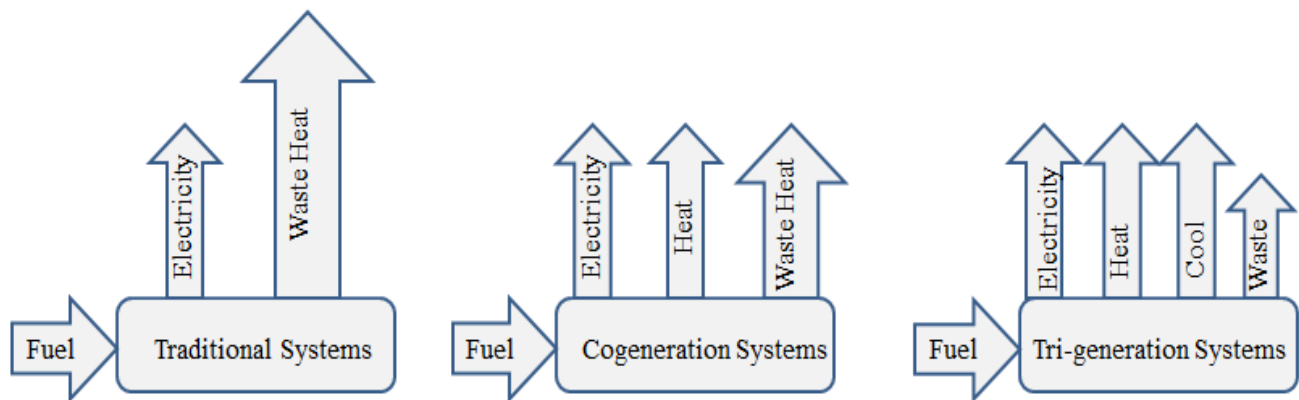


Figure 2.7 - Output of Different Systems

2.1 Cogeneration Systems

Producing heat and electricity at the same time is called cogeneration. Cogeneration can be applied to industrial plants, commercial buildings, and residential use. Different methodologies and techniques have been developed for the cogeneration system, such as; steam turbine, gas turbine, reciprocating internal combustion engine, fuel cell, and Stirling engine [5]. But not all of these systems are applicable for residential purposes. In addition, each type of small scale cogeneration system can be applied for different purposes. The system may satisfy both thermal and electrical demands of the house, or a portion of each thermal and electrical demand, or a combination of full and partial satisfaction of loads. If the cogeneration unit works based on heat demand, it is called a thermal-load following strategy and if it is based on electricity demand, it is called an electrical-load following strategy. A detailed description of efficiencies, principle of operation, and performance characteristics for each reciprocating internal combustion engine, fuel cell, and Stirling engine is provided in this section.

2.1.1 Reciprocating Internal Combustion Engine

One of the most widely used small combined heat and power prime movers is the Reciprocating Internal Combustion Engine (IC Engine). IC engines, due to their well-established technology, are a suitable candidate and a good match for residential cogeneration. Use of the reciprocating internal combustion engine is very common compared to other residential cogeneration systems because of its low capital cost, reliability, ease of maintenance, and low operational cost [11]. The very well established technology of internal combustion engines and competition of manufacturers lowered the price of this reliable prime mover. In this type of cogeneration system, the fuel is either spark-ignited or compression-ignited. Heat and pressure of combustion pushes the piston which is connected to a generator for electricity production. Heat recovery of combustion through cooling water, exhaust gas, and engine oil captures thermal energy [12]. Compared to many other systems, most of the IC engine models have a higher electrical production rate and efficiency, and therefore lower fuel cost [13]. The number of cylinders and the type of fuel can vary according to the size and applications. Figure 2.8 shows a simplified schematic of the IC engine working principle, which includes the heat recovery system, the engine body and the generator.

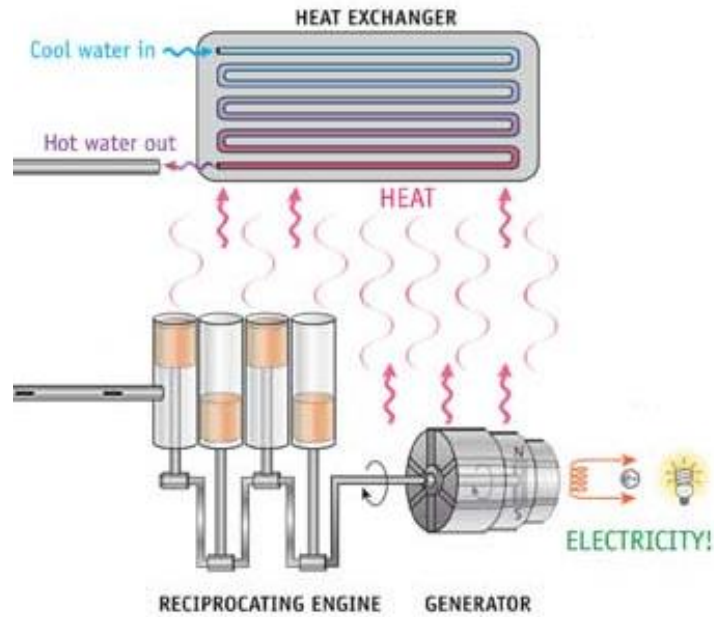


Figure 2.8 - General Schematic Working Principle of Internal Combustion Engine [14]

2.1.1.1 Operation Principles of IC Engines

Two methods of ignition can be used for IC engines; compression ignition and spark ignition. Diesel engines use compression and mostly a four stroke direct injected method. Although they can be used for residential buildings and small scale cogeneration, the main use of diesel engines is large scale cogeneration. The dual fuel operating mode, which can burn natural gas with a small portion of diesel fuel, is one advantageous capability of diesel engines while a down side is the lower temperature compared to spark ignition systems [6, 15]. On the other hand, spark ignition engines, which mostly burn natural gas, because of their heat recovery systems (up to 160°C hot water/20 bar steam) are well suited for small scale cogeneration applications. Natural gas based IC engines are accompanied by low capital cost, fast start up, and are reliable if properly maintained. In addition they have good partial load efficiency, and good heat recovery. Similar to other cogeneration systems, in IC engines a pump circulates the cooling fluid through the jacket of water, which heats up the water [13, 15]. Figure 2.9 shows a simplified schematic of cogeneration with an IC engine and how the heat can be recovered from the exhaust gas, jacket water, and lube oil.

Diesel type engines produce 5 to 20 times more NO_x than natural-gas based spark ignition engines. The NO_x associated with IC engines is thermal NO_x, which comes from N₂ and O₂ reacting at high temperature and is highly dependent on the temperature and the residence time of those gases in the engine. Another type of NO_x production is fuel-bound NO_x and forms when nitrogen is presented in the fuel molecule. Natural gas has a very small amount of nitrogen in its chemical bonds while liquid fuels have more nitrogen bonded in their composition. Therefore, associated NO_x produced by natural gas is relatively less than liquid fuels [13]. In general, high performance operation and low NO_x production cannot occur simultaneously with current technologies.

2.1.2 Fuel Cells

Fuel cell is a technology that potentially produces power and heat directly from the fuel without actual combustion. Nowadays, by improved technology of fuel cells they are more affordable and because of their very low level of emissions and noise, relatively high efficiency, very good response to partial load running, and low maintenance depending to the type of fuel, they are one of the best options for the residential cogeneration systems [6, 5].

Converting chemical energy of hydrogen to electricity is the method which fuel cells uses for power generation. The hydrogen can be derived from hydrocarbon fuels. The electricity produced by fuel cells is direct current (DC). A fuel processor to convert hydrocarbon to hydrogen and a transformer to invert DC to AC are needed [17].

2.1.2.1 Operation Principle of Fuel Cell

Reactions of hydrogen with oxygen produce water. This reaction in the presence of an electrolyte, causes a flow of electric current through an external circuit. Two electrodes and an electrolyte are involved in each fuel cell. Hydrogen acts as a fuel and is oxidized at the (negative) anode. On the other hand, oxygen is reduced at the (positive) cathode while ions move through the electrolyte between electrodes. Also an electrolyte in fuel cells works as a gas separator and electronic insulator [5, 18]. Figure 2.10 shows a basic operation method of a single fuel cell, which in general can produce only a voltage range from 0.6 V to 0.7 V.

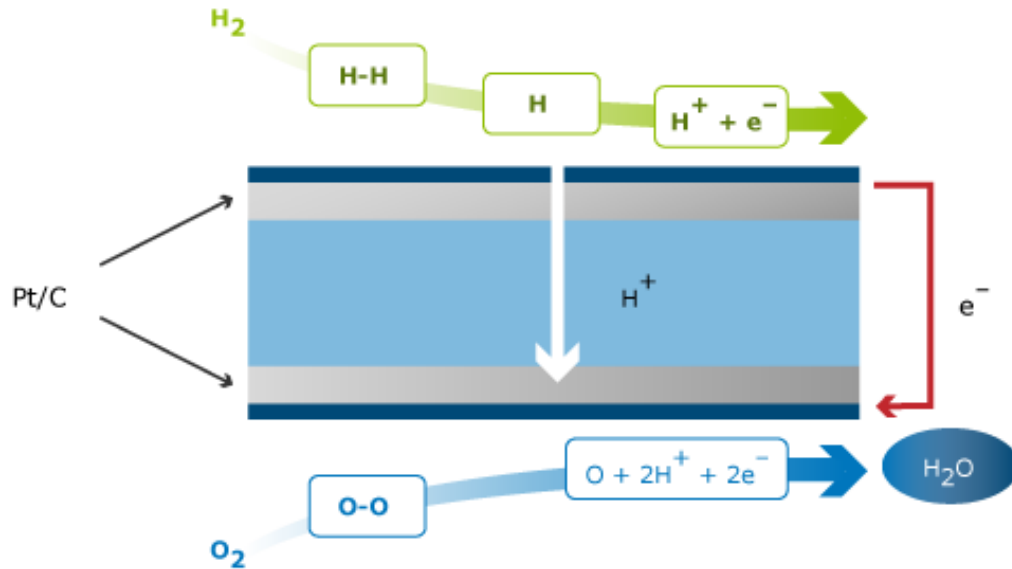
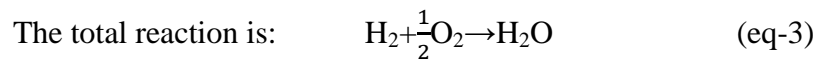
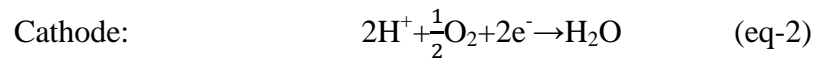
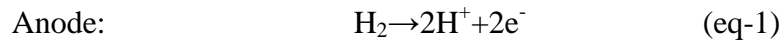


Figure 2.10 - Basic Theoretical Fuel Cell Operation System Based on PEMFC Systems [18]

The following equations show how electrochemical reactions occur:



As mentioned before, a single fuel cell only produces low voltage. Therefore, the practical method to increase the power production is to use a group of cells in series, which is called fuel cell stack. There is a flow plate (separator) between every two cells. Each flow plate is required to be electronically conductive since it is used in one cell on the anode side and for other one on the cathode side. The flow plate also makes an equal distribution of reactants across the cell area [18]. A schematic of a three-cell stack is shown in Figure 2.11.

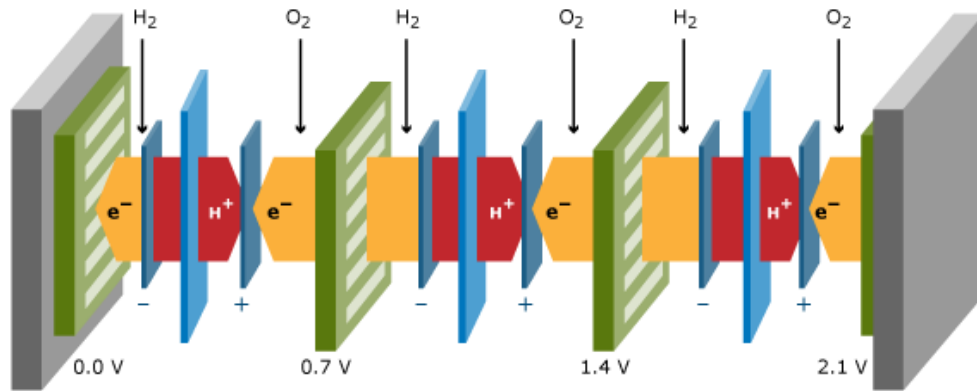


Figure 2.11 -Three-Cell Stack Schematic [18]

2.1.2.2 Different Types of Fuel Cells

There are several types of fuel cell that have appeared during previous years, and the most applicable types are as follow:

- **Alkaline Fuel Cells (AFC)**

In this type of fuel cell KOH (potassium hydroxide) with a concentration of 30% is used as the electrolyte. The fuel is pure hydrogen and the oxidiser is either air or pure oxygen. Use of AFCs is limited because the air has to be cleaned of CO₂ and also only pure hydrogen can be used as a fuel. The AFC process produces heat at 60-80°C, which is low compared to other types of fuel cells [5]. Space crafts are using AFC for their power generation. In AFCs the power density range is between 0.1 and 0.3 W/cm² [18].

- **Polymer Electrolyte Membrane Fuel Cells (PEMFC)**

In polymer electrolyte fuel cells, a solid polymeric membrane, while packed in two platinum-catalysed porous electrodes, is used as the electrolyte and the process temperature is almost 80°C [5]. Both fast start up and being able to start below 0°C makes PEMFCs a good choice for transport applications. In Molten Carbonate Fuel Cells (MCFC) the power density varies with the operating condition and is higher than 0.7 W/cm² [18].

- **Phosphoric Acid Fuel Cells (PAFC)**

In this type of fuel cell liquid H_3PO_4 (phosphoric acid) is used as an electrolyte. The temperature of the process is around 200°C [5]. In PAFCs the power density is around 0.14 W/cm^2 [18].

- **Molten Carbonate Fuel Cells (MCFC)**

The electrolyte in MCFCs is a molten mixture of lithium, sodium and potassium carbonate. The operation temperature can reach as high as 700°C [19]. This type of fuel cell requires carbon dioxide to be delivered to its cathode. Therefore, unlike the other fuel cells, MCFC requires a CO_2 emission control system. In MCFCs the power density range is between 0.1 and 0.12 W/cm^2 . Since the power production range in MCFC systems is from 50 kW to 5 MW typically they have been used in the industrial and commercial sectors [18].

- **Solid Oxide Fuel Cells (SOFC)**

The operation temperature in SOFC is around $950\text{-}1000^\circ\text{C}$ and a ceramic material, Yttria-stabilised zirconia ($\text{Y}_2\text{O}_3\text{ZrO}_2$), is used as a solid electrolyte layer. The fuel can be either pure hydrogen or a mixture of hydrogen and carbon monoxide [19]. Also natural gas or even higher hydrocarbons can be used as a fuel in SOFCs. Available power production ranges in the market for SOFC is from 1 kW to 5 MW . In SOFCs the power density range is from 0.15 to 0.7 W/cm^2 [18].

2.1.2.3 Performance Characteristics of Fuel Cells

According to the literature, PEMFCs and SOFCs are more suitable for small scale cogeneration because of their higher efficiency, lower fuel consumption, and lower environmental impact. The efficiency of fuel cells varies with type and is dependant to the number of cells in series [6]. Consequently, efficiency of a fuel cell system is equal to the total amount of all individual cells. The overall efficiency can reach as high as 80% [17]. Furthermore, some types of fuel cells have a very good response to the partial load and good load following characteristics for both electrically and heat generation. The part load efficiency of those types is even better than reciprocating internal combustion engines [17].

Reforming produces the required hydrogen from the hydrocarbon fuel. Heat is recovered at the reformer and stack of a fuel cell. The PEMFC and PAFC produce low grade heat, which is

suitable for residential buildings. Other types of fuel cells, produce much higher grade heat, and with newer technologies they can be used in residential buildings as well. On the other hand, fuel cell systems depending on their types, require different maintenance. Periodic replacement of the fuel filter, reformer plug, and water treatment beds is mandatory every 2000 to 4000 hours. However, major replacement of the shift catalyzer, reformer catalyzer, and stack is required every four to eight years. Emission mostly happens at the reforming process and is produced less in fuel cells as they do not involve a combustion process. A reformer, in SOFC and MCFC, requires heat and uses the generated heat from the anode. If the reformer's temperature during the process is maintained below 1000°C NO_x formation can be avoided while the required temperature for CH₄ reforming is much lower [6, 17].

2.1.3 Stirling Engine

Stirling engines were invented in 1816 and were widely used during the 19th century. In the 20th century, Stirling and steam engines were replaced by internal combustion engines, which improved the reliability and reduced costs. Recently, the market has again been again attracted to the Stirling engine due to the high efficiency, low negative impact on the environment, and increase in electricity demand [20].

Stirling engines are well-known for their various benefits, such as high efficiency and performance, very low levels of noise and vibration, and almost no maintenance need. Also, because of external combustion, they can work very flexibly by using different types of fuel while products of combustion cannot enter into the cylinder. Stirling engines can be controlled and run by a wide range of energy sources such as oil and natural gas as well as renewable energy sources, like biomass and solar. Compared to other types of engine, Stirling engines have fewer moving components and consequently, less noise and lower maintenance cost [6]. Stirling engines produce 10 times less emission compared to IC engines. Modern Stirling engines preheat the air for an efficient combustion process. NO_x and CO are the prominent emissions produced by Stirling engines while unburned hydrocarbon are insignificant compared to internal combustion engines. In some of the Stirling engines, exhaust and intake air are mixed to decrease the nitrogen oxide formation [21].

2.1.3.1 Operation Principle of the Stirling Engine

Stirling engines are simple in design. They follow the Stirling cycle and work with a compressible fluid (e.g., air, helium, or nitrogen). The closed system of Stirling engines avoids contamination. On the other hand, the working fluid must be a low viscous fluid for pump loss reduction, which can reduce the mass flow rate at the high pressure operation condition [22]. During an isothermal compression process, the engine gains heat at the energy/heat source. The working fluid gas passes through a regenerator body due to a constant volume displacement process and transfers the heat from the fluid to the regenerator. The heat will be recovered by the cool working fluid at the other side of the regenerator and it will be cooled down by the coolant during an isothermal expansion process. The regenerator is a porous metal or a simple matrix of fine wires, which increases the efficiency [5]. The overall working Stirling engine schematic is shown in Figure 2.12.

1-2 & 3-4: Isothermal Compression

2-3 & 4-1: Constant-Volume Displacement

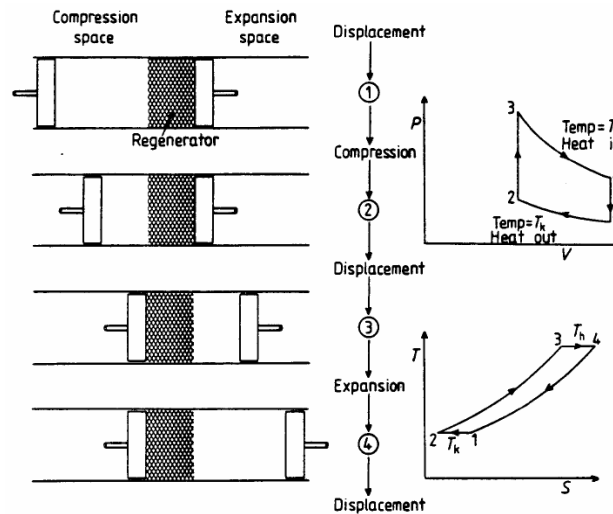


Figure 2.12 - Stirling Engine Working Plan [5]

2.1.3.2 Stirling engine configuration

The first generation of Stirling engines used a kinematic drive method which was a combination of cranks, connecting rods, and flywheels moving all together. Design challenges for crank-driven engines are working fluid leakage and isolation of lubricant. The next

generation of Stirling engines used the free piston drive method. This method replaces the crank with a simple moving part called the free piston and keeps and seals the working fluid for a longer period of time [5, 23]. Basically, in this type of engine, the piston and displacer are dependent on each other. When the displacer oscillates, the piston also has to oscillate. A major force is at the engine axis direction; therefore, angular momentum of the connecting rod is avoided and no lubricant is needed [24].

Stirling engines can be classified by their configurations, called alpha, beta, and gamma. In the alpha type, instead of a displacer, a second piston is used. They move in the same direction to keep the volume constant for the heating/cooling process. The beta version has one displacer and one piston inside a cylinder, while the gamma type displacer and piston are located in different cylinders but connected to each other [6].

2.1.3.3 Performance Characteristics of Stirling engines

In this section the efficiency, heat recovery options and methods, maintenance, and emission of Stirling engines will be discussed. For the optimum design point of the Stirling engine, maximum efficiency and maximum power must be considered. Two power pulses per revolution and continuous combustion result in smooth running with a low level of vibration, noise, and emission. In theory, the efficiency of Stirling engines is higher than that of other engines. The electrical efficiency can reach as high as 40% and the overall efficiency may reach more than 90% [6, 5]. The main source of heat recovery for natural gas fuelled Stirling engines is the cooling fluid. In addition, the exhaust gas heat exchanger, cylinder walls, and lubricant oil are other sources for heat recovery, which improve the efficiency. Because of very high efficiency exhaust heat exchanger, the exhaust gas temperature is very low compared to the combustion temperature and the temperature can be very close to the cooling fluid temperature [6]. Regarding emission, among micro combined systems, Stirling engines are the second best after fuel cells. Because of the low temperature of exhaust gas and continuous, lean combustion, the emissions from Stirling engines are very low compared to IC engines [25]. Stirling engines require maintenance every 5000 to 8000 hours, which is a very long period of time for an engine. On the other hand, free piston engines have no mechanical contact or friction, hence no mechanical maintenance is required. Due to these two reasons, the cost of maintenance is negligible for Stirling engines [6].

2.1.4 Prime Mover Studies

Different micro cogeneration systems have been tested around the world by many researchers, institutes, and universities. Some of the groups have focused on power generation while others have investigated thermal production. Most of the available prime movers in the market have been tested either in laboratories or under real life conditions. The following pages discuss the published results by some of those groups.

2.1.4.1 Cogeneration Test at CCHT House by NRCan

Natural Resources Canada (NRCan) researchers have tested and assessed four different types of micro cogeneration systems at the Canadian Centre for Housing Technology (CCHT) located in Ottawa, Ontario, Canada. Two types of natural gas based Stirling engines, a hybrid internal combustion engine coupled with a furnace, a solid oxide fuel cell, and a Japanese cogeneration¹ system have been tested during 2003 to 2008. Testing all micro cogeneration systems at the same test house under almost the same conditions and demands is unique to this research project. First, they installed a third generation Stirling engine with 736 W electrical and 6.5 kW thermal capacity. The second test was with a fourth generation Stirling engine, which had two power setting modes; 850 W electrical & 6 kW thermal and 1.2 kW electrical & 8 kW thermal. The first engine took the air for combustion from the room while the second was fed by outdoor air. The air intake temperature of the second engine was limited to above -10°C, therefore it was unable to function during very cold winter season. Two separate test strategies of thermal load-following and electric load-following were defined. The results showed that the performance and efficiency of the Stirling engine was higher when it followed the thermal load strategy compared to when it followed the electric load strategy. The Stirling engine consumed almost 20% of its electricity production for the circulation pump in the supply line. The overall efficiency of the Stirling engine based on the HHV of the fuel was estimated at 82.8% during the thermal load following strategy run and 73.9% during the electric load strategy run. The report claimed that the partial load run for the Stirling engine was the reason for the lower efficiency, which is questionable according to the fact that Stirling engines cannot work in partial load. A solid oxide fuel cell was the next cogeneration system installed at the CCHT. The fuel cell was capable of 5 kW electrical and 5 kW thermal productions. The efficiency calculation (HHV

¹ Type and brand of this unit is not specified by the reference source.

based) showed 23.6% of electrical efficiency and 25.4% thermal efficiency. However, a portion of the heat output had to be dumped, therefore the thermal efficiency decreased to 15.6%. Moreover, a hybrid internal combustion engine with 1 kW electrical and 3.25 kW thermal capability was installed and tested. They coupled the IC engine to a furnace to increase the overall thermal capacity to 18 kW. They also installed a Japanese natural gas fueled engine cogeneration system coupled to a ground loop (6 kW electrical & 11.7 kW thermal). However, the efficiency results of the IC engine and Japanese cogeneration system are not available [26, 27].

2.1.4.2 Cogeneration Test in Combustion Research Laboratory at University of Toronto

A research group in the Combustion Research Laboratory at University of Toronto under the supervision of professor Murray J. Thomson experimentally analyzed different micro cogeneration systems on the basis of energy and exergy efficiency. The test was conducted on three types of prime movers all fueled by natural gas. A Stirling engine along with an IC engine and a polymer electrolyte fuel cell (PEFC) were tested. The results indicated that at high supply temperature, the internal combustion engine delivered the highest efficiency, and at low supply temperature the PEFC provided the highest efficiency [28].

An AC-WhisperGen Stirling engine capable of 0.85 kW electrical and 6 kW thermal power productions with a single swirl nozzle and nitrogen as a working fluid was tested. Energy efficiency of 61.6% and exergy efficiency of 36.2% were found for this engine [28, 21].

In addition, a very small PEMFC fuel cell manufactured by EBARA-Ballard was installed and tested. The unit produces 1 kW of electrical and 1.52 kW of thermal power. Natural gas was used to warm up the reformer, which produces hydrogen from the fuel. After achieving a hot stable temperature, natural gas reforms to hydrogen and carbon dioxide. In a cell stack, hydrogen reacts with oxygen and produces electricity. This unit is very small and heats up a 200 L tank to 60°C. Reported energy efficiency for this fuel cell is 74.9% while the exergy efficiency is only 37% because of the low temperature operation [28].

Also, a FreeWatt IC engine with 1.2 kW electrical and 3.26 kW thermal power capacities was tested. This unit works with a single cylinder engine fueled by natural gas along with an

intake air silencer, oil filter, and air filter. This engine provides 76.7% energy efficiency and 57.2% exergy efficiency, which both are the highest efficiencies among the other tested units [28]. Table 2.2 shows the energy and exergy efficiencies of these prime movers.

Another set of experiments was performed on a Stirling engine; this time the engine was fueled by diesel and biodiesel. Using diesel fuel the unit provided 11.7% power efficiency and 78.7% thermal efficiency. On the other hand, burning biodiesel, the Stirling engine could provide 11.5% electrical and 77.5% thermal efficiencies [21, 29].

Table 2.3 shows the details of the system performance.

Table 2.2 - Energy and Exergy Efficiencies for Tested CHP Systems at U of T [28]

<i>Cogeneration</i>	<i>$\eta\%$ El. Energy</i>	<i>$\eta\%$ Ther. Energy</i>	<i>$\eta\%$ Total Energy</i>	<i>$\eta\%$ El. Exergy</i>	<i>$\eta\%$ Ther. Exergy</i>	<i>$\eta\%$ Total Exergy</i>
Stirling Engine (AC- WhisperGen)	7.6	54	61.6	8.2	28	36.2
IC Engine (FreeWatt)	20.6	56.1	76.7	22.1	35	57.2
Fuel Cell (EBARA- Ballard)	29.7	45.2	74.9	31.9	5.1	37

Table 2.3 - WhisperGen DC System Performance [21, 29]

<i>Fuel</i>	<i>Fuel Flow (L/m)</i>	<i>Power (kW)</i>	<i>Heat (kW)</i>	<i>Electricity Efficiency %</i>	<i>Thermal Efficiency %</i>	<i>Total Efficiency %</i>
Diesel	0.0160	1.11	7.44	11.7	78.7	90.5
Biodiesel	0.0155	1.11	7.51	11.5	77.5	89

2.1.4.3 Cogeneration Test in Italy

A collaborative poly-generation research project was conducted at the Università degli Studi del Sannio and Seconda Università degli Studi di Napoli in Italy. They studied many types of poly-generation systems. They also employed a very accurate data acquisition system to collect and record all the sensors readings. They have tested different cogeneration systems and also compared and validated with different studies in the literature. In particular, the Aisin, Dachs, Ecopower and Solo models of micro cogeneration systems were tested by this group. Only the Solo was a Stirling engine and all the other systems were internal combustion engines. The researchers used heaters with electric resistances to simulate the loads, an 80-liter water heater, and a 200-liter hot water storage tank, and three variable speed fan coils [30, 31]. This project is considered to be unique as three types of IC engine with almost the same thermal and electrical capacity under the same conditions were utilized. Although the electrical efficiencies were found to be equal, the thermal efficiencies were different. Among all the IC engines, the Ecopower unit showed the best thermal efficiency. The published report, however, did not provide any particular reason for this difference [30]. Table 2.4 shows the detailed experimental results of the tests for all the four different prime movers. According to the data presented in the Table 2.4, which is a performance comparison between the common and available micro cogeneration systems in the market, the Stirling engine has a higher thermal efficiency and similar electrical efficiency.

Table 2.4 – Performance of Micro CHP Systems [31]

<i>Cogeneration System</i>	<i>Capacity [kW]</i>		<i>LHV Based Efficiency [%]</i>		<i>Type</i>
	<i>Electrical</i>	<i>Thermal</i>	<i>Electrical</i>	<i>Thermal</i>	
Aisin (Toyota)	4.6	11.7	25.5	58.5	IC
Dachs	5.0	12.3	25.5	62.7	IC
Ecopower	4.7	12.5	24.8	66.0	IC
Solo	9.0	26.0	25.0	72.2	Stirling

2.1.5 WhisperGen Stirling Engine

A WhisperGen Stirling engine is installed and operating at TRCA House B. This engine is a natural gas based four cylinder alpha type double-acting unit with a single nozzle for the burner. It is equipped with a cylindrical premix auxiliary burner. Consumer can control the engine by setting the supply temperature and running the auxiliary burner via a very user friendly control system. The generator can produce up to 1000 W of electricity while the thermal output range is between 5.5 kW to 12 kW. The engine itself, consumes 9 W in Standby mode and 100 W during operation. The flow rate of the cooling water can be set by the circulating pump from 8.5 to 15 l/min, which depends on the demand temperature set point. The outlet temperature can reach as high as 85°C. The working fluid inside the engine is pressurized nitrogen. Figure 2.13 shows the simplified schematic of the WhisperGen engine, which the generator is positioned at the bottom of the engine body. Cylinders are located vertically, which the top of cylinders are positioned in the burner, where the nitrogen gas expands in the cylinder. The bottoms of cylinders are at the engine section, where the nitrogen gas compresses. The WhisperGen engine is very small in size, the dimensions are 480 mm × 560 mm × 840 mm and the dry weight is 137 kg [32].

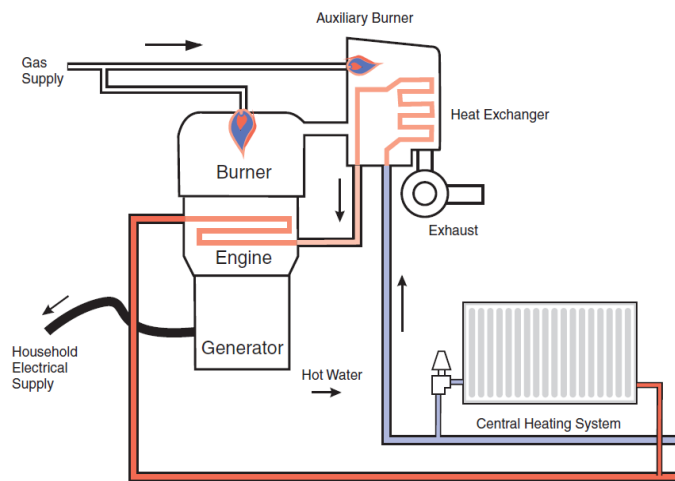


Figure 2.13 - Whispergen Stirling Engine [32]

The WhisperGen Company estimates that a typical household can reduce their electricity bill by 25 to 35% per year [32]. In addition, 1.5 tonnes reduction of carbon dioxide emission per year for each household is estimated. Also, by saving through the electricity generation, the

marginal investment can be paid off during the first three years [32]. Table 2.5 shows the WhisperGen Stirling engine technical specifications.

Table 2.5 - Whispergen Stirling Engine Technical Specification [32]

Component	Description
Engine	4-Cylinder double acting Stirling Engine
Burner	Single nozzle swirl established recuperating
Auxiliary burner	Cylindrical premix surface burner
Generator	4-pole single phase induction motor
Duty cycle	1-24 hours continuous operation
Electrical supply	230V-AC 50Hz (nominal grid voltage)
Electrical output	Nominal mode up to 1000W
Thermal output	Minimum 5kW, nominal mode up to 7kW, maximum 12kW(with auxiliary burner)
Fuel	Natural gas, supply pressure 17-20 mbar
Central heating system	Flow rate 8-15 l/min, maximum supply temperature 85°C

2.2 Tri-generation

Industrial cogeneration systems are very well established. Many years ago, the commercial and industrial sectors recognized the benefits of recovering waste heat from power plants, for which the heat can be used for another industry close to the plant. The idea of poly-generation, which is production of different types of energy together, improved the energy efficiency of the power plants and also lowered the operation cost of industries. Since normally those industries close to the plants do not require all the waste heat, a big portion of the generated thermal energy must be dumped to the environment. Therefore, a heat activated cooling system/Thermally Driven Chiller (TDC) can be used to produce cooling for another industry close to the plant. This procedure will upgrade the system to a Tri-generation system, which can simultaneously produce electricity, thermal energy, and chilled air/water. Compared to cogeneration, tri-generation is normally accompanied by an increase in energy efficiency.

In 1990, the European Commission set up the “Europe 2020” strategy known as “20-20-20” to reduce greenhouse gas emissions by 20%, increase the share of renewable energy by 20%, and increase energy efficiency by 20%. Since then, many manufacturers in Europe have been focused on a plan to minimize the residential sectors role in energy consumption [33]. Nowadays, finding a residential micro cogeneration unit is very easy and accessible specially in Europe. Many different types and brands with various thermal/electrical sizes are available with a reasonable and affordable price.

Continuous thermal production in addition to power generation is not economically feasible all year round. In the hot season, the heating demand of a residential building is very low but the cogeneration unit produces the same thermal energy as it does in the winter time. However, installing a small TDC in parallel with the cogeneration system would upgrade to a micro tri-generation system. The residential micro tri-generation system would be capable of heat and electrical generation in winter and also supply chilled water to meet the house cooling demand in the summer.

Residential micro tri-generation is not a well-established system and is not recognized as economically feasible yet. Currently, only a few companies are producing a very small number of micro tri-generation units and these systems are not readily accessible.

2.3 Heat Activated Cooling Systems

After choosing a cogeneration system, a TDC is the main component in any tri-generation system. In heat activated systems, unlike in conventional vapor compression cycles, the cooling/chilling process is not achieved by any mechanical or electrical power. Rather, absorption systems, adsorption systems, and thermo-chemical accumulators (TCA) are the main options to be used as a heat activated cooling system. There are different operation principles for cooling systems. Analysis of the industrial process in cogeneration energy production, and the huge amounts of wasted heat at those plants raised the idea of using the heat for cooling. The waste heat can be a good match and useful source for cooling production through a heat activated refrigeration system [34]. Use of heat for the cooling production may lead to electricity consumption reduction and also reduced CO₂ emission [35].

2.3.1 Absorption Systems

The condenser, evaporator, absorber, and generator are four essential components of an absorption cycle, which works based on two different pressure stages [34]. Figure 2.14 shows a schematic of the absorption system. Two evacuated vessels are connected to each other; one of the vessels contains the liquid refrigerant and the other contains the absorbent/refrigerant solution. The solution absorbs the vapor of the refrigerant and decreases the temperature at the other tank (refrigeration effect). In the meanwhile, the solution absorbs more of the refrigerant and becomes more dilute. The whole process is called *absorption* which is exothermic as the system must reject the heat to the outdoors to keep the absorption process in action [35]. When the solution is saturated, again the system is required to separate out the refrigerant from the diluted solution. Applying thermal energy reproduces the refrigerant effect at the system. The chemical and thermodynamic characteristics of the working fluid have the most important effect on the performance of the absorption system. The mixture must not be toxic and explosive. In addition, high heat of vaporization and high concentration within the absorbent are required for the refrigerant [36, 35]. The heat exchanger inside the condenser and the absorber are connected to a cooling tower. The evaporator produces the chilled water for the building, and the generator is connected to a heat source.

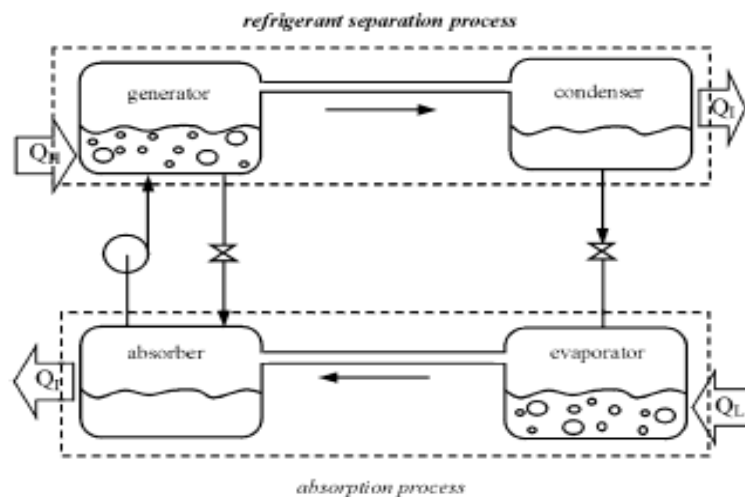


Figure 2.14 - Absorption Process [35]

The low pressure of the evaporator forces refrigerant to evaporate. When it returns to the liquid phase in the absorber, the refrigerant content of the sorbent solution increases. During the

next stage because of high pressure in the generator, the sorbent solution will boil to separate the refrigerant, at that point, the solution will be capable of sorption again. The condenser will condense the refrigerant and it goes to the evaporator. However, to achieve a continuous operation, the sorbent solution must be circulated between the absorber and the generator [34].

LiBr absorption chillers are very sensitive to leakage because of corrosion of metallic material. Also, incondensable gases cause inefficient absorption process in the absorber, which requires a hermetic or airtight design. However, to remove the incondensable gases a system purge is required to operate at least every few days [36].

Crystallisation is a common problem with absorption systems. Although absorption machines are equipped with a control mechanism to prevent crystallisation, this problem may occur because of shutting down the machine, insufficient purging, and heat input to the generator caused by a problem in the cooling tower [34].

2.3.2 Adsorption Systems

Forming a molecular or atomic film of a gas/liquid on a solid surface is called adsorption. An evaporator, condenser, and two adsorption chambers are the essential parts of each adsorption chiller. In this type of chiller, two adsorption chambers switch to the desorbing/adsorbing options. The working principle of an adsorption chiller is explained by the following two stages [37, 38].

In the first stage, as Figure 2.15 shows, hot water from a heat source passes into Chamber #1 to desorb the silica gel/zeolite. At that point, the sorbent is regenerated, and extracted water vapour from the sorbent goes to the condenser and will be condensed from a gas to the liquid phase. Condensed water will be circulated to the bottom of the machine in a closed loop for re-use. Meanwhile, water vapour from the evaporator goes into Chamber #2 and will be adsorbed by the sorbent. In order to have a continuous adsorption process, the heat must be removed and Chamber #2 requires cooling. The evaporator removes the heat from the product, which is chilled water. From the low pressure in the evaporator, the refrigerant changes to the gas phase. As Figure 2.16 shows, in second stage, two chambers will switch over in their operation mode when the sorption is saturated with water vapour to a qualified amount. At that point, the heat source is connected to the Chamber #2 and the cooling water, which comes from a cooling tower, is connected to the first Chamber [39, 40, 37].

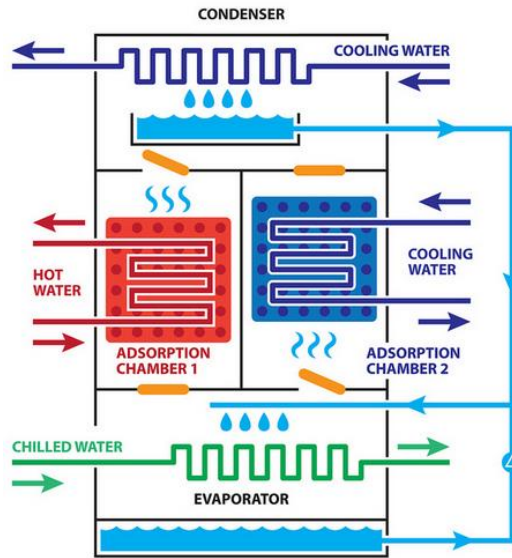


Figure 2.15 - Adsorption Process First Stage [39]

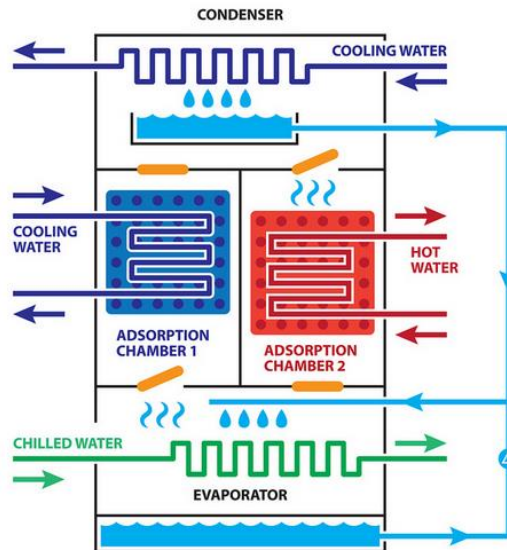


Figure 2.16 - Adsorption Process Second Stage [39]

Most of the available technologies in the market use water as a refrigerant and zeolite or silica gel as an adsorbent. Also, adsorption chillers are available in a wide range of cooling capacities from 5 kW to 500 kW. The typical coefficient of performance (COP) for the adsorption chillers is close to 0.6 when the charging temperature is 80°C. However, adsorption

chillers are able to work with the temperature down to 50°C. The produced chilled water could be as cold as 3°C. Other advantages of adsorption chillers compared to absorption systems are the use of a natural refrigerant (water or ammonia) as the working fluid, operation life times that can be as long as 30 years, maintenance and operation costs that are very lower and no crystallisation or corrosion issues [39, 40, 37].

2.3.3 Available Technologies in the Market

PolySMART, a project funded by the European Union, which consists of 32 partners, to develop a set of technical solutions for the poly-generation market, performed market research to find potential available technologies in cogeneration and heat activated cooling systems. They considered a wide range of capacities from that of a single-family user to multi-family consumers. Table 2.6 shows the summary of market available CHP capacities and Table 2.7 shows the summary of market available TDC capacities.

Table 2.6 - CHP Range of Specification [41]

Engine Type	Number of Samples	Range of Max Temperature Supply (°C)	Range of Heat Production (kW)	Range of Power Production (kW)	Total Efficiency (%) [LHV Based]
IC Engine	16	75 – 96	10 – 79	4 – 50	71 – 93
Stirling Engine	3	85	37 – 310	9 – 75	87
Micro Turbine	3	92 – 95	65 – 98	30 – 70	70 – 82

Table 2.7 - TDC Range of Specification [41]

Type	Number of Samples	Range of Charging Temperature (°C)	Range of Chilled Water Temperature (°C)	Range of COP	Cooling Capacity (kW)
Absorption	6	75 - 96	7 – 16	0.6 – 0.78	2.5 – 71
Adsorption	4	75 - 85	9 - 15	0.4 – 0.6	4.5 - 35

2.3.4 Climate-Well

A Swedish company, ClimateWell AB, has invented a highly efficient heat activated cooling system which has been tested for large buildings and offices powered by solar energy (solar evacuated tubes) as its heat source. Due to a lack of solar potential and also the relatively inexpensive price of natural gas in Canada, there is an interest from both ClimateWell and a North American natural gas distributor, Union Gas Ltd, to test and evaluate the feasibility of this cooling system in Canada as a part of tri-generation. A potential option of heat production to charge the cooling system is a Stirling engine. Preliminary analysis showed that integrating the Stirling engine and ClimateWell may turn out to a feasible, cost effective, and environmentally friendly micro Tri-generation system.

The ClimateWell chiller is a Thermo Chemical Accumulator (TCA) system. The unit works in liquid, vapor, and solid phases. It is believed that this system would be as efficient as a traditional absorption system [42].

The ClimateWell chiller is able to store heating energy and produce cooling in a highly efficient manner. The chiller operates in three different modes; charging, heating, and cooling. During the charging process Lithium Chloride salt dries, which means energy stored in the unit and as a result that energy can be used when there is a demand [43]. Both the charging and

discharging cycles require heat rejection. Table 2.8 illustrates the Climate-Well technical specifications.

The most significant difference between the ClimateWell TCA and conventional absorption/adsorption technology is the three phase process, which include solid, vapour, and solution phases. The traditional absorption/adsorption process occurs between two phases only. It is either solution and vapour or solid and vapour. ClimateWell uses LiCl-H₂O as the working fluid. The chiller contains two barrels (see Figure 2.19). Having two barrels allow the unit to charge one barrel and discharge the other at the same time. Each barrel is a vacuumed and closed system, which includes four parts as follow: condenser/evaporator, reactor (absorber), solution store, and water store. The charging process occurs in the desorption phase while discharging is an absorption phase [43, 44].

Table 2.8 - Climate-Well Technical Specifications [43]

Heat Source Circuit	Flow		25-30 L/min
	Typical Power Range		15-20 kW
	Operation Temperature	In	85°C -110°C
		Out	75°C -100°C
Distribution Circuit	Flow		25-30 L/min
	Operation Temperature	In	15°C -21°C
		Out	10°C -16°C
	Heat Rejection Circuit	Flow	
Typical Power Range		20-30 kW	
Operation Temperature		In	30°C -45°C
		Out	<30°C
Energy for Charging of One Cycle	57 kW per barrel		
Energy Storage Capacity for Cooling	56 kWh (28 kWh per barrel)		

2.3.4.1 Charging Process

During the charging process, the heat exchanger inside the condenser is connected to the heat rejection circuit and the heat exchanger inside the reactor is coupled to the heat source circuit as shown in Figure 2.17. In this TCA unit, the LiCl solution is pumped and sprayed over the heat exchanger in the reactor to increase the heat transfer area. Because of the heat provided by the heat source, the solution reaches the saturation point during the desorption process. Because the heat exchanger allows a continuous desorption process, solid crystals will eventually form. At that point, water is evaporated. Water vapor enters the condenser where it is condensed into the liquid phase. Since the condenser is connected to a heat sink, it removes the heat from the water vapor. The condensed liquid water enters into the water store. The solid crystals formed during the desorption process will fall to the vessel due to gravity. A sieve will prevent them from falling into the solution store. This process results in a slurry formation at the bottom of the vessel [44].

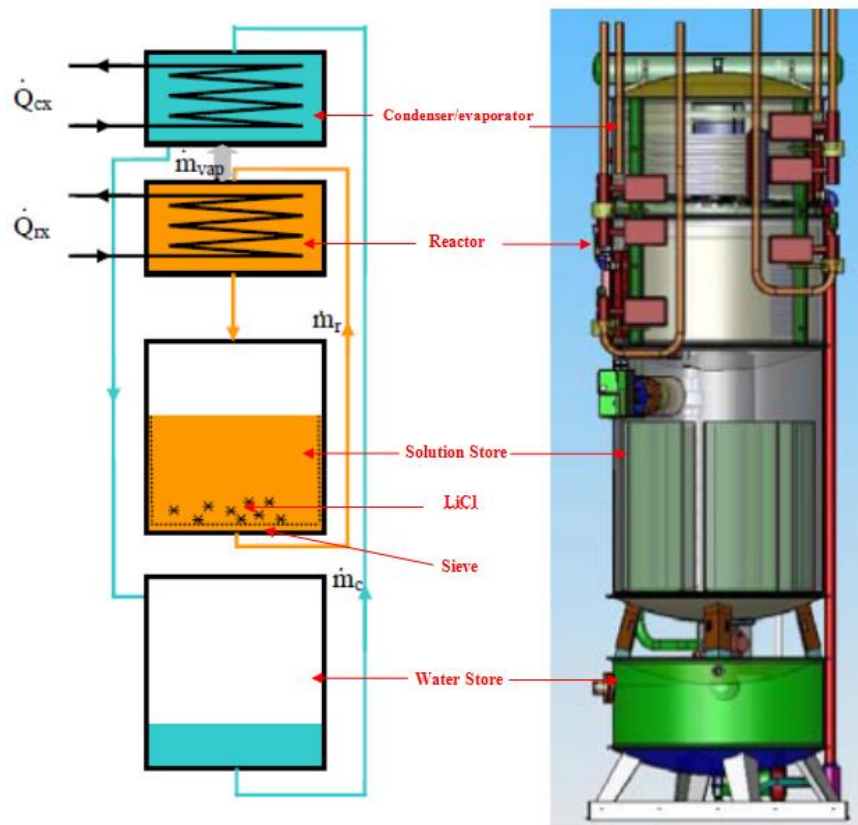


Figure 2.17 - Schematic of a single Barrel of ClimateWell [44, 45]

2.3.4.2 Discharging Process

During the discharging process, the heat exchanger inside the evaporator is connected to the chilled water supply circuit, which goes to the air handling unit of the building. At that point, heat exchanger inside the reactor is connected to the heat rejection circuit by switching the valves. Discharging process is reversed. In this process, saturated solution from both the water store and the solution store is pumped over the heat exchanger in the evaporator. The evaporator acquires the heat from the building and produces vapour. Water vapor enters to the reactor where it is absorbed by the saturated LiCl slurry. Saturated solution can absorb vapour and become unsaturated. It then falls to the solution store and by dissolving the solid crystals, it becomes saturated again. This saturated LiCl is then pumped to the absorber again and thus the absorption process continues until all the solution is unsaturated. The heat of condensation and binding energy release is transferred to the environment. By the end of the absorption process, the solution store is filled with unsaturated LiCl solution and the water store is emptied [44, 45].

This machine is able to restrict the charging process to two phases to prevent unwanted crystal formation in the pipes. However, during the cooling down of the solution crystals will form. The discharging process occurs after all crystals have been dissolved, therefore the discharging process starts with three phases and eventually will continue into the two phase regime. Since the ClimateWell machine runs both units simultaneously, while one of the units is being charged the other can be discharged. Then the units will switch the operation mode and it takes at least 10 minutes to supply chilled water again [44, 45].

Figure 2.18 shows the temperature of the reactor and condenser/evaporator of a barrel for both charging and discharging processes. The blue line indicates the temperature of the reactor and the red line indicates the temperature of condenser/evaporator. As Figure 2.18 illustrates that the temperature of the reactor increases by the heat source during the charging and condenser's temperature is constant since it is connected to the heat sink. Also Figure 2.18 shows the discharge process temperatures as well, when the reactor is connected to the heat sink and the temperature at evaporator is very low and it is connected to the AC line.

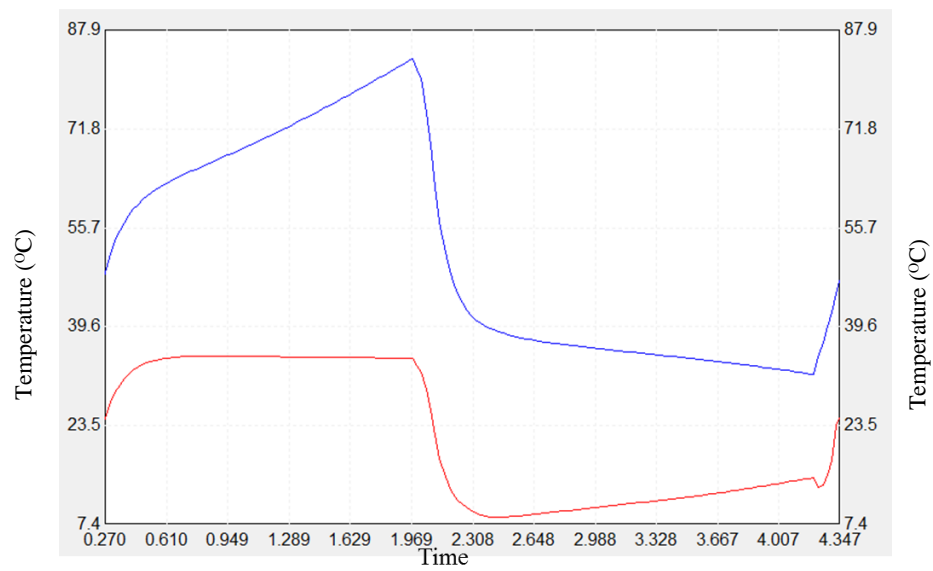


Figure 2.18 - Temperature of the Reactor and the Condenser of a Barrel During Charging and Discharging

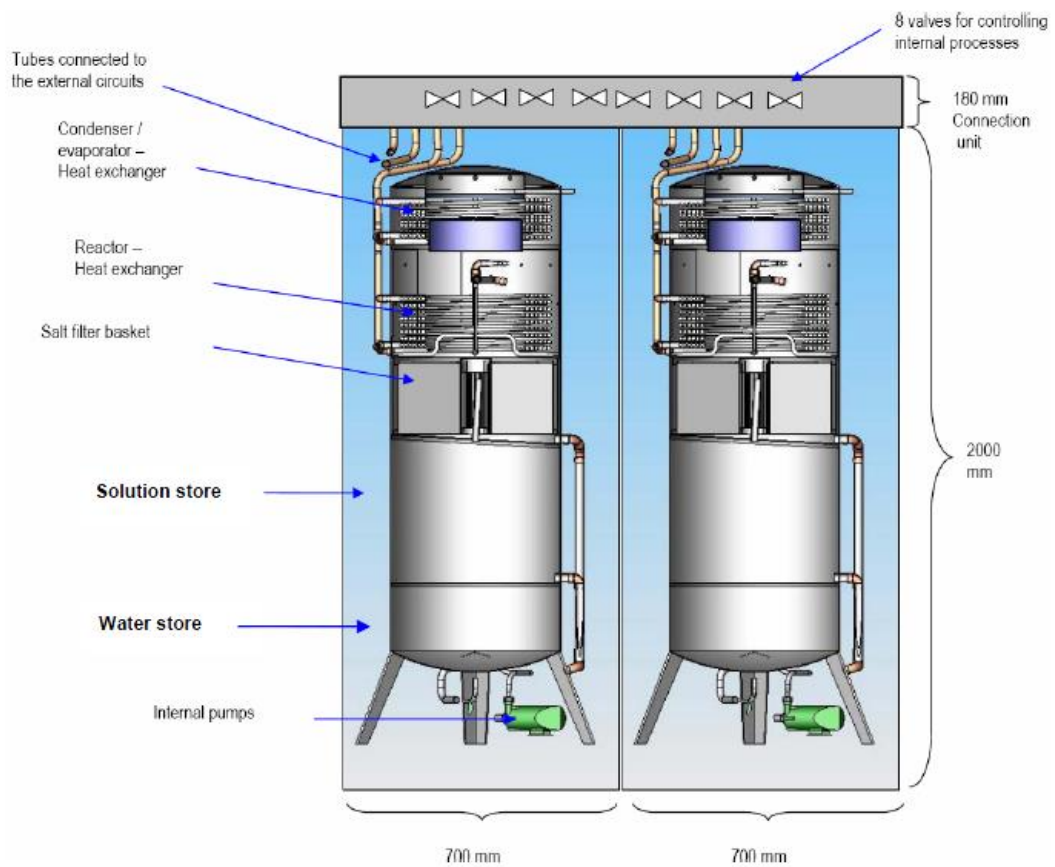


Figure 2.19 - ClimateWell Machine [44]

Chapter 3 - TRCA House

In Ontario, the Toronto and Region Conservation Authority (TRCA) works to promote sustainable technologies for buildings. TRCA along with the Building Industry and Land Development (BILD) Association have implemented the “Archetype Sustainable House” (ASH) project at the Living City Campus at the Kortright Center in Vaughan (north of Toronto), Ontario, Canada. A national design competition in 2006 resulted in the current design of the archetype house. The Archetype Sustainable House is designed to demonstrate practical sustainable energy technologies in near and medium terms through research, demonstration, education, training, market transformation and many partnership programs [46, 47].

The Archetype House consists of two fully-instrumented semi-detached houses, which establish the next generation of green homes. The first house is called House A and demonstrates currently available technologies, while the second house is called House B and uses the most advanced and innovative technologies that will be used in the near future [9]. These two houses are the first housing project in Canada that achieved a Platinum LEED certification [48]. In addition, the houses are also certified by the Energy Stars® and R2000 programs [47].

House A and B are shown in Figure 3.20. The House A is on the right side in Figure 3.20 and the House B can be seen on the left side. Also Figure 3.21 shows the front view of the houses. There is an in-law suit attached to the House B.

House B is designed to test and put into practice new technologies, and is equipped with a very accurate data collection system along with House A. The operating systems of the house are capable of being programmed to simulate real life occupancy conditions. Therefore, House B was selected as the field test site for the tri-generation project. After a series of preliminary tests and feasibility analysis, the system was designed and installed in House B for the experimental work.



Figure 3.20 - Rear View of TRCA Houses – North Side [47]



Figure 3.21 - Front View of TRCA Houses – South Side

3.1 “House A & B” Descriptions

In general, House A and House B are similar but there are differences in details such as window types, floor areas, house volumes, and mechanical systems. There is an in-law suite

attached to House B, with 32 m² of floor area. It is a separate living room above the garage. It is interconnected with House-B via a wooden platform [49].

Basement walls for both houses are made of RSI² 3.54 (R³20) Durisol blocks. Most of the other walls use RSI 5.31 (R30) and also include other insulation materials. In House A, three inches of a fire resistant Roxul Batt Fiber insulation, for a total of R30 is applied [47]. In House B, two different types of spray foam are used: the Heat-Lock Soya Polyurethane Foam and the Icynene spray foam. Using sprayed foam minimizes air leakage. House B is equipped with triple glazed low E (emissivity) argon filled windows while a double paned low E fiberglass framed windows are installed at House A. An RSI 7 (R40) panel using Styrofoam is installed for the roof in both houses [10, 50]. Details on the structural features are summarized in Table 3.9.

Table 3.9- Structural Features of the Twin Houses [9]

Features	House-A	House-B
Basement walls	RSI 3.54 (R20) with Durisol blocks	RSI 3.54 (R20) with Durisol blocks
Wall insulation	Roxul Batt Fibre (R21) + 3" Styrofoam	Heat-Lock Soya Polyurethane Foam / Icynene spray foam
Walls (including insulation)	RSI 5.31 (R30)	RSI 5.31 (R30)
Windows	2.19 W/m ² ·K (0.39 Btu/ft ² ·°F) and double paned, low "E", fiberglass framed	1.59 W/m ² ·K (0.28 Btu/ft ² ·°F) and all triple glazed, low "E", with argon filled
Roof	RSI 7 (R40) Structurally Insulated Panels (SIPs), which are insulated Styrofoam panels	RSI 7 (R40) Structurally Insulated Panels (SIPs), which are insulated Styrofoam panels

² RSI is the standard metric form of the thermal resistance for construction material. The number in front of the RSI is the value of the thermal resistance or the thermal insulance of the material with units of (m²·K)/W

³ R value is the imperial equivalent of the RSI (1 h·ft²·°F/Btu = 0.176110 K·m²/W or 1 K·m²/W = 5.678263 h·ft²·°F/Btu

3.2 Mechanical Systems

3.2.1 House A

Since the focus of this project is on House B, this study will not go through the details of mechanical systems in House A. A brief explanation of the systems is given. A flat plate solar collector along with a wall mounted mini boiler is used to supply the hot water. For cooling and heating purposes, a two-stage air source heat pump is connected to the air handling unit (AHU) to supply the conditioned air to the house. Also the house is equipped with a heat recovery ventilator (HRV) [49].

3.2.2 House B

House B is equipped with more advance technologies compared to House A. Since the purpose of this house is to test and experimentally investigate energy efficiencies, different redundant HVAC systems are installed in parallel. This section describes most of the equipment in House B prior to installation of the tri-generation project items. For domestic hot water production two tanks were installed in series. The first tank is a pre-heat tank, which is heated partially by a solar collector through the tank's upper coil. The second tank is a time of use (TOU) tank, which is electric powered and has electrical element to maintain the water heated to 60°C. The lower coil of the first tank could be connected alternatively to either the ground source heat pump (GSHP) installed at the house, or the Stirling engine cogeneration system. As a result, the domestic hot water can be heated by four different systems; the solar collector, GSHP, Stirling engine cogeneration unit, and electricity [49].

The house can be heated either through the in-floor radiant system for all three storeys and basement or the multi zone air handling unit, which circulates the warm air into the different zones of the house. The multi zone air handling unit is able to supply the air for all or any specific zone without any effect on the other zones. Therefore, this system helps the building to save the energy and only heats up or cools down the zones as required [49].

The required hot water for the in-floor system and the air handling unit can be produced by either the GSHP or the Stirling engine cogeneration system. The Stirling engine burns natural gas. The GSHP uses two horizontal loops. It also supplies chilled water to the air handling unit

during the cooling season. For both cooling and heating purposes, a buffer tank is used to store the chilled/hot water to prevent or minimize the short cycling of the GSHP or the Stirling engine. The house is also equipped with an energy recovery ventilator (ERV). In addition, a grey water heat exchanger for heat recovery and a 10 m³ underground cistern, which collects the rain water for toilet flushing and gardening, are included at the house [46, 49]. A detail specification and energy performance of the Stirling engine cogeneration system have been reported in Chapter 2, Section 2.1.5. Detail specification of the equipment and the manufacturer/distributor is shown in Table 3.10.

Table 3.10 - Detail Specifications of Equipment, and Manufacturer/Distributor [46]

Equipment	Technical Information	Manufacturer/Distributor
Evacuated tube solar collector	Gross Area: 2.88 m ² (31 ft ²), Absorber area: 2.05 m ² (22 ft ²)	VISSMANN Manufacturing Company
Solar hot water tank	Capacity: 300 Litres (79 USG)	VISSMANN Manufacturing Company
Auxiliary hot water tank	Capacity: 175 Litres (50 USG), Maximum heating capacity: 6 kW (20 MBH)	GSW Water Heating
Buffer tank	270 litres (71 USG)	GSW Water Heating
Ground source heat pump (GSHP)	a) Heating capacity at 0°C (32°F) Entering Water Temperature (EWT) and 1.04 Litres/sec (16.5 GPM) water flow rate, COP: 3.0 (13.3 kW) b) Cooling capacity at 25°C (77°F) Entering Water Temperature (EWT) and 1.04 Litres/sec (16.5 GPM) water flow rate, COP: 2.86 (12.66 kW), EER: 12.86 c) Length of horizontal loop: 152.39m (1000'), Number of loop: 2, Depth of ground level: 1.83m (6')	WaterFurnace International, Inc.
Air handling unit (AHU)	a) Maximum heating capacity at 82°C (180°F) Entering Water Temperature (EWT): 28 kW (95 MBH) b) Cooling capacity: 5.27 to 12.3 kW (1.5 to 3.5 tons) c) Nominal air flow rate: 660 Litres/sec (1400 CFM)	Ecologix Heating Technologies Inc.
Energy recovery ventilator (ERV)	a) Heating capacity at -15°C (5°F) supply air temperature Sensible recovery efficiency: 55% , Latent recovery moisture transfer: 0.26, Net air flow rate: 52 Litre/sec (110 CFM) b) Cooling capacity at 35°C (95°F) supply air temperature Total recovery efficiency: 41%, Net air flow rate: 50 Litres/sec (106 CFM)	Venmar Ventilation Inc.
Drain water heat exchanger	Length: 91.44 cm (36"), diameter: 7.62 cm (3")	RenewABILITY Energy Inc.
Micro CHP system	Electrical power: 1 kW (3.4 MBH), Thermal energy: 12.0 kW (40.98 MBH)	Whispergen Limited

Chapter 4 - Methodology

In this chapter a detailed description of the tri-generation system is discussed. The details of the design procedure along with all sensors and meters, which were added to the house to monitor the new integrated system, are explained. The monitoring system's structure and the data collection system are described. Moreover, specification of the working fluid inside the system is defined. Also, the methods of the energy, consumption, and generation efficiency calculation were analyzed.

The methodology that is used in this study is a combination of data analysis and computer simulation. The real time data set is recorded from the tests of different mechanical systems via a data acquisition system. The test series have been performed during different times of the year under different conditions such as various outdoor temperatures and different cooling and heating demands.

The methodology can be summarized in the following points:

- Collected data is used to evaluate the performance of individual mechanical equipment, using energy and efficiency equations and any other indices depending on the type of studied equipment and available data.
- The outcome of the pervious analysis is compared with results from the literature and manufacturer performance data. Differences are investigated to explore all possible reasons for deviations of expected performance, which may include: improper installation, controls, operation outside of manufacturer specification ranges, or any other mechanical shortcomings of the studied equipment or the system of equipment.
- The studied mechanical equipment is simulated in TRNSYS 17 using the provided model by ClimateWell, adjusted model of the CHP, and current built-in commercial TRNSYS types for the heat rejection circuit. Simulation parameters for the equipment are derived from the experimental data analysis and from the manufacturers' data sheets.

- Based on results from the previous steps, the models are fine-tuned, using the various calibration tools available in TRNSYS 17, to meet the actual expected experimental observations.
- The finalized model is applied to different cities in Canada to estimate the cost and energy efficiency of the system under different climatic conditions.

4.1 Description of the Tri-generation Project

The TRCA houses are equipped with over 300 sensors of different kinds such as; flow meter, Wattnode, RTD probe, matched delta T, air temperature, relative humidity, and pressure sensors. All of these sensors are recalibrated on a regular basis.

As mentioned in Chapter 2, the WhisperGen Stirling engine was in service at the TRCA house since 2009. Prior to design and installation of the tri-generation project, the Stirling engine was tested to supply hot water either to the domestic hot water tank or to the buffer tank for space heating purposes under different conditions. The feasibility analysis based on the results of these series of tests, showed that the Stirling engine with minor adjustment could be a suitable option to be integrated with the ClimateWell chiller.

The ClimateWell unit is a thermo chemical accumulator, which is required to reject heat during both charging and discharging processes in order to perform effectively. Therefore, three essential circuits must work at the same time to run the chiller. The first circuit, as it is shown in Figure 4.22, is for charging the chiller, which connects the hot water supply and Stirling engine, to the ClimateWell unit. It is a closed loop circuit and the hot water returns to the cogeneration unit after passing through a heat exchanger inside the chiller. The second circuit, which is also shown in Figure 4.22, is needed to connect the chiller to an air handling unit (AHU). This circuit is also a closed loop, which supplies chilled water from the ClimateWell unit to the air handling unit. The AHU has two coils in series and chilled water returns to the chiller after traversing both coils. Since the chiller is required to reject the heat, third circuit is the heat rejection loop. There are two options to reject the heat: either rejecting the heat to the environment or recovering the waste heat as much as possible. Since that waste heat could be used to warm up the domestic hot

water, a complex circuit was designed to recover the waste heat, which is shown in Figure 4.23. In this circuit, hot water goes through three cascade tanks using five different coils to recover the heat to preheat the city water for domestic use. After passing through the three tanks, if the water temperature is still high, it passes through an outdoor fan coil as well, since the return temperature to the chiller has to be lower than 25°C. During this process the hot water cools down and returns to the ClimateWell unit. Figure 4.22 shows the general schematic of the tri-generation system. All three circuits including three heat recovery tanks and the outdoor fan coil are shown in Figure 4.22.

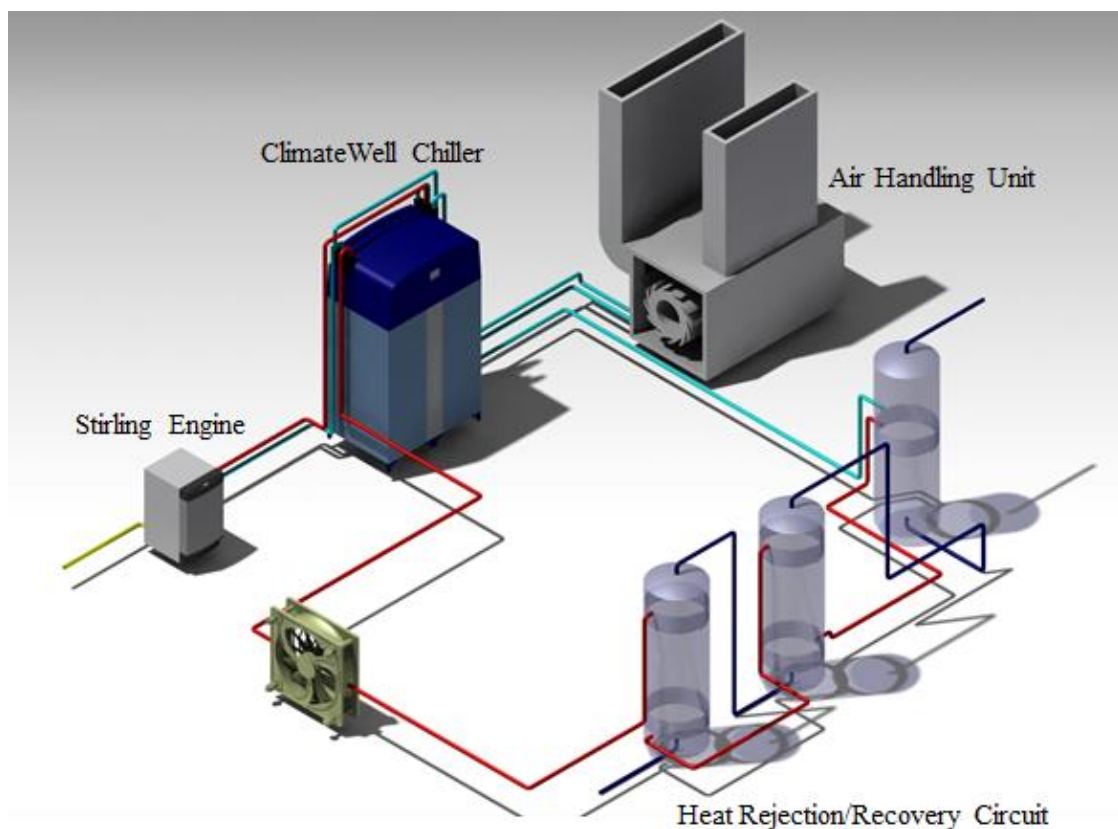


Figure 4.22 - General Schematics of Tri-generation System

Although Figure 4.22 shows the overall schematic of the integrated system, more details of sensors, piping, pumps and others is shown in Figure 4.23. Each of the three circuits requires a pump and an expansion tank. Moreover, in order to record data, additional temperature sensors and flow meters were needed, which were installed and described in Section 4.4.

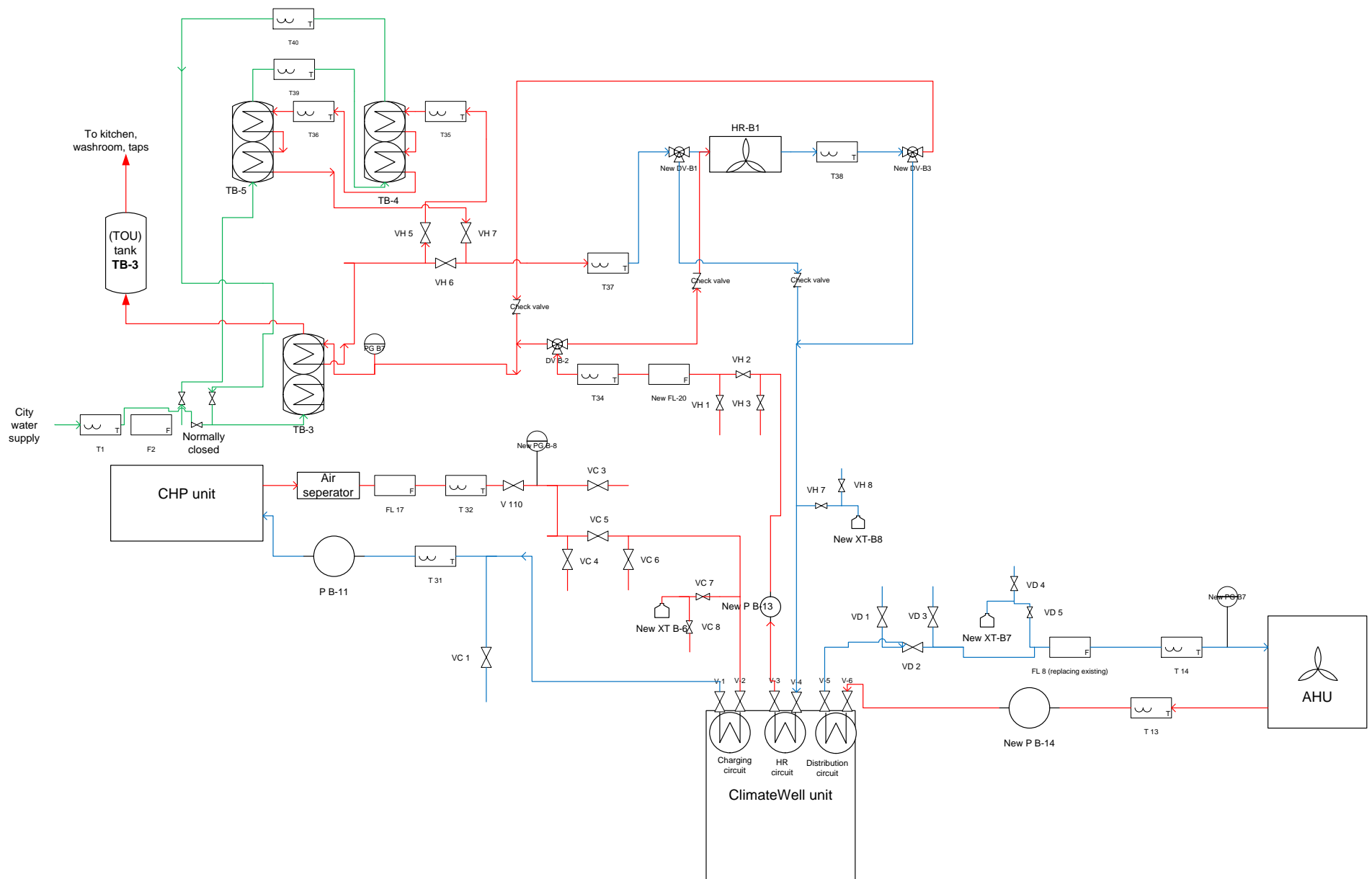


Figure 4.23 - Detail Schematic of the Tri-generation System

4.2 Monitoring System

The long term monitoring system at the Archetype Houses was developed, installed, and employed by former graduate students. An accurate data acquisition system capable of recording data from over 300 sensors in 5 second intervals was already implemented. In order to test and analyze the performance of the tri-generation system many of the existing sensors (such as outdoor temperature sensors, city water temperature sensors, temperature and flow rate sensors of the inlet and outlet of the air handling unit, natural gas meter, exhaust temperature sensor, etc.) were used [49, 51].

4.2.1 DAQ System

In order to monitor and record all relevant data for the newly integrated system, a number of additional temperature sensors, flow meters, and watt-nodes were installed. Temperature sensors of the supply and return loop in the heat rejection circuit, along with many temperature sensors for different heat rejection configurations are some of the newly added and installed sensors. The output signals for all of these sensors are in milliamps and these signals are converted to the temperature or the flow rate units by LabVIEW software [46]. Previous graduate students employed the LabVIEW Development Suite 8.6 [9] to develop the real-time monitoring system. The LabVIEW software, as it is shown in Figure 4.24, provides all of the live data readings in its graphical front panel. Therefore, in order to observe the sensors' readings of any instrument, the front panel shows all of those data without probing the Channel ID. Figure 4.24 shows a window for the cogeneration system and its sensors, while similar windows for each of AHU, ERV, solar collectors, GSHP, radiant in-floor heating, and DHW are available [10].

In general, all of the raw signals sent from the sensors are converted and post-processed at the background of the front panel to the engineering units, applying the offset of calibration values. All data are stored in a Microsoft SQL server database. A Channel ID and Module are assigned for each sensor [9].

The addresses and IDs of all the newly installed and existing sensors are listed in Appendix A. The Channel ID and Module number are needed to extract the secondly, minutely, and hourly data for each sensor in the different time intervals from the SQL software.

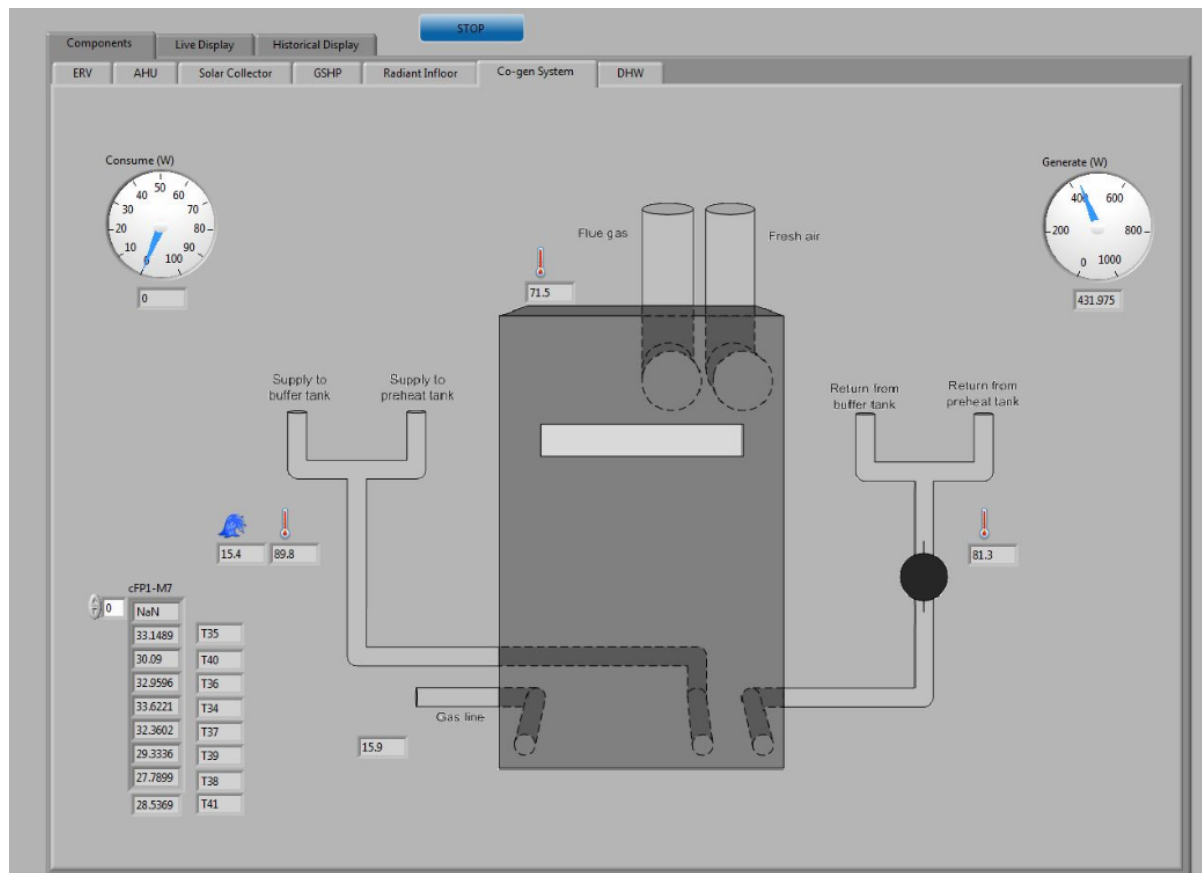


Figure 4.24 - Front Panel of LabVIEW Program at TRCA

4.2.2 ClimateWell Database

The ClimateWell chiller is able to be set for a specific delivery temperature. The unit can switch between charging and discharging modes alternately. The ClimateWell chiller is equipped with temperature sensors for the inlet and outlet of both the reactor and condenser in each barrel and also a flow meter for the air conditioning circuit. There is a control system panel inside the unit, which automatically saves all of the readings into its database using a log interval of 10 seconds. The memory of this database is able to keep the data for 30 days [52].

Although the ClimateWell chiller saves all the data to its database, the data is not accessible on a real time monitoring basis. Therefore, during the ClimateWell installation process at the TRCA house, temperature sensors and flow meters that required were considered and connected to the DAQ system. Moreover, the ClimateWell sensors were also connected to the spare channels of the DAQ system as a backup measure.

4.2.3 Sensor Calibration

The calibration process finds systematic bias and corrects the raw values which are read by the sensors [9]. Since one of the goals of this project was to achieve accurate monitoring and data recording of the tri-generation system, calibration was critical to ensure the correctness of the sensors. Sensors were calibrated with an off-line technique, which compared data read from the sensor with a high-quality calibrator and indicates the differences [49].

4.2.3.1 Temperature Sensors

In addition to many existing temperature sensors at the TRCA houses, seven new resistance temperature detector (RTD) Pt-500 probes were installed. This type of temperature sensor must be fitted in a sensor pocket and cannot be installed directly in the flow. There is a platinum electric resistor inside the sensor, which changes the voltage with the temperature. Measuring the resistance value gives an analog indication of the temperature. [53]

To calibrate the RTD probes, Hart Scientific 9102S handheld dry-wells and MICROCAL 20DPC calibrators were used. These handheld calibrators use metal blocks, which have a well drilled into it to insert the RTD sensor and accurately calibrate them [54]. This calibrator device was used to determine the offset for both the existing and new temperature sensors from the set point of 5°C to 95°C with 15°C intervals.

4.2.3.2 Water Flow Meters

A rotary Proteus 800 series flow meter was installed for each of the circuits. This type of flow meter measures and monitors liquid flow from 0.2 to 225 L/min with the accuracy of $\pm 2\%$. The sensor is equipped with a three-color LED light. A trip point has to be set. When the flow rate is 15% higher than the trip point the light is green, within 15% difference by trip point the light is amber, and the red light indicates a flow rate lower than the trip point [55].

In order to calibrate flow meters, the guideline of the National Institute of Standards and Technology (NIST) was employed [56]. A known amount of water in a closed loop after passing through the sensor was collected in a bucket with known volume within a defined time period. These data were compared with the SQL server database and the offset was calculated.

4.3 Working Fluid and Its Properties

Density of water varies from 999.82 kg/m^3 to 950.05 kg/m^3 with the temperature change from 4 to 100°C , while the specific heat (C_p) of water does not vary significantly and its range is from $4.178 \frac{\text{kJ}}{\text{kg.K}}$ to $4.219 \frac{\text{kJ}}{\text{kg.K}}$ for the same temperature range [57]. A water–Propylene Glycol (PG) solution (55:45) was suggested as a working fluid by ClimateWell. After the installation and filling the water loops, the percentage of the PG-water solution was experimentally tested and resulted in 35% water-PG solution which has a -18°C freezing point. The density of the water-PG solution varies inversely with temperature. On the other hand, the specific heat of water-PG solution increases with temperature rise. Since both the density and the specific heat play direct roles in the energy calculations, the maximum possible error was calculated and studied. The difference in density and specific heat for 30%, 35%, and 40% PG-water solutions are shown in Appendix B. The density of the 35% water-PG mixture varies between 1053.5 kg/m^3 and 992.3 kg/m^3 and the specific heat from $3.628 \frac{\text{kJ}}{\text{kg.K}}$ to $3.956 \frac{\text{kJ}}{\text{kg.K}}$ [58].

There are three circuits in the tri-generation project, which work in different temperature ranges. The temperature in the charging circuit is from 80°C to 100°C while it is between 5°C and 20°C in the discharging circuit, and 20°C to 45°C in the heat rejection circuit. The error of considering constant density and specific heat in each of those circuits for the energy equations was estimated. The maximum error in each time step was $\pm 3.7\%$, but the maximum error during each process/cycle or time interval was $0.7\%^4$, which is negligible. A sample of error consideration is also provided in Appendix B. Therefore, an average value of the density and specific heat for each of the circuits were considered and it can be found in Table 4.11. Although constant values were considered for these circuits and calculations, a specific constant value was used for each of the circuits and corresponding temperature ranges, which significantly decreased the error in the calculation.

⁴ Since during each cycle the positive and negative errors cancel out each other, the final/cumulative values correspond to a smaller error.

Table 4.11 - Constant Density & Specific Heat Values of Water-PG 35% Solution

Water-PG solution 35%	Discharge Circuit (5-20°C)	Heat Rejection Circuit (20-45°C)	Charge Circuit (80-100°C)
Density (kg/m ³)	1049.42	1038.78	1000.41
Specific Heat ($\frac{kJ}{kg.K}$)	3.65	3.71	3.90

4.4 Energy Consumption, Generation and Efficiency Equations of Equipment

The equations regarding to the energy consumption/generation and also thermal/electrical efficiencies of the Stirling engine and ClimateWell are discussed in this section. In addition, sensors locations and matching addresses for the LabVIEW program are included in the equations.

4.4.1 WhisperGen Stirling Engine-Micro Combined Heat and Power (CHP) Unit

In studying the cogeneration system, special attention was paid to the electrical and thermal energy generation, and the performance of the system as determined by its electrical, thermal and total efficiency. Electrical efficiency is defined as net electrical energy produced divided by the input energy given by the higher heating value (HHV) of the natural gas. Thermal efficiency is defined as generated thermal energy divided by input energy given by the HHV of the natural gas. Accordingly, in Chapter 5, results are presented on an hourly and daily basis, which gives a broad overall view of performance. Figure 4.25 demonstrates the sensors location/LabVIEW addresses and output/input of the Stirling engine. As it is shown in Figure 4.25, temperature sensor in the supply line is T32 and for return it is T31. The flow meter for this circuit is FL17⁵ and also the gas meter is called NG2.

1. Thermal energy generation by Stirling engine:

$$\dot{Q} = (\rho\dot{v})_{\text{supply}}c_p(T_{\text{supply}} - T_{\text{return}}) = \rho \times \text{FL17} \times c_p \times (T32 - T31) \quad (\text{Eq-4.1})$$

Where c_p and ρ values can be found in Table 4.11.

⁵ All the “FL” readings from the SQL are in L/min . They must be converted to m^3/s by: $FL \times \left(\frac{0.001m^3}{L}\right) \times \left(\frac{min}{60s}\right)$

2. Thermal Efficiency:

$$\eta_{thermal} = \frac{Net\ E_{generation}}{E_{gas}} = \frac{(\rho\dot{v})_{supply}c_p(T_{supply} - T_{return})}{\dot{v}_{gas} * HHV} \times 100$$

$$= \frac{Thermal\ Energy\ Generation\ (kWh)}{Fuel\ Energy\ Consumption\ (kWh)} \times 100 \quad (Eq-4.2)$$

3. Electrical Efficiency:

$$\eta_{electrical} = \frac{E_{generation}}{E_{gas}} \times 100 = \frac{Electrical\ Output\ (kWh)}{Fuel\ Input\ (kWh)} \times 100 \quad (Eq-4.3)$$

4. Overall Efficiency:

$$\eta_{overall} = \frac{[Electrical\ output\ (kWh) + Thermal\ output\ (kWh)]}{Fuel\ input\ (kWh)} \times 100 \quad (Eq-4.4)$$

Where η is the efficiency of the engine and E is the energy (kJ). All temperature readings from the sensors are in °C. Densities of the working fluid, ρ , in the formulas are in kg/m³. \dot{v} is the volumetric flow rate and its unit is m³/s. The unit of higher heating value (HHV) is kJ/L and c_p is the specific heat with the unit of kJ/kg. K.

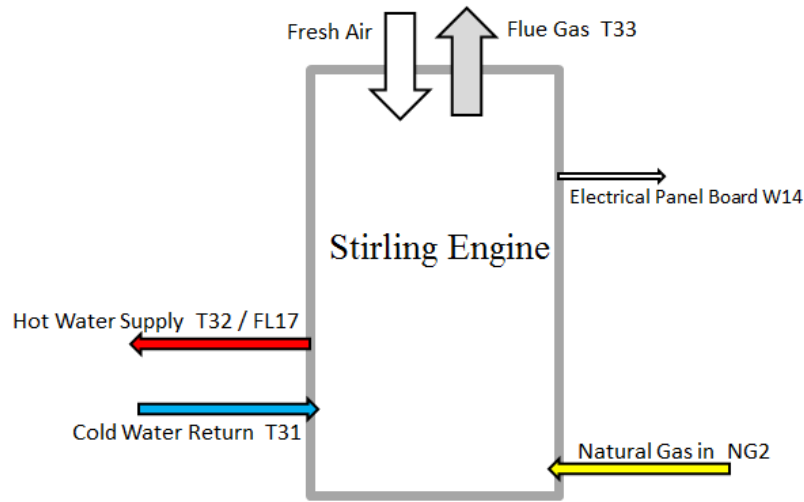


Figure 4.25 - Micro CHP Unit - Sensor Locations

4.4.2 ClimateWell Chiller

The tri-generation project at the TRCA house does not study the chemical reactions inside the ClimateWell chiller unit, but rather the intention of this research is to study absorbed, rejected, and

produced energy by the chiller and how proper integration of the unit into existing house with a cogeneration unit is achieved. Therefore, all three circuits that are connected to the chiller are equipped with temperature sensors and flow meters. Temperature differences were measured. Energy differences were calculated, using recorded flow rates and temperature differences. Figure 4.26 demonstrates the sensors location/LabVIEW addresses and output/input of the ClimateWell chiller. As it is shown in Figure 4.26, all three circuits are connected to the chiller. The temperature sensors in the charging loop, which is connected to the CHP unit along with temperature sensors in heat rejection loop and AC loop are shown in Figure 4.26. Also Flow meters Channel IDs are provided. Calculation of the coefficient of performance (COP) of the unit was carried out by the following equations:

1. Thermal energy absorbed by ClimateWell:

$$\dot{Q}_{Abs} = (\rho\dot{v})_{supply}c_p(T_{supply} - T_{return}) = \rho \times FL17 \times c_p \times (T32 - T31) \quad (Eq-4.5)$$

2. Thermal energy rejected to the heat sink:

$$\dot{Q}_{Rej} = (\rho\dot{v})_{out}c_p(T_{out} - T_{in}) = \rho \times FL20 \times c_p \times (T34 \text{ or } T37 - T41) \quad (Eq-4.6)$$

The heat rejection circuit has multiple configurations, therefore:

- If the working fluid in the heat rejection circuit, first passes through the three tanks and then the outdoor fan-coil; use T34 sensor in Equation 4.6
- If the working fluid in the heat rejection circuit, first passes through the outdoor fan-coil and then three tanks; use T37 sensor in Equation 4.6

3. Cooling production by the ClimateWell:

$$\dot{Q}_P = (\rho\dot{v})_{supply \text{ to AHU}}c_p(T_{return \text{ from AHU}} - T_{supply \text{ to AHU}}) = \rho \times FL8 \times c_p \times (T14 - T13) \quad (Eq-4.7)$$

4. COP of the ClimateWell Chiller:

$$COP = \frac{Q_P}{Q_{Abs}} = \frac{\rho \times FL8 \times c_p \times (T14 - T13)}{\rho \times FL17 \times c_p \times (T32 - T31)} \quad (Eq-4.8)$$

Since the working fluid is the same in both circuits, the c_p and ρ are canceled and the equation is as follows:
$$\text{COP} = \frac{\text{FL8} \times (T14 - T13)}{\text{FL17} \times (T32 - T31)}$$

(Eq-4.9)

Where the c_p and ρ values can be found in Table 4.11

Figure 4.26 demonstrates sensor locations.

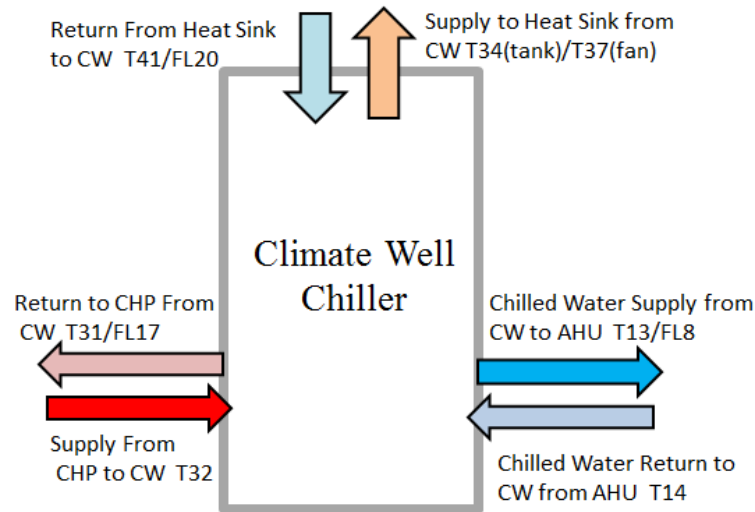


Figure 4.26 - ClimateWell Unit - Sensor Locations

All the Channel/Module addresses and ID's for the temperature sensors (T)'s and (FL⁶)'s are provided in the sensor list in Appendix A.

4.4.3 Heat Rejection System

The ClimateWell chiller requires a heat rejection system. In order to reject sufficient heat and also recover the waste heat for domestic use, a complex circuit including three tanks and a fan were installed. For the heat recovery/rejection system all of the tanks and the fan are considered as one system, which has two different aspects; the rejected energy, and the recovered energy for the house. Also the energy rejected by each tank or the fan can be estimated based on measured temperatures and flow rates. Figure 4.27 demonstrates the heat rejection system along with its sensors. Other

⁶ All the "FL" readings from the SQL are in $/min$. They must be converted to m^3/s by: $FL \times \left(\frac{0.001m^3}{L}\right) \times \left(\frac{min}{60s}\right)$

sensors which are located between tanks are not shown in Figure 4.27 and a list of them is available in Appendix A.

1. Thermal energy rejected by the heat rejection system:

$$\dot{Q}_{Rej} = (\rho\dot{v})_{out}c_p(T_{out} - T_{in}) = \rho \times FL20 \times c_p \times (T34 \text{ or } T37 - T41) \quad (\text{Eq-4.10})$$

2. Thermal energy recovered for the domestic hot water use through the heat recovery system:

$$\dot{Q}_{Recovered} = (\rho\dot{v})_{citywater}c_p(T_{out} - T_{in}) = \rho \times FL2 \times c_p \times (T23 - T1) \quad (\text{Eq-4.11})$$

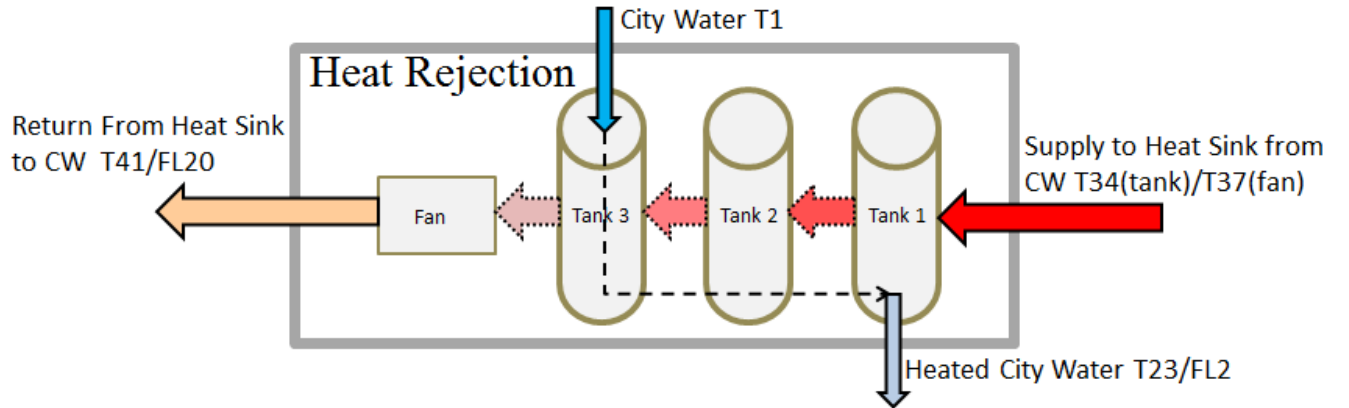


Figure 4.27 - Heat Rejection/Recovery System - Sensors Locations

4.4.3 WhisperGen Stirling Engine Model in TRNSYS 17

In order to simulate the overall tri-generation system, TRNSYS 17 software was employed. The chiller type and model in TRNSYS 17 were provided by the ClimateWell Company. The heat rejection circuit was modeled using available standard types of tanks and a fan coil module in TRNSYS. The cogeneration type in TRNSYS needed to be generated. A Fortran skeletal model of an auxiliary burner, which is called Type 6 in TRNSYS library, was employed and modified based on the real experimental correlations and was renamed Type 222. In order to do so, multiple working

cycles were considered. The best fit of the thermal generation for a normal cycle was chosen. A normal cycle of the Stirling engine heats up the water to the higher set point, then the engine shuts off until the water cools down and reaches the lower set point and again the heating process starts. Therefore, to model the most suitable output and find the closest cyclic behavior of the engine by the simulation software, two polynomial equations were developed: one for the heating process, another for the cooling process. The efficiency of the engine was determined experimentally and it varies with different supply temperature. Therefore, those two polynomial equations, which were used to model the thermal production of the engine, were calculated based on the efficiency, supply temperature, and return temperature. Three modes were defined: shut down mode, heating mode, and cooling mode. Type 222 was programmed based on following characteristics:

Inputs:

$$\dot{m}_{in}, T_{in}, \dot{m}_{Fuel}$$

Outputs:

$$\dot{m}_{out}, T_{out}$$

Constants:

$$c_p, \rho$$

All modes:

$$\dot{m}_{in} = \dot{m}_{out}, \quad \dot{Q}_{in} = \dot{m}_{Fuel} \times HHV$$

Mode 1 – Shut down mode

$$T_{out} = T_{in}$$

Mode 2 – Heating mode

$$\eta_{heating} = [(-0.0033(T_{out})^2) + (0.3425(T_{out}) - 8.1631)]$$

$$T_{out} = \frac{\eta_{heating} \times \dot{Q}_{in}}{\dot{m}_{out} \times c_p \times \rho} + T_{in}$$

Mode 3- Cooling mode

$$\eta_{cooling} = [(-0.0098(T_{in})^2) + (1.1363(T_{in}) - 32.064)]$$

$$T_{out} = T_{in} - \frac{\eta_{cooling} \times \dot{Q}_{in}}{\dot{m}_{in} \times c_p \times \rho}$$

Chapter 5 - Data Analysis

In this chapter, the experimental results of the proposed research are discussed. Also, the expected results based on the simulated model are studied. The Stirling engine cogeneration system was tested under different outdoor temperatures and loads. Many sets of data were recorded and analyzed. The thermal and electrical efficiencies along with the cyclic behaviour of the engine were investigated. Moreover, the fuel consumption and maximum and minimum thermal/power productions were studied. All these tests were conducted for the second round using the auxiliary burner of the engine, which enhanced the thermal production of the engine. Accordingly, a feasibility analysis was conducted to find out the possible options of how to implement the tri-generation system. The required time and energy for both charging and discharging cycles were calculated. After installing the chiller, a series of tests was planned and all the related data were recorded. The charging and discharging performance analysis is provided. In addition, the performance of the heat rejection circuit was discussed. Moreover, the predicted results of the simulated model were compared to the experimental data and discrepancies were investigated.

5.1 Preliminary Experimental Results of the Stirling Engine

The electrical and thermal energy generation, and the performance of the system as determined by its electrical, thermal and total efficiency were tested and assessed. The electrical efficiency is defined as the net electrical output energy divided by the input energy given by HHV of the natural gas. The parasitic electrical losses due to cycling, in the start-up and shut down are also included in the calculation of overall electrical efficiency. The efficiency is found on daily basis in order to account for the effects of on/off cycling [59]. Thermal efficiency is defined as the thermal output energy divided by the input energy given by HHV of the natural gas. Results are presented on daily basis as well as cyclic, which gives a broad overall view of performance [59].

5.1.1 Daily Breakdown of Thermal Energy Production of TRCA House

Since 2009, a Stirling engine based cogeneration unit at the TRCA archetype sustainable house (ASH) was installed and intended to cover the domestic hot water and space heating needs. During the feasibility tests and before installing the ClimateWell chiller, in order to investigate the thermal and electrical capability of the engine, series of tests were scheduled to meet the thermal demand of the house. Hence, the thermal energy production through the Stirling engine was required to be equal to or higher than the total thermal demand of the house. To demonstrate the daily thermal demand and production, an experimental heating performance evaluation was made during March 2011, which is shown in Figure 5.28. As Figure 5.28 illustrates, the daily thermal production of the Stirling engine varies for different days and it is directly dependent on the daily heating demand of the building. On the other hand, heating demand of the house is affected by the outdoor temperature. Lower outdoor temperature results in higher heating demand. Therefore, the engine is required to be run longer time in colder days.

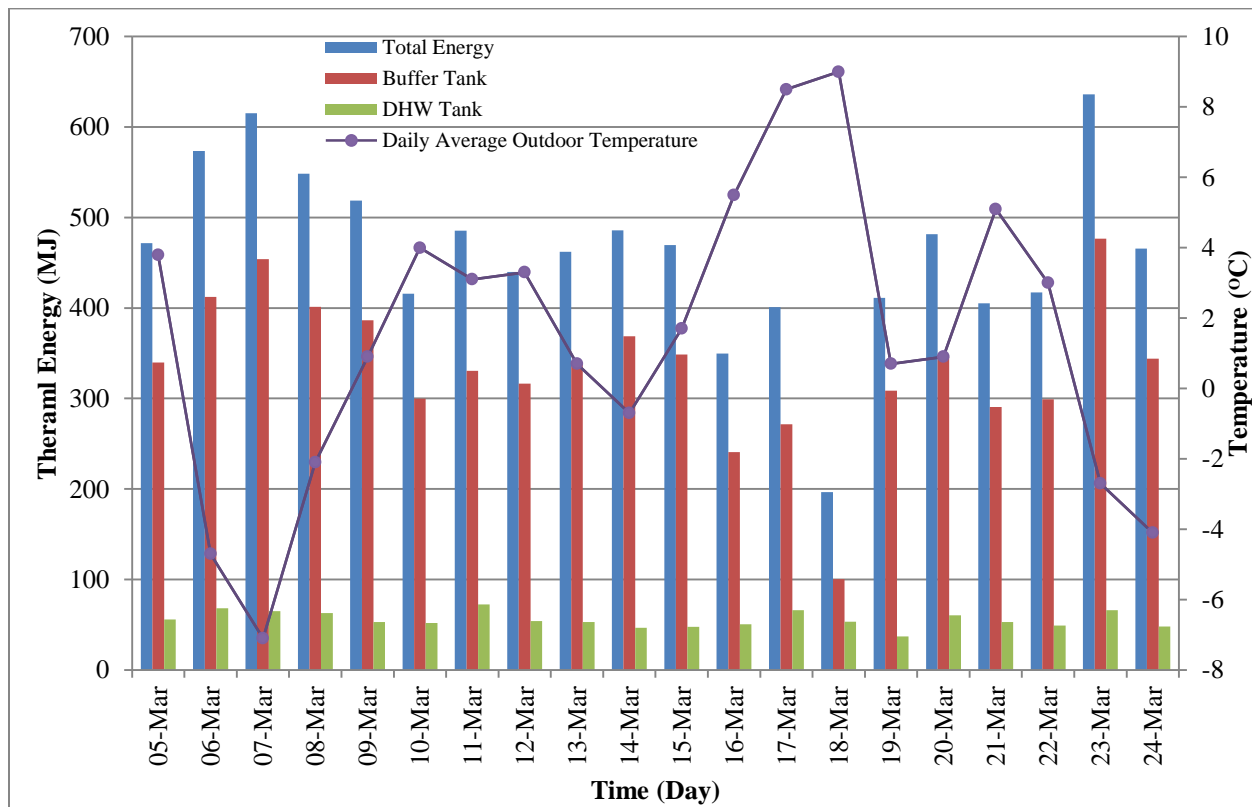


Figure 5.28 - Daily Thermal Energy Production of the Stirling Engine - March 2011

Table 5.12 shows the daily average, minimum, and maximum outdoor temperatures, thermal energy productions, domestic hot water thermal demands, and space heating demands. The maximum thermal energy generation for the space heating occurred in the coldest day of the test period and the minimum thermal energy generation corresponds to the warmest outdoor temperature. Domestic hot water usage depends on the defined occupancy schedule of the house and end use appliances schedule. Therefore, maximum or minimum of thermal energy production in one day is not necessary the sum of maximum or minimum of thermal energy for domestic hot water and space heating production of the same day. For instance, the minimum thermal energy production for domestic hot water was on March 19, but the minimum of thermal energy production for space heating and total energy production occurred on March 18.

Table 5.12- Daily Maximum, Minimum, and Average at House B – February and March 2011

		Minimum	Average	Maximum
Domestic Hot Water	MJ/Day	37	56	72
	kWh/Day	10.27	15.55	20
Space Heating	MJ/Day	100	334	477
	kWh/Day	27.77	92.77	132.5
Average Outdoor Temperature (°C)		-7.1	1.44	9
Thermal Energy Production	MJ/Day	154	390	543
	kWh/Day	42.77	108.3	150.8

5.1.2 Thermal Efficiency of Stirling Engine

The efficiency of the CHP unit is one of the most important factors of this system. Therefore, thermal efficiency of the unit was analyzed in this section. Daily results show that the average thermal efficiency was 78.3% while the minimum and maximum thermal efficiencies were 63.6% and 83.5% respectively. Based on the experimental observation, the thermal efficiency of the CHP is not dependent on the outdoor temperature. Rather, it is dependent on the supply temperature. However, the supply temperature is inversely related to the outdoor temperature. As a result, the supply temperature is dependent on the outdoor temperature due to higher heating demand of the house. As it is shown in Figure 5.29, the thermal efficiency of the Stirling engine is highly dependent on the supplied water temperature. The higher the supplied temperature, the lower the efficiency is.

Since the efficiency of the engine is directly dependent to the duration of the cycles as well, it is observed that at some temperature because of different cycling time, the efficiency varies. All these thermal efficiencies are calculated when the engine was run only with the main burner and not the auxiliary burner. The 5% error bars are shown in the graph to provide an accurate representation of the results. In winter 2012, series of tests were conducted to evaluate the performance of the engine with auxiliary burner. The result is provided later in this chapter.

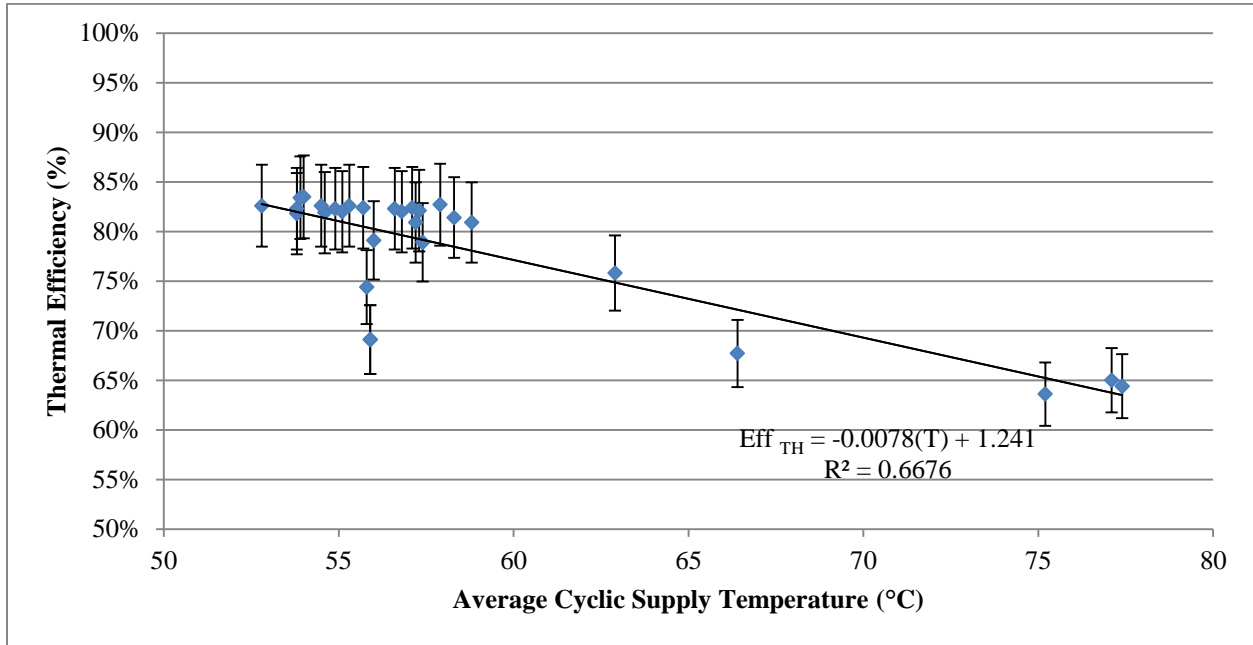


Figure 5.29 - Thermal Efficiency of Stirling Engine versus Supplied Temperature

5.1.3 Electrical Output of the Stirling Engine, Daily Break Down and Efficiency

The advantage of the combined system compared to other systems is simultaneous electric power generation with thermal generation. The amount of electricity produced by CHP systems vary by the size of the units but during running the cogeneration system, this amount is almost constant and the fluctuation is negligible [60, 6]. The Stirling engine unit consumes a small portion of the produced electricity for its controller circuits. Also at the TRCA House extra power is consumed by the circulation pump which circulates the water for the space heating and to the domestic hot water tank. Figure 5.30 shows the daily electrical production of the Stirling engine along with the controller consumption and the circulation pump consumption. The results showed that the average electrical efficiency of the engine was 11.1%, while the minimum of 9.4% and the maximum of 12.3% were also observed. In general, the electrical efficiency of the cogeneration unit compared to the thermal

efficiency was much lower. The lower thermal demand results in shorter cycle, which reduces the electrical efficiency due to higher electrical consumption during start-up period. Therefore, minimum electrical and thermal efficiency do not occur at the same time necessarily. Also maximum of those may or may not happen at the same cycle.

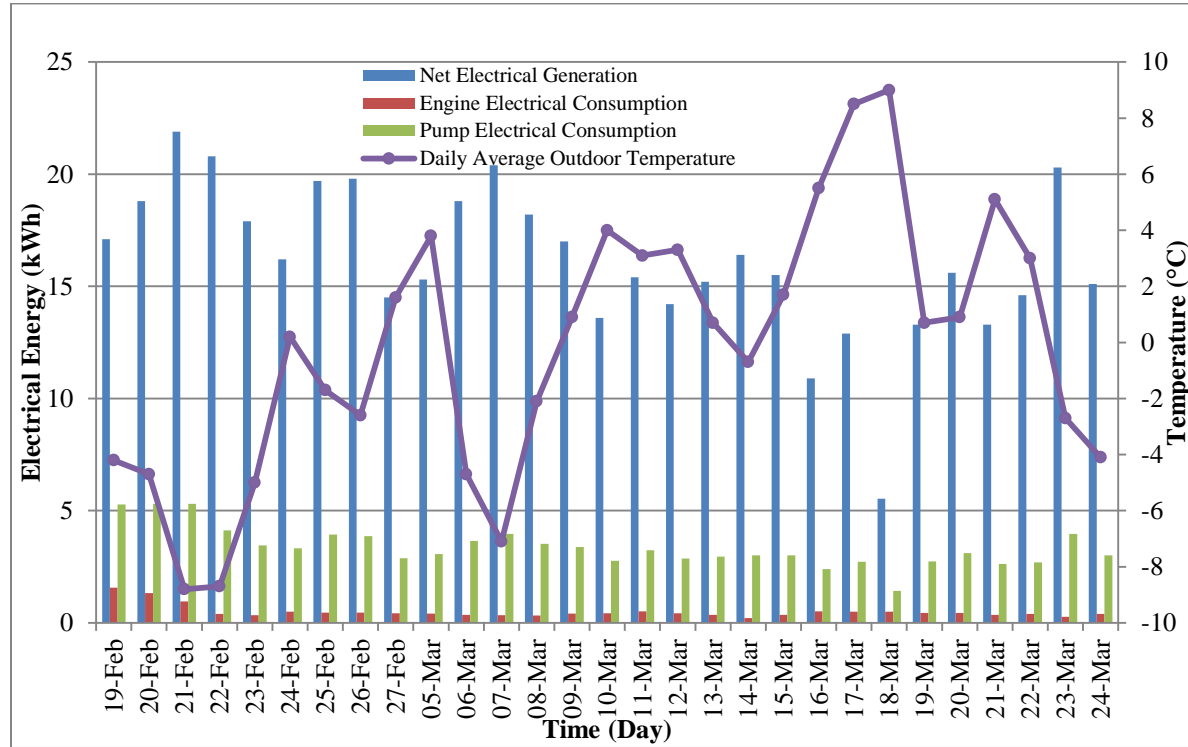


Figure 5.30 - Daily Electrical Production of Stirling Engine-Winter 2011

The overall efficiency of the CHP system is calculated by [5] :

$$\text{Overall Efficiency} = \frac{\text{Useful Thermal} + \text{Net Electrical Output (kWh)}}{\text{Fuel input} \times \text{HHV (kWh)}}$$

Therefore, the overall efficiency achieved by the Stirling engine during the experiment was 89.3% for the average and 73.1% and 95.4% for minimum and maximum respectively. Table 5.13 shows the minimum, maximum, and average efficiencies of the Stirling engine during the test period.

Table 5.13 - Efficiencies of the Stirling Engine – Winter 2011

	Minimum	Average	Maximum
Electrical Efficiency %	9.4	11.1	12.3
Thermal Efficiency %	63.6	78.3	83.5
Overall Efficiency %	73.1	89.3	95.4

5.1.4 Cyclic Behaviour of Stirling Engine

To obtain a reliable result from the Stirling engine, the behavior of every single cycle of operation must be assessed. A cycle is the period when the thermal and electrical generation process starts until the engine completely stops. The LabVIEW program reads the temperature sensor in the buffer tank and sends a signal to the co-gen system to start when the buffer tank water temperature is below the low temperature set point and whenever it reaches the high set point, the program shuts down the co-gen unit. In other word, the LabVIEW program controls the Stirling engine based on the defined set point temperatures. Thus, the water temperature in the buffer tank is always between two set points. Figure 5.31 shows the Stirling engine performance on a typical winter day (February, 20, 2011) when the daily average ambient temperature was -4.7°C . Figure 5.31 illustrates seven complete cycles with different lower set points at the buffer tank. In this experiment, first cycle with the lower set point of 48°C , the second cycle with 55°C , next four cycles with 78°C , and again from 7 pm the lower set point was at 65°C , while all high set point was at 90°C . The engine stops burning gas because of safety issues when the supply temperature reaches 90°C but the reason that the temperature at the engine reaches 93°C is that the water is still gaining heat from engine to meet the higher set point temperature at the buffer tank. Basically, the pump circulates water after each shut down to decrease the engine body's temperature but for the first few minutes right after the shut-down process, the working fluid still heats up because of the residual heat of the engine.

The average temperature difference between the supply line and return line is 7°C with a very small variation and this almost constant temperature difference produces an average thermal output of 8600W. This is mainly dictated by the internal heat exchanger in the cogeneration unit. The average gas consumption is 13.5 l/min as shown in Figure 5.31. There is a peak load for the gas consumption at the beginning of each cycle which is 17 l/min and it lasts for the first few minutes until the system reaches the steady state. The gas consumption graph of the engine has the same pattern for the whole year and it is indirectly dependant on the outdoor temperature. Also it is almost constant through each cycle. Therefore, the energy input to the system, which is the fuel input/natural gas, is almost constant.

As Figure 5.31 shows, the average coolant flow rate is close to 17 L/min in a typical day. The flow rate can be set to higher or lower rate through the variable speed circulation pump. The flow rate is close to 13 L/min when the engine is connected to the DHW tank, which is due to the

restriction in the tank's lower heat exchanger. As it is mentioned before, the thermal input is almost constant. Consequently, when the flow rate is lower, the cycle becomes shorter. But the average supply temperature and flow rate must meet the minimum requirements of the house demands. Accordingly, the controller program reads the buffer tank's temperature and the supply temperature then it controls the engine to run shorter/longer cycles. Figure 5.32 shows the thermal and electrical production during a typical working cycle of the Stirling engine. Constant electricity production along with stable thermal production are two main characteristics of any working cycle.

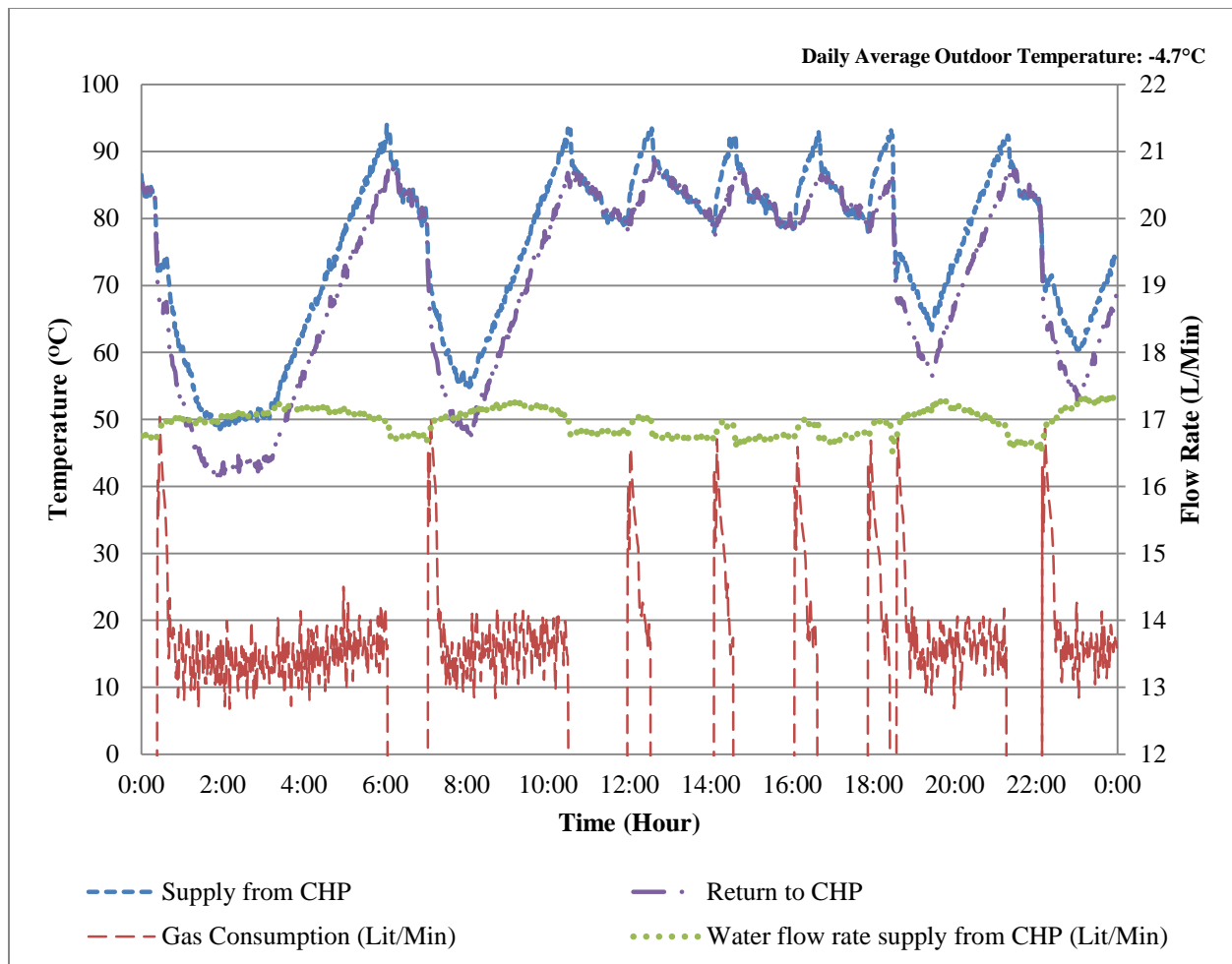


Figure 5.31 - Stirling Engine Performance – February 20, 2011

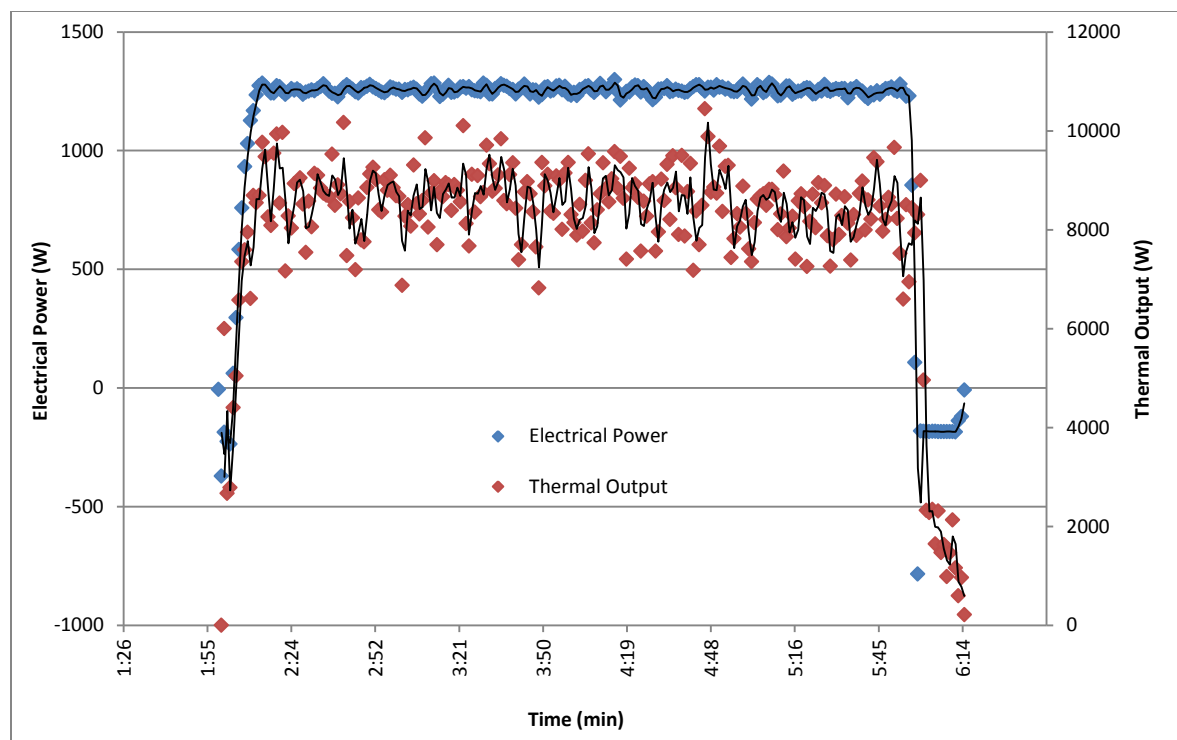


Figure 5.32 - Typical Cyclic Behavior of the Stirling Engine

5.1.5 Stirling Engine Performance with a Built in Auxiliary Burner

In addition to many tests on the Stirling engine with the main burner, series of tests were scheduled and conducted for this engine to study the performance of the cogeneration system using the internal auxiliary burner. The ClimateWell chiller requires a heat source, which can be provided by the hot water in the range of 80 to 120°C. The Stirling engine, as it is shown previously, is able to provide continuous thermal energy, but there are some difficulties. The WhisperGen engine shuts down due to the safety issues when the temperature reaches 85°C. Also that highest range of temperature from the Stirling engine only covers the lowest range of temperature requirement of the ClimateWell.

In order to solve the safety shut off issue, a 110 Ω electrical resistor was added to the safety circuit and the internal control unit of the Stirling engine was upgraded to send the safety signal when the temperature reaches 95°C instead of 85°C. Accordingly, the auxiliary burner of the engine was used to investigate the performance of the engine at a higher temperature set point. Figure 5.33 shows a typical cyclic behavior of the engine on October 18, 2012 with a lower set point temperature of 80°C and higher set point of 95°C using the auxiliary burner. A new circulation pump was

installed and the flow rate was 15 L/min. Although in general the supply and return temperature trends look like the same as the main burner, there are significant differences in details.

Employing the auxiliary burner successfully increased the peak supply temperature up to 95°C. The on/off cycles' duration significantly decreased. Previously, each cycle's duration was almost two hours, which was decreased to an average time of 30 minutes. This helps the charging process since the average supply temperature in the same time interval is higher than previous results. A bigger pump with a higher flow rate capacity will help to avoid the short cycling. A continuous thermal production without on/off cycles is an ideal charging process for the ClimareWell chiller.

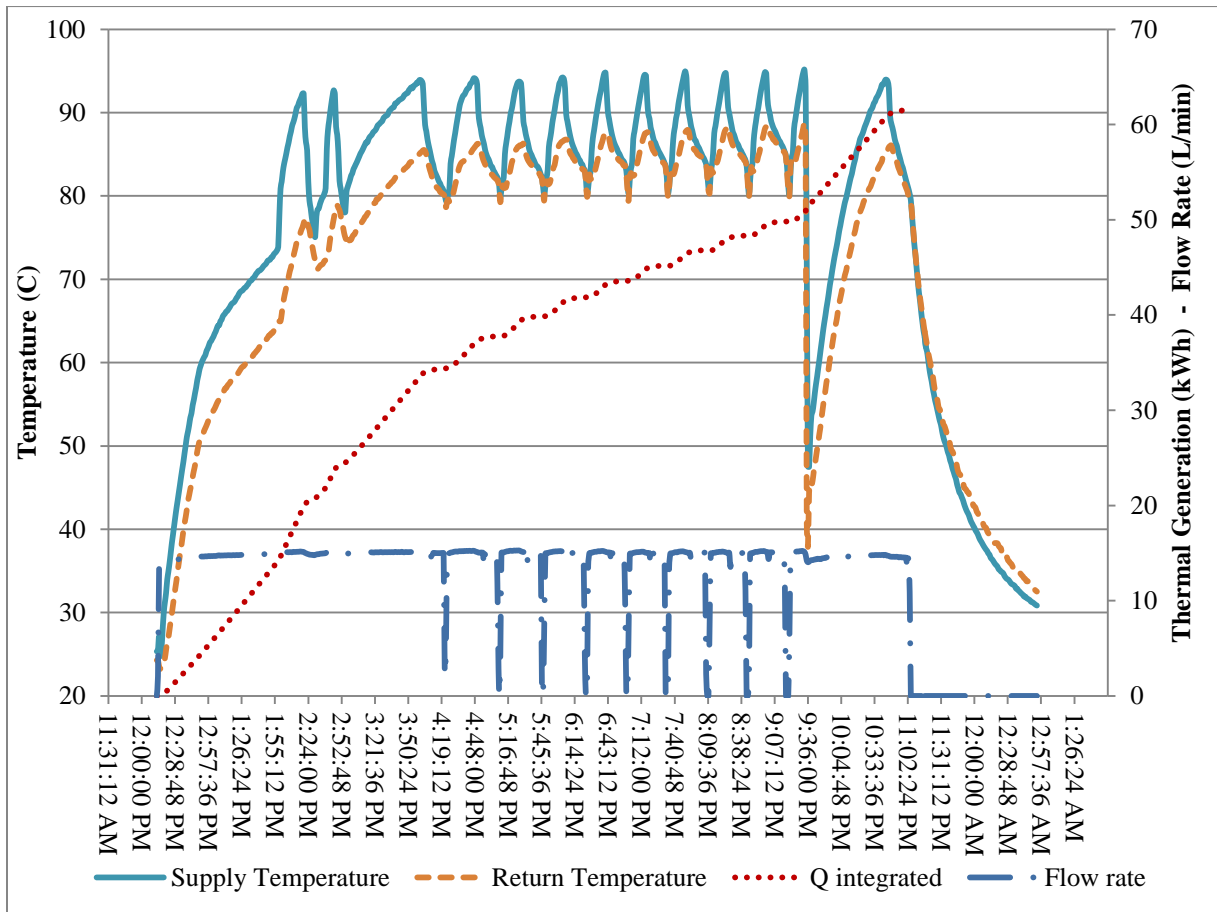


Figure 5.33 - Stirling Engine Performance with Auxiliary Burner - October 18, 2012

5.2 Feasibility Analysis

The Whispergen Stirling engine was installed in House B. A series of tests was conducted to investigate the capability of the engine to charge the ClimateWell chiller. The engine's performance was studied and the thermal energy generation of the engine according to the outdoor temperature was carried out. On the other hand, House B was simulated and calibrated by Safa in 2011 [51], using TRNSYS software [51]. The predicted heating demand of the house was compared to the experimental thermal energy production. After the relationship between demand and production was established, the heat activated cooling system was considered as a source of heating demand in the cooling season and the same established relationships were used to predict the charging time and gas consumption.

5.2.1 Heating and Cooling Demand and Production

The calibrated TRNSYS model [51] and Toronto metropolitan weather data are used to extract the cooling and heating demands of the house. Accordingly, the maximum heating demand is 8.02 kW and maximum cooling demand is 4.86 kW. Figure 5.34 illustrates the predicted hourly demand of the house by the TRNSYS software, using the long term average Toronto weather data. This graph was used to assess the capability of the proposed heating/cooling integrated system.

During the first and second series of tests on the cogeneration system, collected data were used to determine accurate amount of thermal energy production for the space heating and domestic hot water production of the House B on a daily basis.

Figure 5.35 shows the experimental results of those tests. Figure 5.35 also shows the relation between the Stirling engine's thermal production at the House B and daily average outdoor temperature. The heating demand of the house decreases when the outdoor temperature is higher, therefore, the thermal generation was less during those warmer days. The average thermal production in typical winter day, during the testing period, is from 60 to 100 kWh.

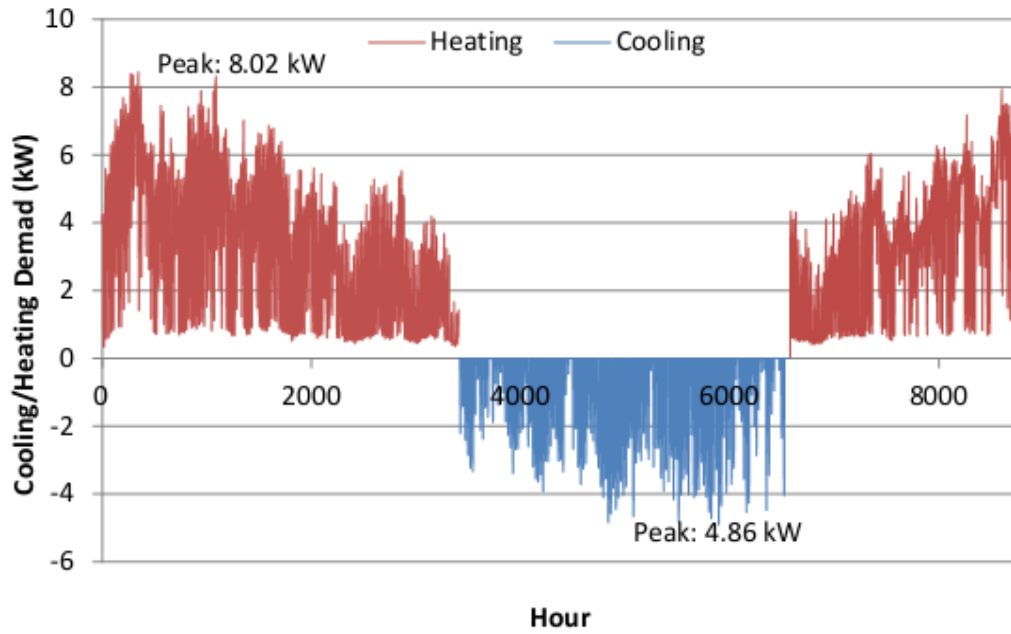


Figure 5.34 - Predicted Heating and Cooling Deamnds of House B by TRNSYS Software

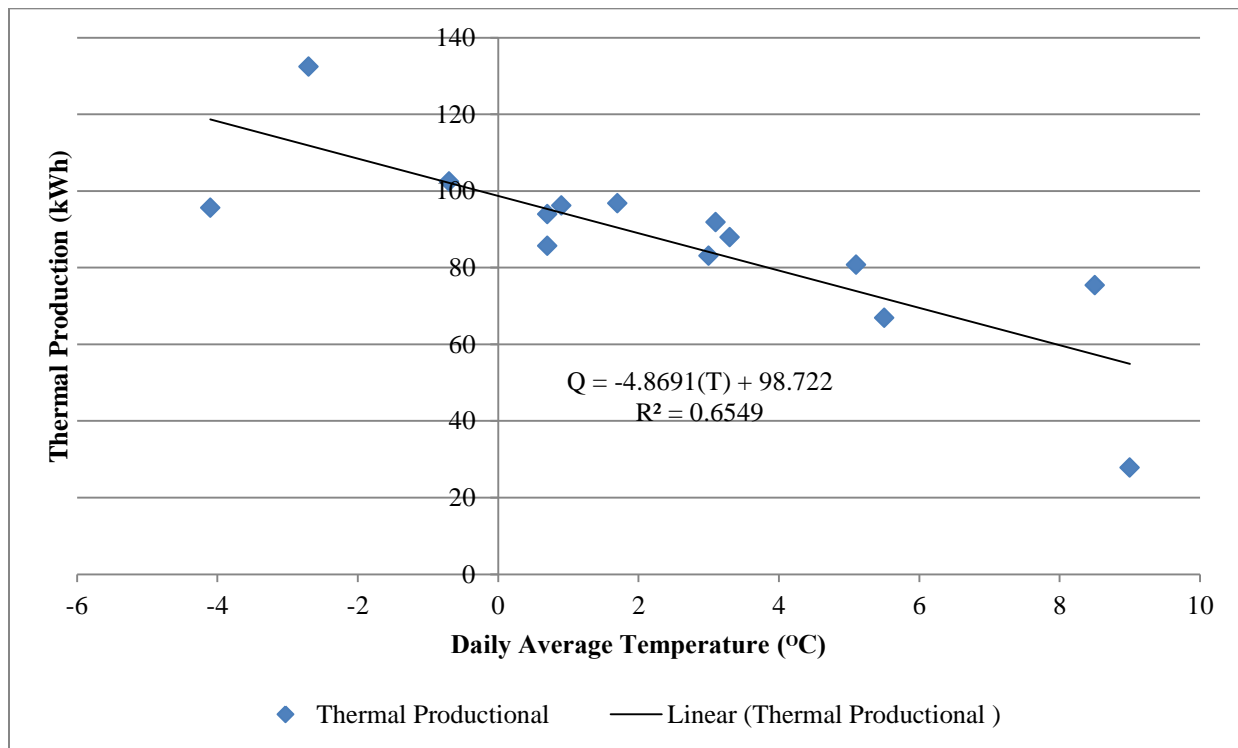


Figure 5.35 – Experimental Thermal Energy Generated versus Daily Average Temperature

The calibrated TRNSYS model [51] was used to study the thermal demand of the house and the required thermal energy production of the Stirling engine. Figure 5.36 shows the result of thermal demand of House B without the in-law suit, which is simulated by the TRNSYS software, versus daily average outdoor temperature. As it is shown in Figure 5.36, the predicted thermal demand of the house varies from 40kWh to 110kWh depending on the outdoor temperature. Using a trend line and pattern of Figure 5.36, the thermal demand of House B was developed for the temperature range of a winter season.

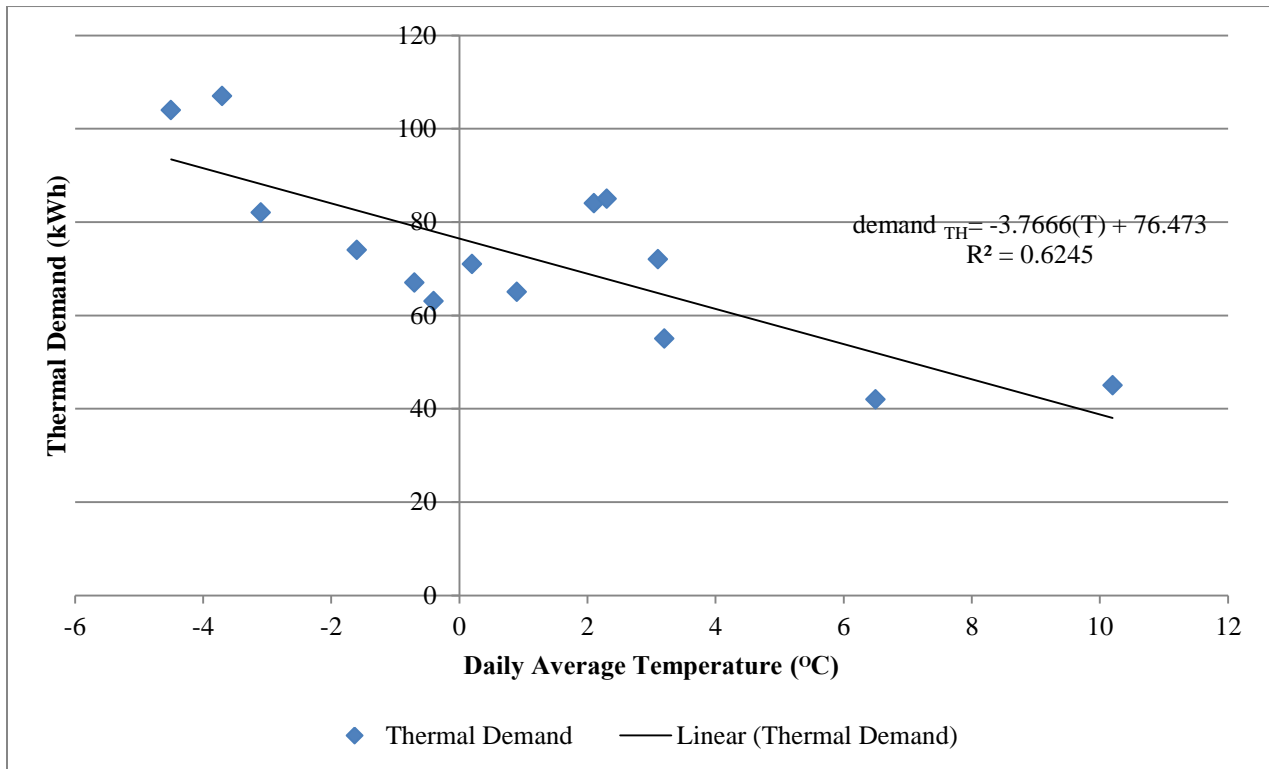


Figure 5.36 - Thermal Demand of House B Prediction by TRNSYS

Both of the experimental and simulated results from CHP tests and TRNSYS software were compared in Figure 5.37. It was observed that actual thermal production is consistently 22% more than the heating demand predicted by TRNSYS model. Since the DHW load is included in the model, this discrepancy occur because the in-law suite demand is excluded in the model while the experimental thermal production data from the Stirling engine includes space heating requirement of the in-law suite as well. Based on the TRNSYS daily average temperature output for Toronto, the minimum daily average temperature is -21°C and the maximum is 25°C, while the maximum daily

average temperature in the heating season is 12.15°C. Therefore, the prediction graphs are generated according to these domains.

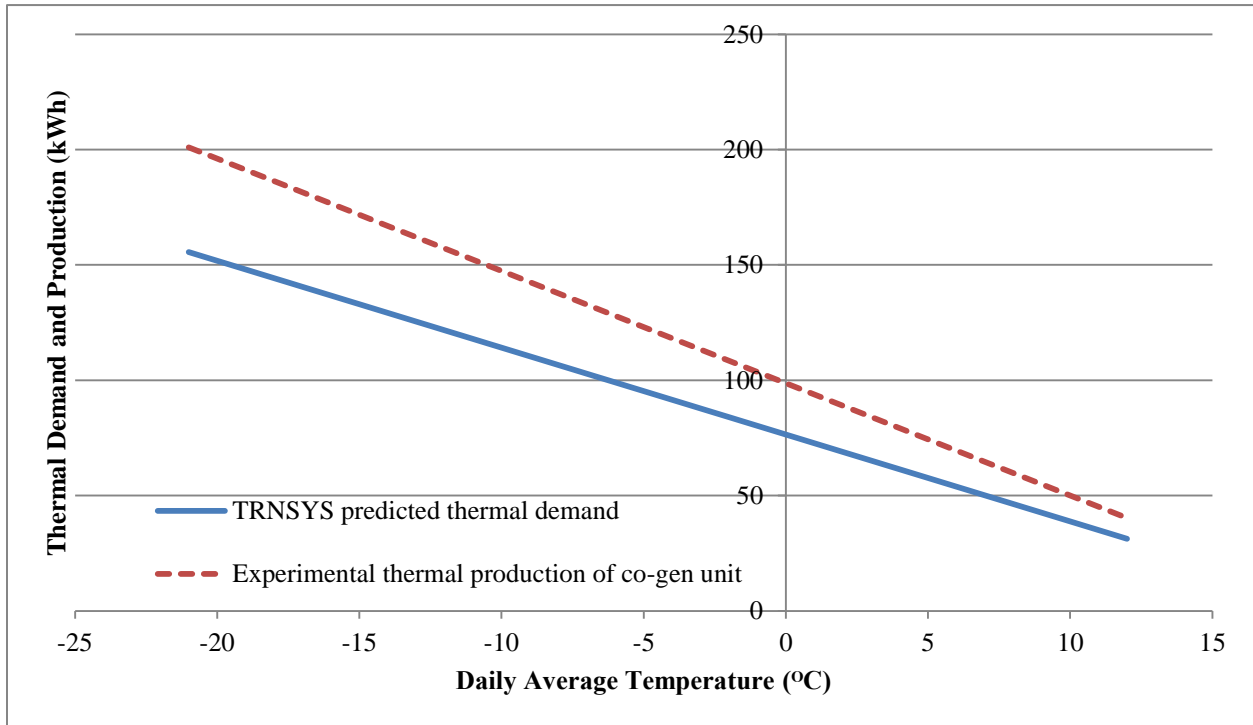


Figure 5.37 - TRNSYS House B simulated model Predicted and Experimental Thermal Output vs Average Daily Outdoor Temperature

The TRNSYS model of House B was employed and cooling demand of the house was carried out. The predicted cooling demand was normalized based on the daily average outdoor temperature. The trend line of the cooling demand prediction is shown in Figure 5.38 with the blue line. Since the ClimateWell chiller's COP was reported by the manufacturer's manual as 0.5, the same methodology as heating season was used to estimate the required thermal energy for charging the chiller during cooling season. The same 22% offset was also considered to avoid the possible errors.

Figure 5.38 also shows how much thermal energy is required to be generated by the Stirling engine to charge the ClimateWell chiller based on the daily average outdoor temperature.

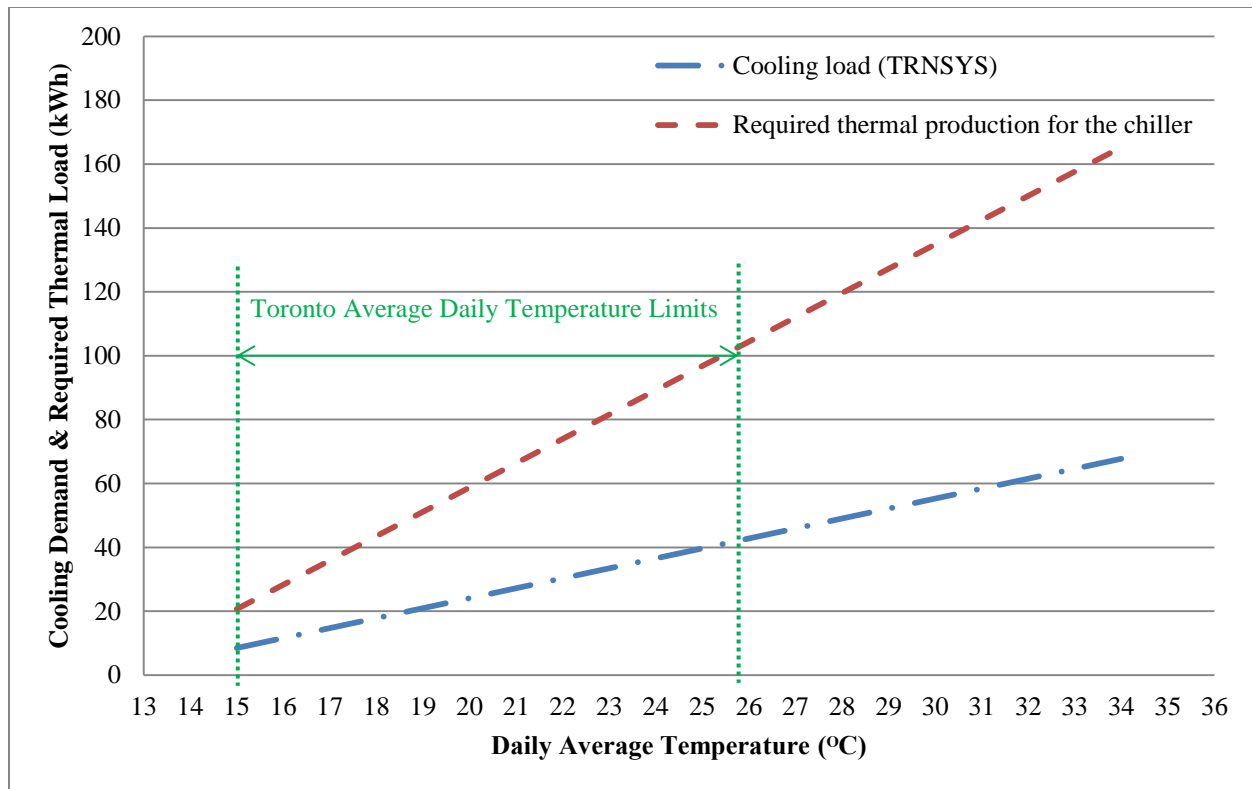


Figure 5.38 - Predicted Cooling Demand (TRNSYS) of House B and Required Thermal Load vs Average Daily Temperature

The same methodology was used with different COPs rather than 0.5 and the results are available in Appendix C.

5.2.2 Time of Running Stirling Engine and Gas Consumption

In this section, the gas consumption of the Stirling engine and the required time of running the engine to produce the demanded thermal energy for both cooling and heating seasons are studied. In Figure 5.39, in addition to the thermal generation and TRNSYS predicted lines, time and corresponding gas consumption are considered as well. All the on/off cycles, start up and warm up processes are considered in the time of running for the calculation. Using Figure 5.39, and knowing the daily average outdoor temperature, the thermal demand of the house can be estimated and also it can be predicted how long the engine is required to run and how much gas will be consumed during that run. Figure 5.39 also shows that if the average outdoor temperature is less than -17°C , the cogeneration unit must work the whole 24 hours and any temperature below -17°C requires more than 24 hours, which is impossible. Six data point as examples are shown in Table 5.14 to illustrate how to use the Figure 5.39.

Table 5.14 - Numeric Sample of Heating Season Demands

Daily Average Outdoor Temperature (°C)	TRNSYS Predicted Heating Demand (kWh/day)	Actual Thermal Production (kWh/day)	Gas Consumption (m ³ /day)	Co-gen Run Time (hr/day)
-15	132.9	171.7	15.8	23.0
-10	114.1	147.4	14.3	20.1
-5	95.3	123.0	12.8	16.9
0	76.5	98.7	11.4	13.7
5	57.6	74.3	9.9	10.4
10	38.8	50.0	8.4	7.2

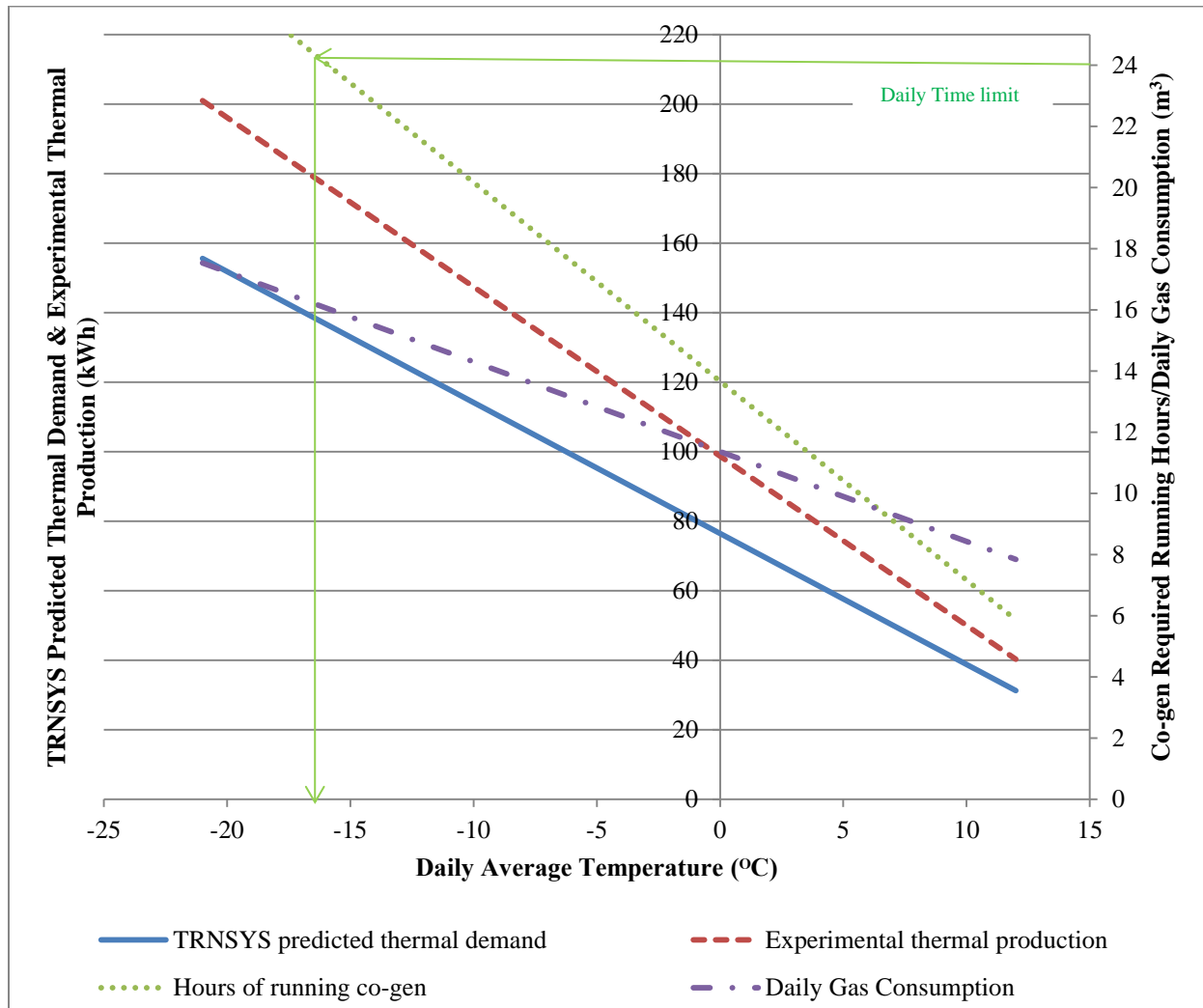


Figure 5.39 - TRNSYS Thermal Prediction & Required Run Time & Gas Consumption

Accordingly, the same procedure was repeated to determine the heating demand of the chiller to be charged in the cooling season. Figure 5.40 shows the details of the cooling demand of the house by using TRNSYS software, which corresponds to the thermal energy required by the chiller and also

predicted Stirling engine run time and gas consumption for the charging process. The COP of the chiller is considered 0.5 in these calculations according to the manufacturer data sheet, also other COPs such as 0.3, 0.35, 0.4,...,0.6 are shown in Appendix C. Five data point as examples are shown in Table 5.15 to show how to use the figure.

Table 5.15 - Numeric Sample of Cooling Season Demands

Daily Average Outdoor Temperature (°C)	TRNSYS predicted Cooling Demand (kWh)	Required Thermal Production to Charge the Chiller (kWh)	Gas Consumption (m ³)	Time (hr)
18	17.8	43.5	5.1	4.5
20	24.0	58.7	6.7	6.4
22	30.3	73.9	8.4	8.3
24	36.5	89.2	10.0	10.3
26	42.8	104.4	11.7	12.2

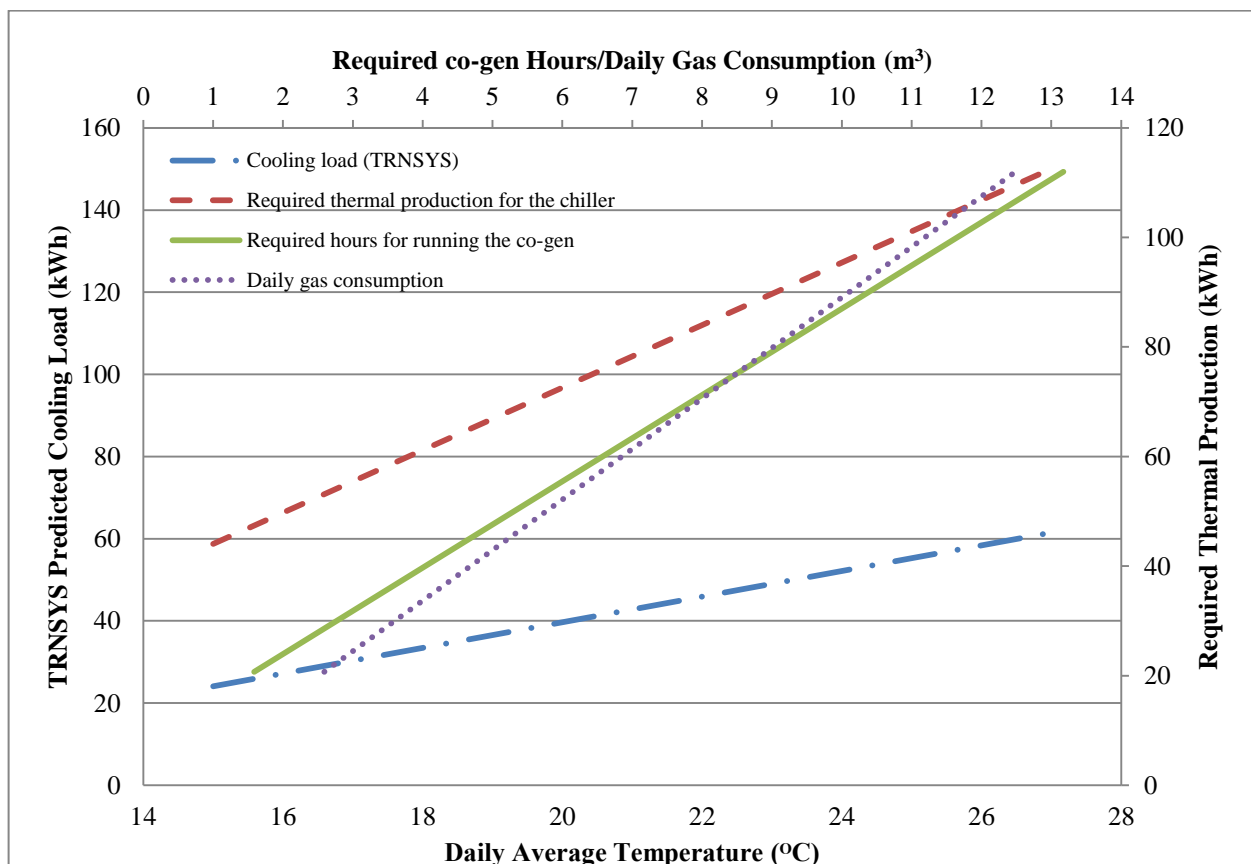


Figure 5.40 – TRNSYS Cooling Prediction & Required Co-gen Run Time & Gas Consumption

5.2.3 Extrapolating the Heating and Cooling Demands and Gas consumption

In order to investigate the feasibility of integrated system, it is very important to study the annual energy consumption, cost, and emissions of the system. After conducting the preliminary tests and feasibility analysis, the results were extrapolated for the whole year. The expected consumption was calculated based on the long-term average weather data of Toronto. The overall pattern of the gas consumption was carried out.

The daily heating and cooling demand of the house, which is extracted from the TRNSYS software, is shown in Figure 5.41. Moreover, required thermal load for the cooling season is included in Figure 5.41. The purple dotted line indicates the amount of thermal energy required to be generated in order to charge the chiller for meeting the cooling demand.

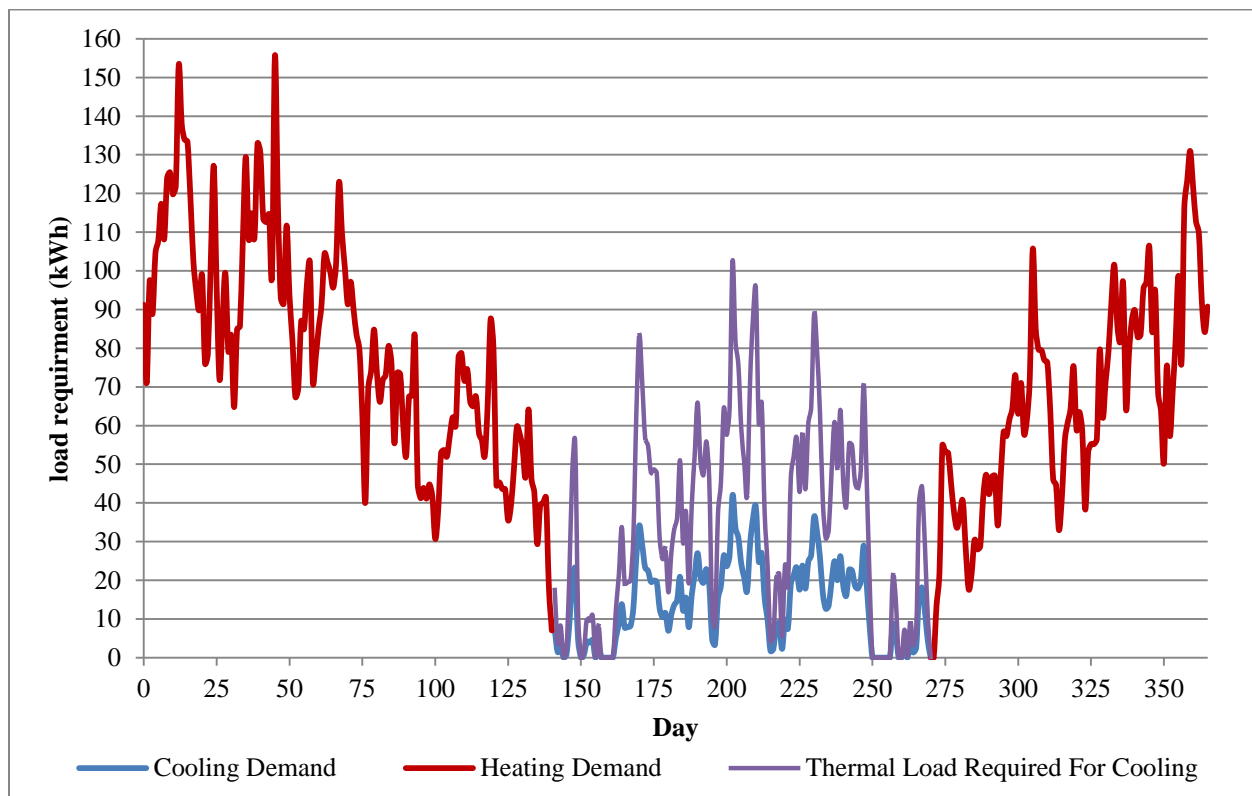


Figure 5.41 - Daily Demand of House B

Figure 5.42 shows the cumulative heating and cooling demand of House B along with estimated annual natural gas consumption using the tri-generation system. According to the Statistics Canada, the average natural gas consumption per household in Ontario is 90 gigajoules or 25,000 kWh [61]. As it can be seen in the Figure 5.42, the annual heating demand of House B is 17581 kWh,

which is 70.3% of an average household demand in Ontario. Since the Archetype Sustainable House is very well insulated and air tight, it was expected to see this difference. The annual cooling demand of the house is 1809 kWh. In order to charge the ClimateWell chiller with the Stirling engine, 4414 kWh of thermal energy generation is required. Accordingly, the estimated natural gas consumption for the total of heating and cooling season based on the thermal efficiency is 2443 m³. As a result, it is observed that although the tri-generation system burns natural gas during both winter and summer time, because of high efficiency of the Stirling engine and also well insulated house, the annual natural gas consumption is less than an average household, which only uses natural gas during the heating season.

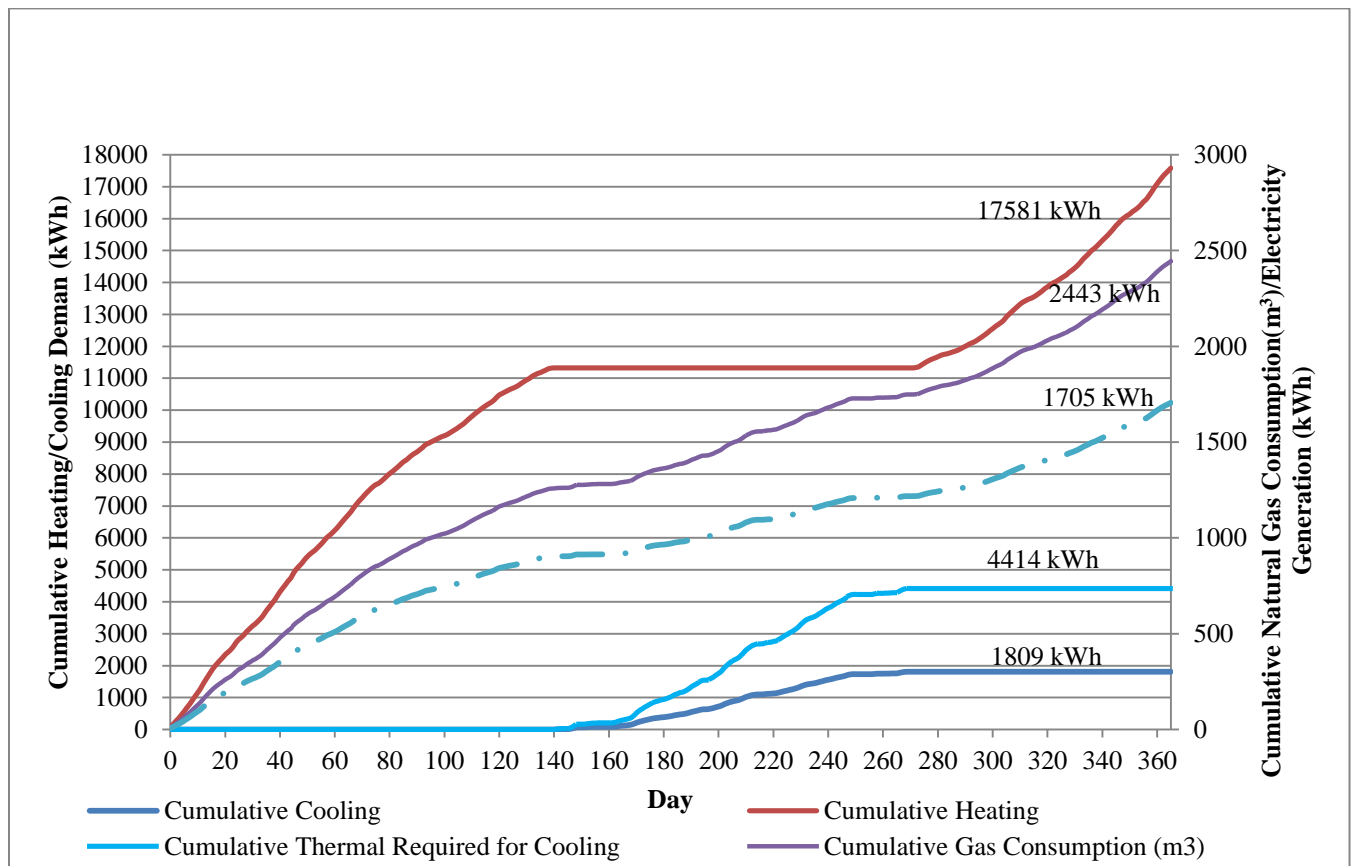


Figure 5.42 - Cumulative Heating and Cooling Demand of the House

Figure 5.43 illustrates the estimated daily natural gas consumption's pattern for the entire year along with the average outdoor temperature in Toronto. A regular residential home with a conventional air conditioning system does not consume natural gas during the cooling season while the proposed tri-generation system requires to burn natural gas for the whole year. The green line in

the Figure 5.43 shows the pattern of gas consumption a cogeneration system while the pink line illustrates the gas consumption pattern of a tri-generation system. The yellow area shows the gas consumption difference between cogeneration and tri-generation system, which corresponds to 469 m³ of natural gas with the cost of \$131. As mentioned previously, because of the sustainable house, the annual gas consumption is less than average household. Using the tri-generation system in a non-sustainable house decreases the electricity consumption and grid dependency.

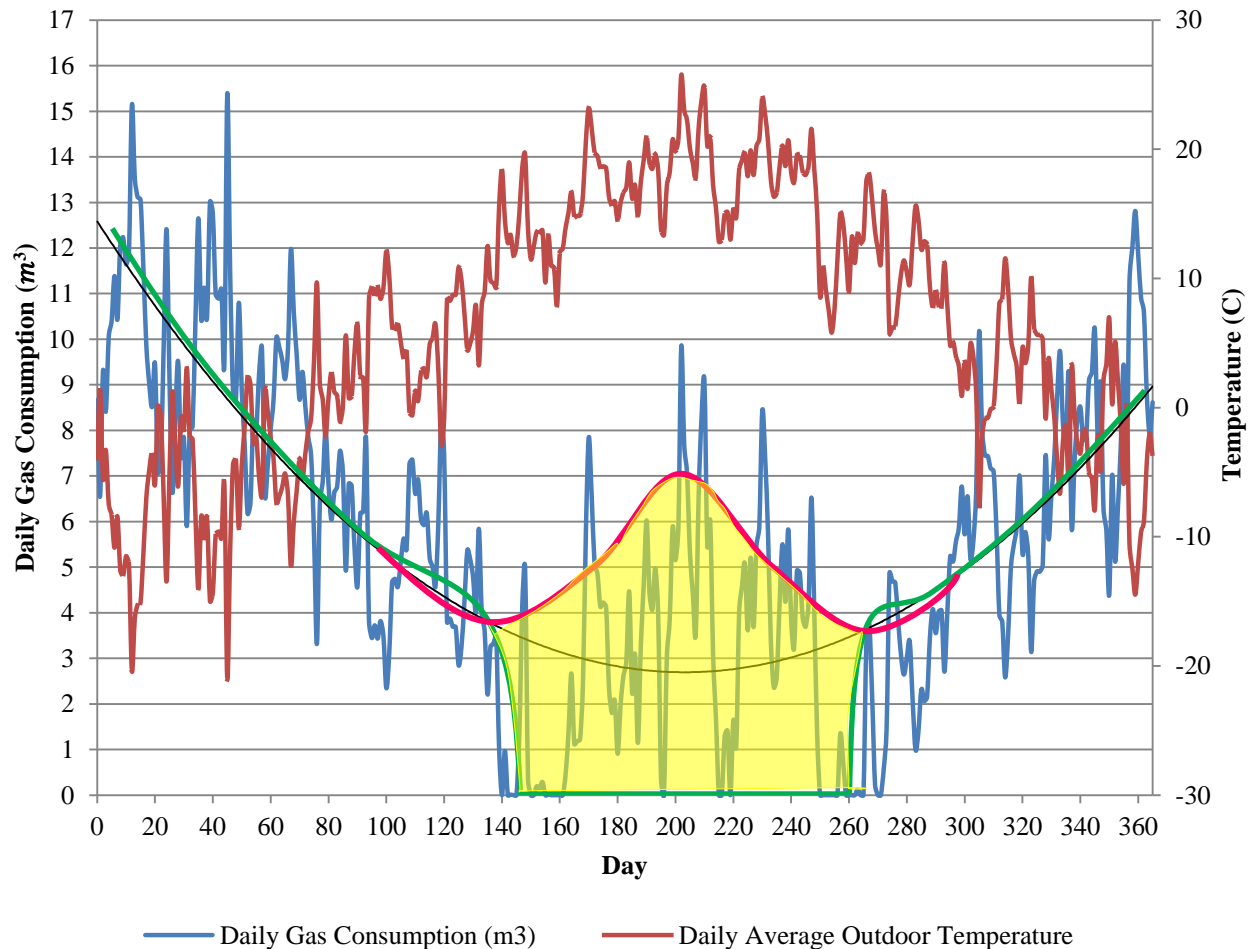


Figure 5.43 - Estimated Daily Gas Consumption vs Daily Average Outdoor Temperature

5.2.4 Prediction for Other Canadian Cities

All the previous analyses and figures are based on the Toronto weather data. The same methodology was used to study the feasibility of micro residential tri-generation system for other Canadian cities such as Vancouver, Montreal, Halifax, and Edmonton. The TRNSYS model of House B was used with those cities' weather library and the annual heating and cooling demands

were estimated. Considering the same integrated system in the same house located in different Canadian cities, the annual natural gas consumption and also the annual electricity generation were predicted. Figure 5.44 shows the annual cooling demand, annual electricity generation, and also annual natural gas consumption of House B in different cities. Halifax has the lowest cooling demand among all these cities and Montreal has the highest cooling demand. Edmonton consumes more natural gas than other cities because of the long heating season and also comparable cooling demand.

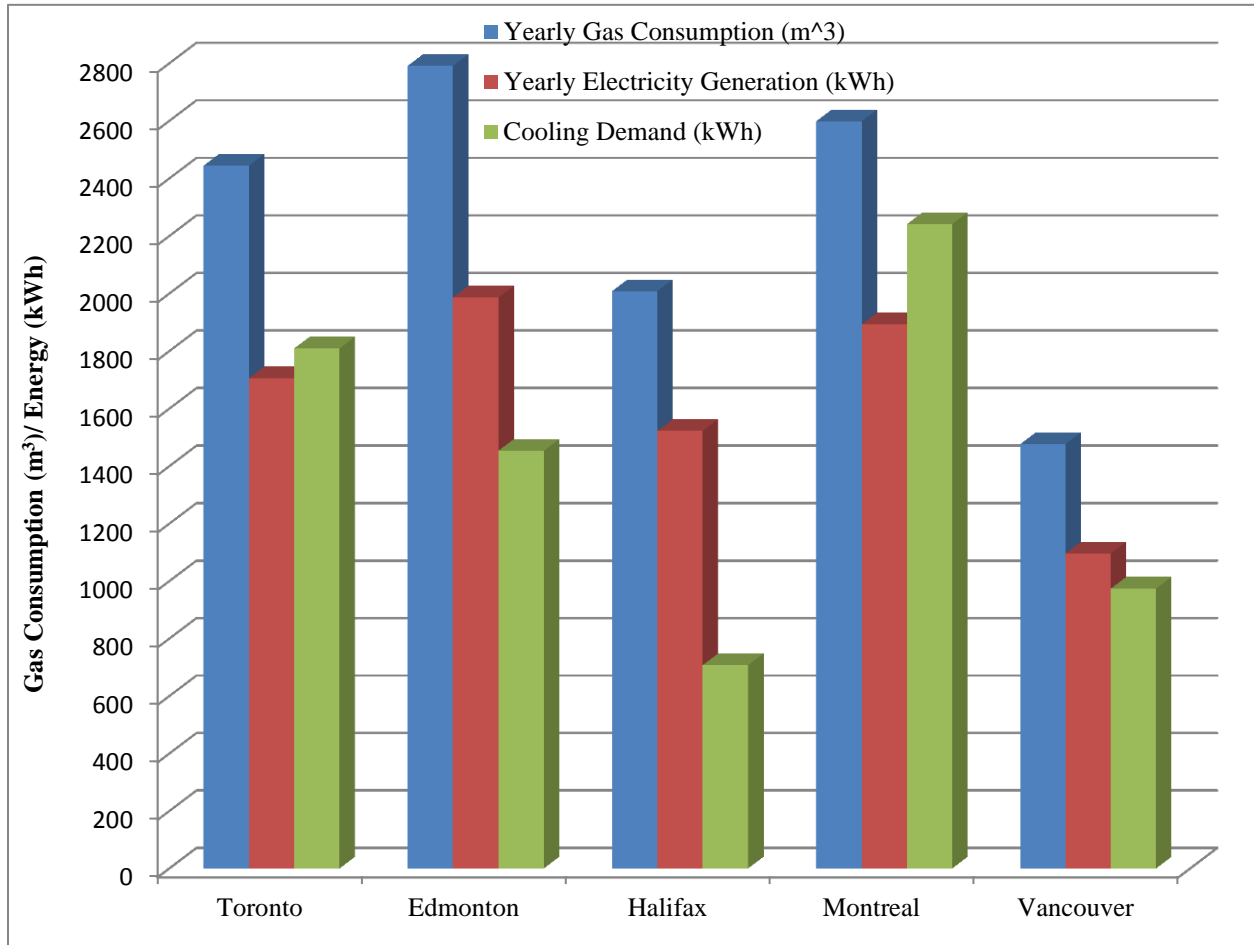


Figure 5.44 - Annual Demand and Corresponding Gas Consumption in Different Canadian Cities

5.2.5 Cost and GHG Emission in Toronto

As it is discussed in Section 5.2.3, using the Stirling engine cogeneration in a residential building, because of electricity generation decreases the cost of operation. Based on the predicted results of annual gas consumption and electricity generation Table 5.16 was generated. The natural gas price was considered 28 ¢/m³ based on a benchmarking research by Mahssa GhajarKhosravi

[62] using the 2012 price list of Enbridge Gas [63] and the electricity price was considered \$0.124/kWh based on a benchmarking of residential electricity bills⁷, using the 2012 price list of Toronto Hydro [64]. Also the GHG emission factor in Ontario for the electricity was calculated based on 100g CO₂/kWh and 180.3g CO₂/kWh for the natural gas [65]. According to Table 5.16 the predicted annual cost of natural gas for tri-generation system is \$684.04, which electricity generation saves \$211.48. The net energy cost is \$472.56.

Table 5.16 - Cost and GHG Emission in Toronto

Annual Natural Gas Cost	\$684.04
Annual Cost Saving by Electricity Generation	\$211.48
Annual GHG Emission Production by Natural Gas	4777.9 kg CO ₂
Annual GHG Emission Saving by Electricity Generation	170.55 kg CO ₂

In order to compare the operation cost of the proposed tri-generation system with non-integrated systems, operation cost and GHG emissions of two different systems considering ASH heating and cooling demands were calculated and provided in Table 5.17. Both two cases are using a furnace for the space heating and an electrical air conditioning system for the space cooling. The efficiency of the furnace in one the cases is considered 90%, which is also equipped with an air conditioning system with a Seasonal Energy Efficiency Ratio (SEER⁸) of 14 (COP=4.1). The second comparison case is defined as a system including a furnace with 80% efficiency and also an air conditioning system with SEER of 10 (COP=2.93). The annual natural gas cost, electricity cost, and total annual operation cost of both two systems were calculated and compared with the proposed tri-generation system in Table 5.17. Also the total GHG emission production regarding to the gas and electricity consumptions of both systems were provided accordingly. As a result, the tri-generation system is expected to produce more GHG emissions annually with a lower annual operation cost.

⁷ Fixed costs and tax are not included in the electricity price.

⁸ The Seasonal Energy Efficiency Ratio (SEER) is also the COP expressed in BTU/W·hr, but instead of being evaluated at a single operating condition, it represents the expected overall performance for a typical year's weather in a given location.

Table 5.17 - Cost and GHG Emission Comparison Between Tri-generation and Conventional Systems

	Tri-generation System	Furnace (90% Efficiency) AC (SEER=14 or COP=4.1)	Furnace (80% Efficiency) AC (SEER=10 or COP=2.93)
Annual Natural Gas Cost	\$684.04	\$611.88	\$667.51
Annual Electricity Cost	-\$211.48	\$54.70	\$76.55
Annual Operation Cost	\$472.56	\$666.58	744.06
Annual GHG Production	4607.35 kg CO ₂	3530.95 kg CO ₂	3865.56 kg CO ₂

5.3 Tri-generation System's Experiments

After a comprehensive tests and feasibility analysis of the Stirling engine and after the design of the piping, fittings, and sensors were completed, the integrated tri-generation system was installed at the TRCA archetype sustainable house (ASH) in summer 2012. Due to the complications of the system and spate of sensors, the commissioning process took longer than it was expected and finished by the end of the cooling season. Since House B is equipped with different HVAC systems, a ground source heat pump was used to heat up the house through the in-floor heating system to simulate the artificial cooling demand for the house. As the experiment was carried out during the October and November of 2012 (fall season), the GSHP maintained the indoor temperature around 24°C in order to create the cooling demand.

In this section, experimental results of the residential tri-generation system including experimental analysis of energy consumption, generation and energy storage are discussed. This chapter also includes experimental results related to the charging and discharging behaviour of the ClimateWell chiller.

5.3.1 Charging Behavior of the ClimateWell

After commissioning the tri-generation system several tests were carried out to analyse the charge and discharge behavior of the ClimateWell chiller. This chiller is able to store the thermal

energy and release it in a form of cooling effect when it is needed. As it is discussed in Chapter 2, the chiller requires a thermal source to be charged. The thermal source must supply 15 to 25 L/min flow rate of working fluid while the temperature is higher than 80°C. The chiller will be charged faster if the supply temperature is higher. The chiller has two barrels, which can be charged one at a time. During charging process of each barrel the second barrel can be discharged and produce chilled water if there is a cooling demand in the building, otherwise the full barrel will remain charged until there is a demand. Reactor's valve of respective barrel is open during the charging process, which allows the high temperature working fluid to enter into the reactor to start the desorption process. Water vapour will be released due to the desorption process and enters to the condenser. Therefore, the condenser heat sink's valve is open to allow the working fluid in the heat rejection loop enter the condenser and keep it cool enough for the condensation. One way to understand which barrel is charging and which one is discharging is to look at the valve positions at the ClimateWell data log.

As it is discussed in Section 5.1, a Stirling engine cogeneration unit was employed to charge the chiller. The auxiliary burner was used during the charging tests. Figure 5.45 shows four charging period that Stirling engine cogeneration performed. Difference in the charging duration is because of the manual or automatic swaps between two barrels, which caused the rapid temperature drop. The red line in Figure 5.45 shows the supply temperature and blue line is return temperature to the CHP unit from the ClimateWell chiller. Temperature difference between supply and return corresponds to the absorbed energy at the chiller. Due to overheating of the cogeneration unit, there are multiple on/off cycles in each charging cycle, which reduces the efficiency and makes the charging process longer. An ideal supply and return temperature for the charging process is drawn by the dotted lines, which increases the temperature after each swap and maintains it above 90°C until next swap. A possible solution to eliminate the on/off cycling is to increase the flow rate of working fluid by replacing the circulating pump.

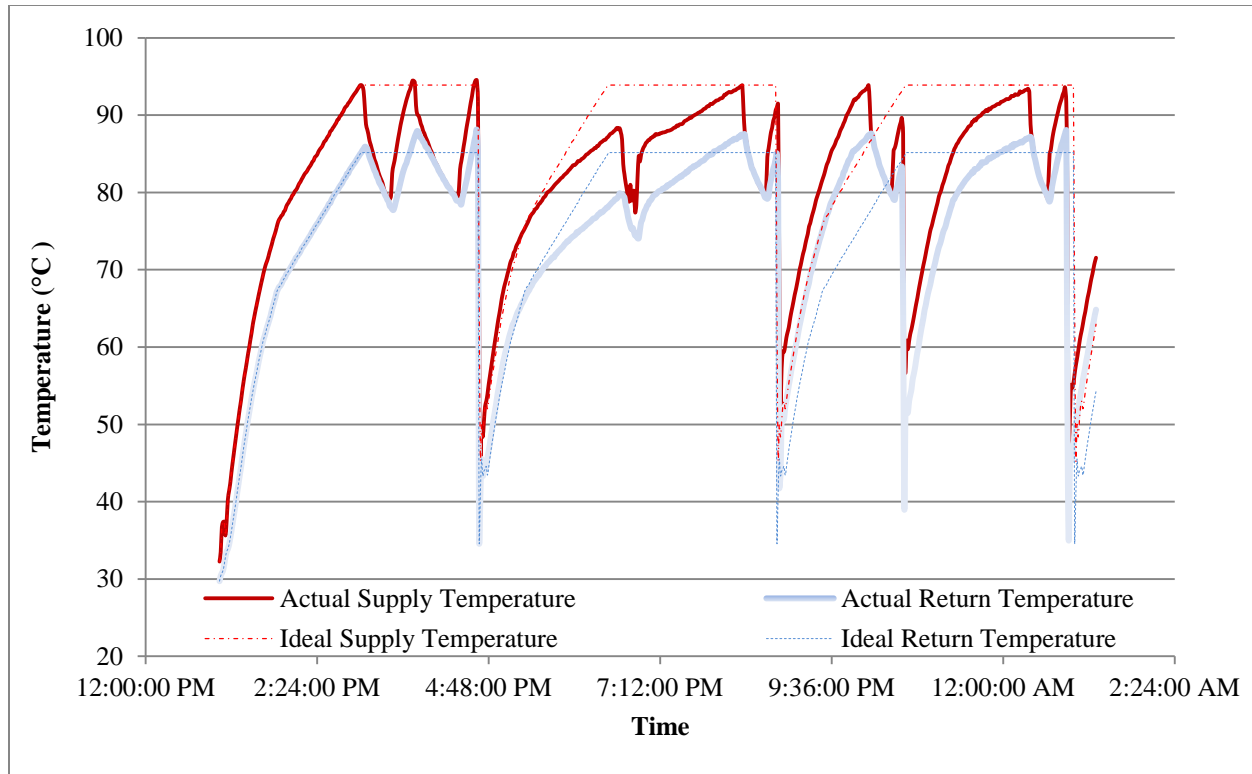


Figure 5.45 - Supply and Return Temperature for both Ideal and Actual Conditions

In order to demonstrate the charging process in detail, one set of charging experiment data that took place on October 20th 2012 and last 416 minutes (from 4:19am to 11:15am) was chosen. It is one of the longest charging periods of Barrel A and the barrel was initially completely discharged.

Figure 5.46 shows the temperature and the flow rate data with respect to time that were collected from different sensors during the charging cycle of Barrel A. From Figure 5.46, it is noted that the supply temperature from the CHP unit reached to its highest limit, which is 95°C while the flow rate of the working fluid in the charging loop was almost 15 L/min. The return temperature was consistently 10°C lower than the supply temperature, which shows a low heat storage rate in the chiller. One possible reason for the low heat transfer rate is the vacuum level of barrels in the ClimateWell unit, also the flow rate is lower than expected, which is another possibility. From the Figure 5.46, also it is observed that temperature of working fluid dropped 6 to 10°C through the heat recovery circuit. The supply temperature to the DHW tanks was between 20°C and 30°C and the return was from 14°C to 19°C while the flow rate of this loop was 14 L/min. It is observed that during on/off cycles of the CHP unit, when the supply temperature in charging loop drops, the condenser heat rejection valve closes and it opens again during next cycle. As a result, on/off cycling

not only decreases the charging efficiency and increases the charging time, but also interrupts the heat rejection process as well.

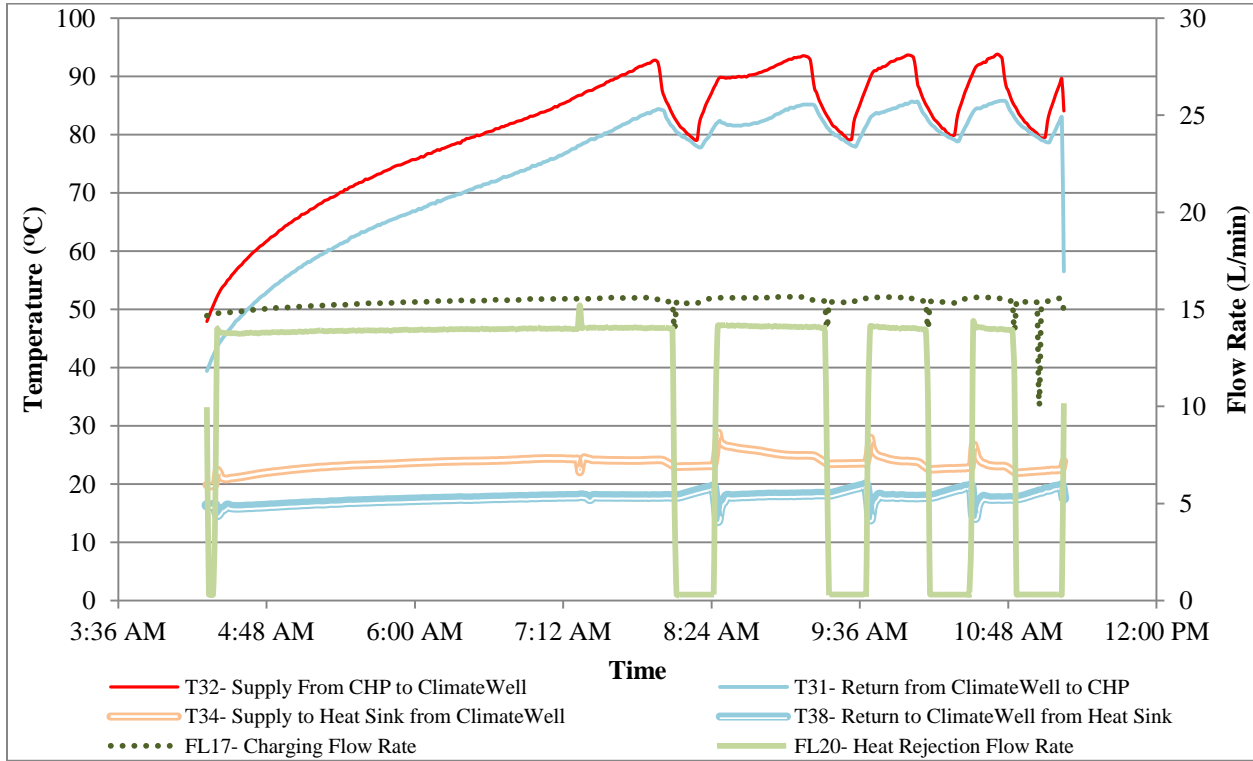


Figure 5.46 - Temperature and Flow Rate of Different Sensors During Charging Process vs Time

Figure 5.47 shows the heat transfer rate, $\dot{Q}_{\text{generation}}$, and total energy production, $Q_{\text{generation}}$, by the Stirling engine during the charging cycle. Figure 5.47 shows a steady heat transfer rate from the start until the on/off cycling began. The average steady heat transfer rate was close to 9 kW and during the cycling period, the heat transfer rate was unstable and it changed from 1 kW to 8.5 kW. According to the cogeneration unit manufacturer the nominal thermal output of the engine is 7 kW with the maximum of 12 kW [66]. From the Figure 5.47, it is also observed that heat transfer rate from the engine decreased during last cycles and when it was close to the end of the charging cycle. Overall, throughout this charging period, 48.63 kWh energy was generated by the Stirling engine.

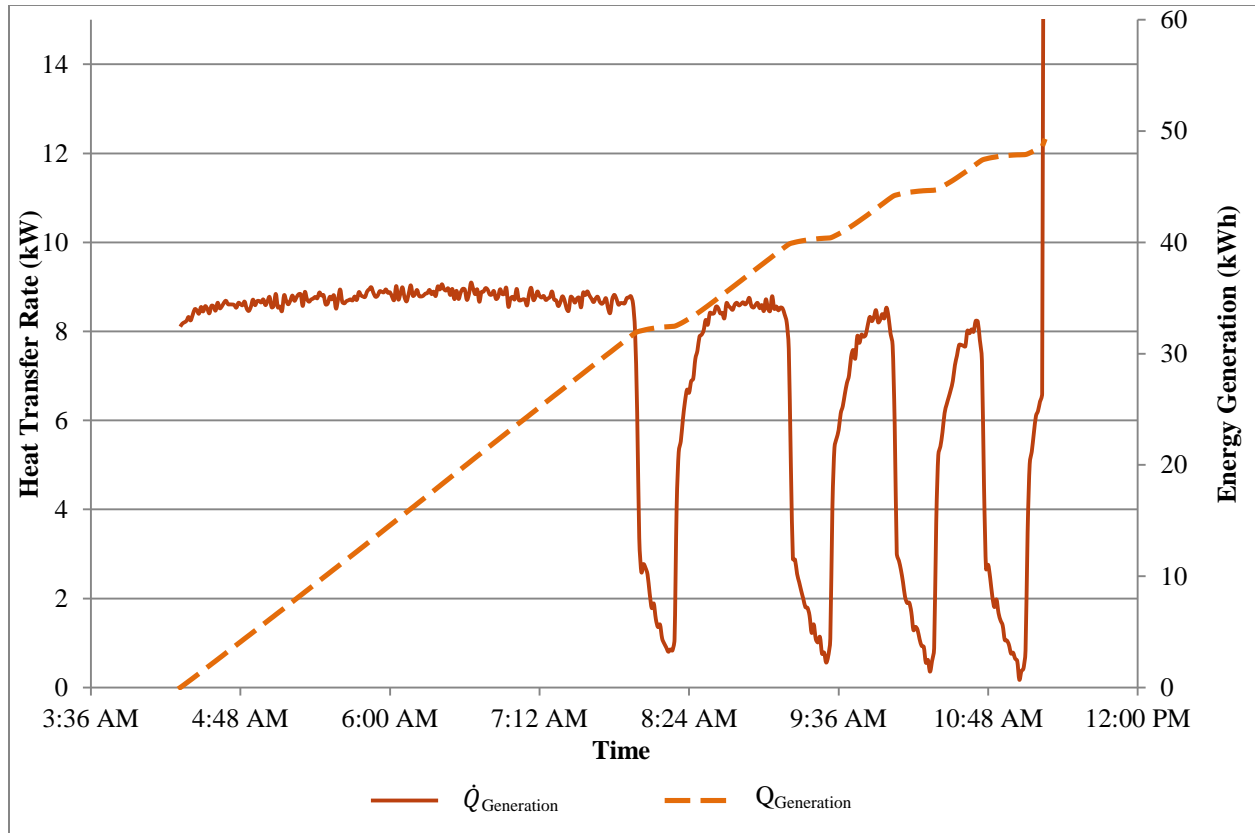


Figure 5.47 - Heat Transfer Rate and Cumulative Energy Generation by the Stirling Engine

Figure 5.48 illustrates the rate of heat rejection and rate of heat storage for the same charging period. At the start of the charging process the stored energy heat transfer rate was higher than the rate of rejection since the desorption process requires lots of energy to start. After almost one hour of charging process the rate of energy storage and rejection stabilized. It is observed from Figure 5.48 that the stabilized rate of heat transfer to be stored in the chiller is almost 3.3 kW and rate of heat rejection is close to 5.8 kW. As mentioned before, as a result of cycling behavior of the Stirling engine, the heat rejection valve in condenser (CHS) closes. Therefore, the heat rejection rate fluctuates when the CHP reaches to its cycling point. This variation in the heat rejection rate directly affects the energy storing rate. Also it is shown that the highest heat rejection rate occurs right after the CHS valve is opened.

Figure 5.49 shows the total thermal and electrical energy generated by the CHP, energy rejected to the heat recovery system, and energy stored in the ClimateWell chiller during the same charging process. In this particular charging period, the cumulative energy generated was 48.63 kWh, while the total energy rejected was 31.90 kWh and chiller stored 16.76 kWh.

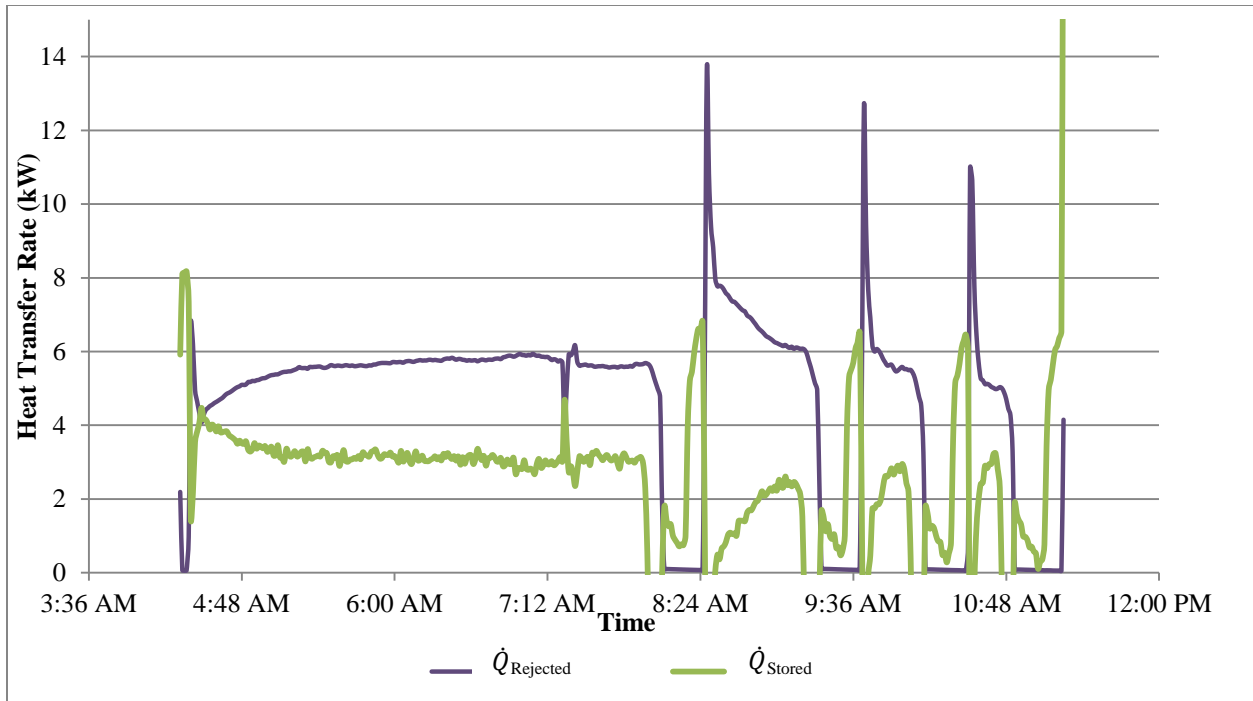


Figure 5.48 - Stored and Rejected Heat Transfer Rate

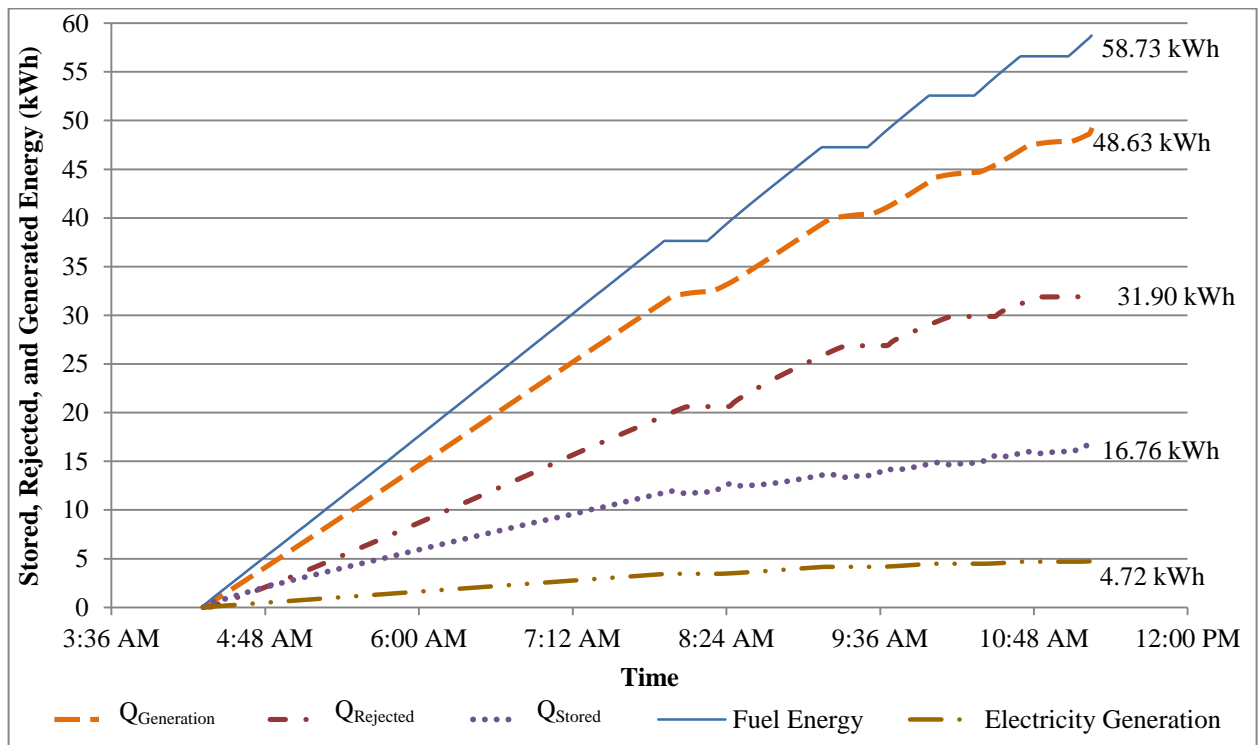


Figure 5.49 - Cumulative Stored, Generated, and Rejected Energy During Charging Period

As it is shown in Table 5.18, the natural gas consumption for this charging period was 5.59 m³, which corresponds to 211.45 MJ or 58.73 kWh. The overall efficiency of the Stirling engine was calculated as 90.03%, which corresponds to 82.8% of thermal efficiency and 8.03% of electrical efficiency. On the other hand, 65.63% of the generated thermal energy was rejected and 34.47% of that was stored into the chiller.

Table 5.18 - Charging Process Results

Fuel Consumption	58.73 kWh
Generated Thermal Energy	48.63 kWh
Generated Electrical Energy	4.72 kWh
Stirling Engine Thermal Efficiency	82.80%
Stirling Engine Electrical Efficiency	8.03%
Stirling Engine Overall Efficiency	90.03%
Rejected Energy	31.90 kWh
Percentage of Rejected Energy	65.63%
Stored Energy	16.76 kWh
Percentage of Stored Energy	34.47%

Since the ClimateWell chiller rejects a lot of thermal energy, a heat recovery system was designed to utilize the rejected energy for the domestic hot water production, using multiple tanks in series and an outdoor fan-coil. Tanks were named as TB-3, TB-4, and TB-5. The working fluid, which needs to be cooled, enters a coil inside the TB-3, then two coils of TB-4, and at the end two coils of TB-5 then finally goes through the fan-coil and returns to the ClimateWell unit. On the other hand, domestic main water fills all three tanks in reverse. The main water fills TB-5, TB-4, and TB-3 in sequence.

Figure 5.50 shows the temperature of the working fluid in heat rejection circuit in different locations. The red line shows the temperature of the working fluid when it leaves the chiller. The dotted lines are the temperatures of the working fluid right after TB-3, TB-4, and TB-5 and the brown line is the temperature of the working fluid after passing through the outdoor fan-coil, which directly returns to the ClimateWell chiller.

The temperature drops less than one degree after the TB-3. This is because, only the top heat exchanger of the tank TB-3 was used for the heat rejection during the experiment. The temperature drops one to two degrees across the TB-4 and three to four degrees across the TB-5. This is because the main domestic cold water first fills up the TB-5. Therefore, the maximum rate of heat rejection happens at this tank. At the end, the working fluid passes through the outdoor fan-coil and the temperature drops two to three degrees before returning to the ClimateWell chiller.

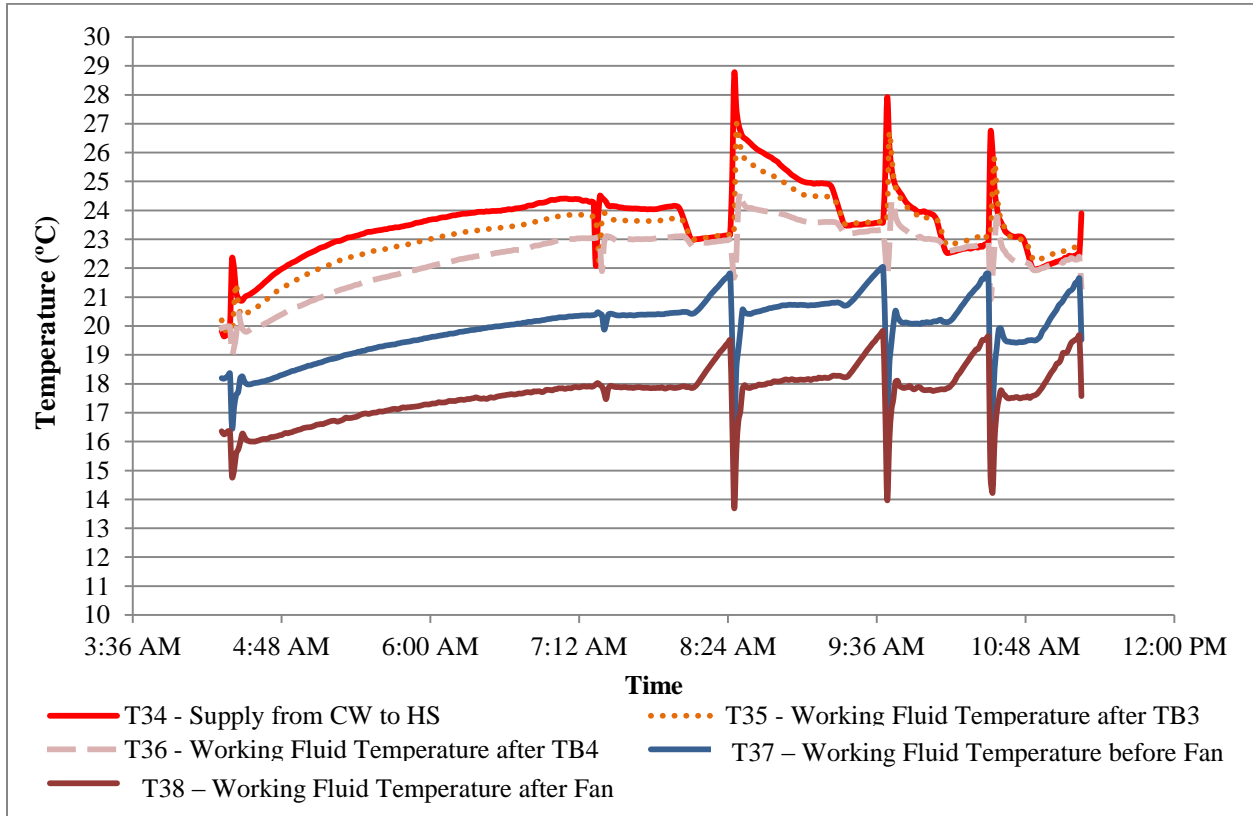


Figure 5.50 - Temperature Variation of Working Fluid in the Heat Rejection Circuit

As shown in Figure 5.51, the domestic main water temperature was at 12.6°C, while the flow rate of DHW draw was almost 3.5 L/min during this charging process and both the temperature and flow rate was almost constant. It is observed from Figure 5.51 that the domestic main water temperature increases after each tank. TB-5 increased the domestic main temperature between 6°C to 9°C. TB-4 could increase the temperature by 2°C to 4°C and TB-3 only increased the temperature by 1°C. The domestic main water temperature after the heat recovery was between 20°C and 25°C. Figure 5.52 shows the share of each tank and outdoor fan-coil in the heat rejection circuit. It is

observed that TB-5 and the fan-coil with 41.49% and 36.33% share are the most effective components in this system and TB-3 with only 8.04% is the least effective one.

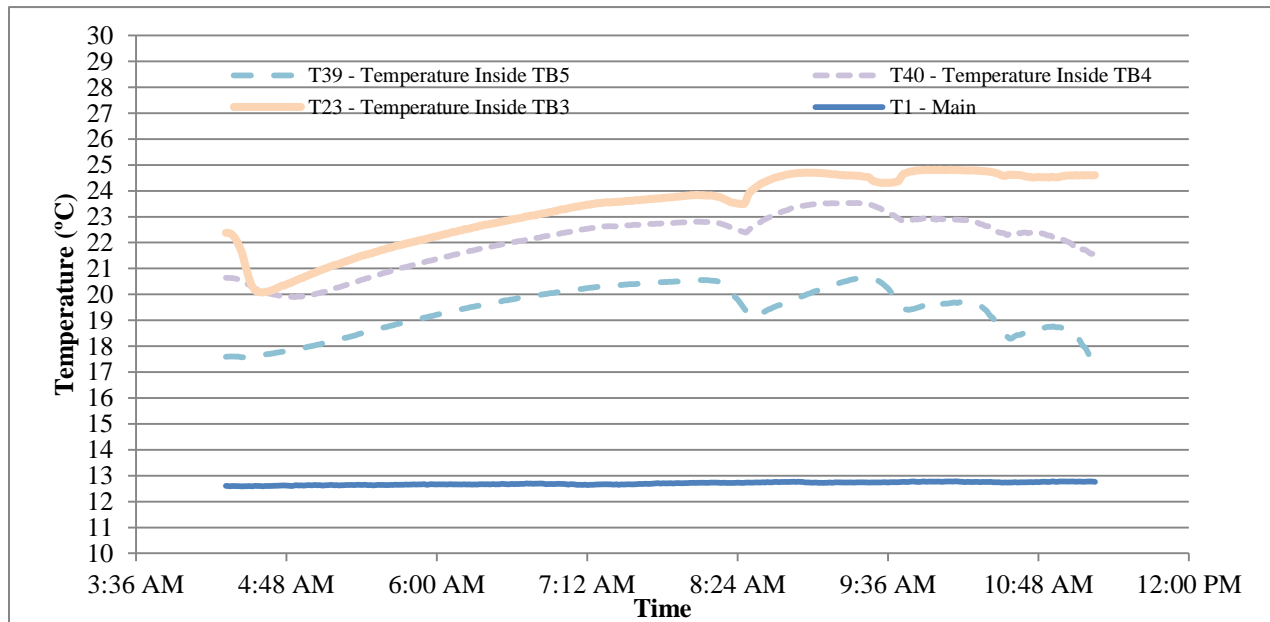


Figure 5.51 - Temperature Variation of Main Domestic Water in Heat Recovery Circuit

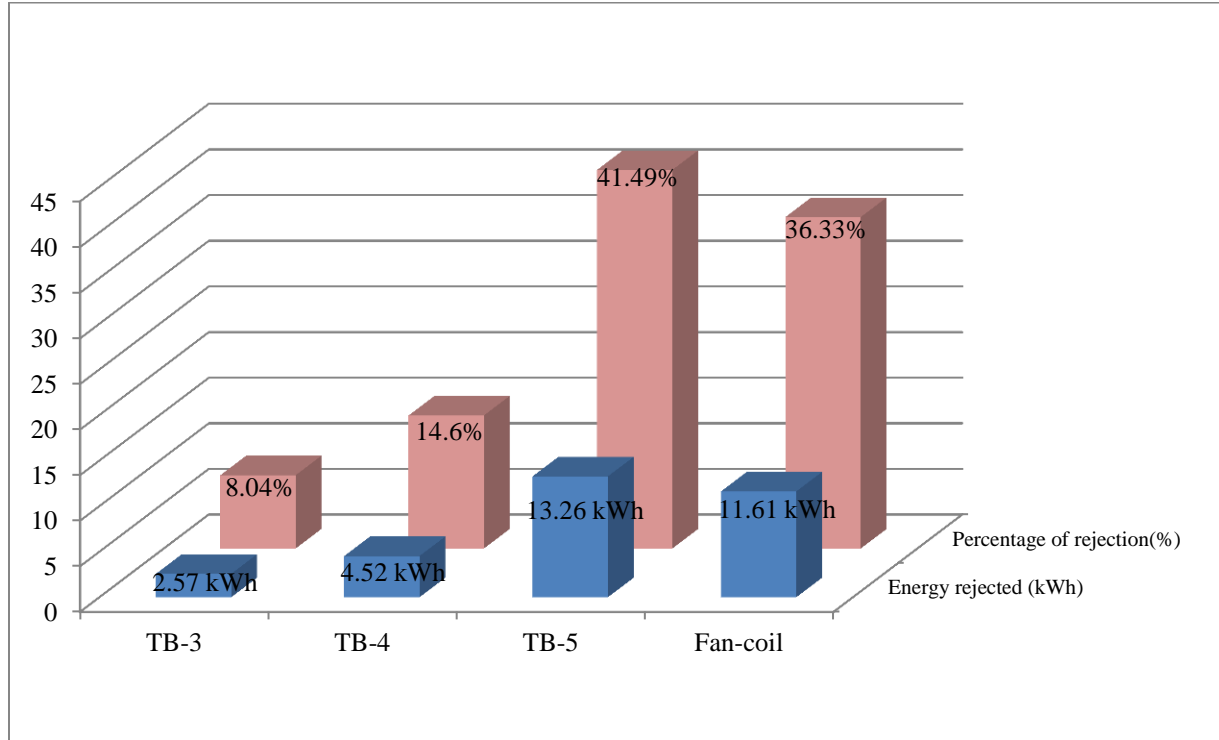


Figure 5.52 - Share of Each Component in the Heat Rejection Circuit

5.3.2 Discharging Behavior of the ClimateWell Chiller

Discharge process, releases the stored energy in the chiller in the form of cooling effect. Condenser air conditioning (CAC) valve opens and water inside the condenser evaporates. The water receives required energy of evaporation from the building space. Water vapor enters to the reactor of the respective barrel where it absorbs by the unsaturated crystal salts and rejects its energy through condensation. At this time, the reactor valve (RHS) connects to the heat rejection circuit to release this condensation energy.

A typical discharging cycle as a show case was selected. This discharge period data collected on October 20, 2012 from 11:36am to 9:01pm, which took 385 minutes to perform. Since there was no natural cooling demand in October, required cooling demand was artificially provided by the in-floor heating system that was connected to the ground source heat pump. The GSHP heated the house and the chiller cooled down the house.

In Figure 5.53, the blue line shows the temperature of the supplied chilled water from the ClimateWell chiller to the AHU. The supply temperature was 8.5°C at the start of the process and increased to 15°C as the barrel discharged. Although the manufacturer claimed that this unit is able to produce the chilled water down to 7°C, the experimental result never showed less than 8°C. The chilled water passes through two coils in series at AHU and returns to the ClimateWell unit. Figure 5.53 also shows the return temperature from the AHU to the chiller by the red line. The temperature difference from supply to return varied from 4°C at the beginning of the cycle to 2°C by the end of the process. The flow rate was almost constant at 11.8 L/min. Figure 5.54 shows the heat transfer rate of discharge process at the AHU and also the cumulative energy, which discharged during this process. The discharge process began with a heat transfer rate of 3.3 kW and as the discharge period continued, the rate of heat transfer decreased to 1.5 kW. According to manufacturer, cooling power of each fully charged barrel is from 3 to 3.5 kW. This rate depends on the heat rejection quality and level of charging. Cooling power is higher when the barrels are fully charged. Also from Figure 5.54, it was observed that 18.11 kWh of the stored energy inside the ClimateWell chiller was used to produce cooling.

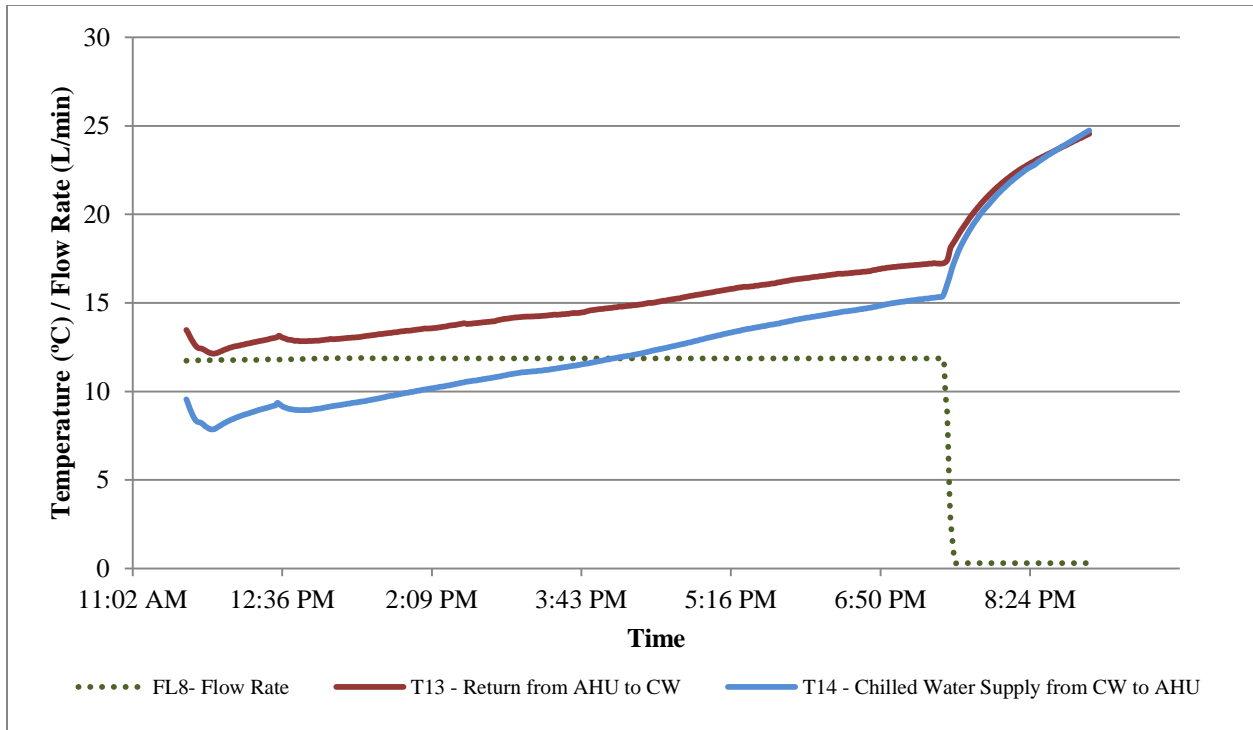


Figure 5.53 - Temperatures and Flow Rate of the AC Loop

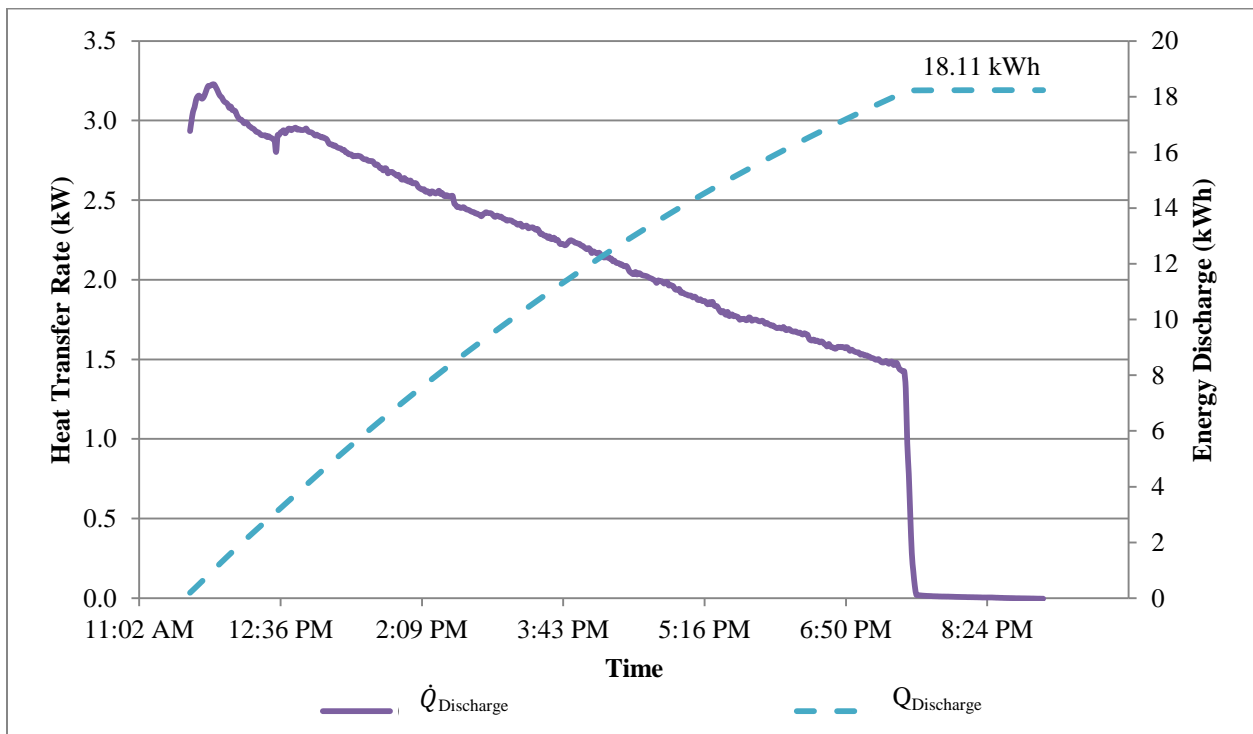


Figure 5.54 - Discharge Rate and Total Discharged Energy

Figure 5.55 shows the heat rejection rate during the discharge period, which started from 7 kW from the beginning and dropped to 2 kW at the end of the process. During this experiment 24.24 kWh of energy was rejected from the chiller. The same heat recovery process also was applied to preheat the domestic main water.

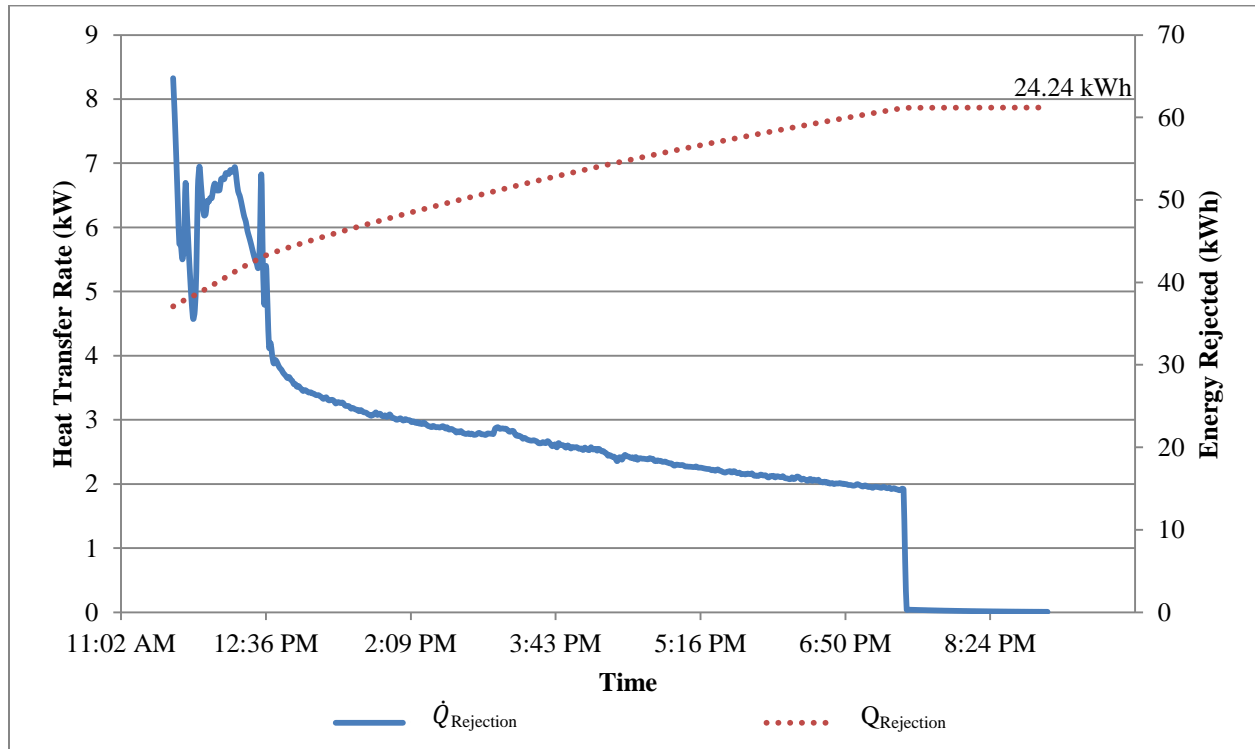


Figure 5.55 - Rejected Rate and Cumulative Rejected Energy

Theoretical COP of the TCA cycle is 0.68 [67] and according to the manufacturer the practical COP of the ClimateWell chiller is from 0.52 to 0.58. Based on limited experimental testing, data analysis of the ClimateWell chiller at the TRCA Archetype Sustainable House (ASH) always showed a COP of between 0.3 and 0.4, which is lower than what manufacturer claimed. The ClimateWell chiller performance is highly dependent on the level of charge and also charging/discharging condition, which is recommended by a charging temperature of higher than what CHP supplied. Therefore, one possible reason that the experimental COP was much lower than expected COP, can be the low charging performance.

5.4 TRNSYS Simulation for Charging and Discharging Optimization

In this section a simulated model of the tri-generation system is discussed and analyzed. This model is used to find the optimized charging and discharging processes. Also the results of simulation as an ideal case and experiments as an actual case are compared and possible improvements are provided.

TRNSYS (TRaNsient SYstem Simulation Program) is a transient system energy modeling software designed to solve complex energy system problems and it is commercially available since 1975. The software uses individual components referred as types connected to each other. Each type represents one part of the system. It recognizes a system description language where the user specifies the components that constitute the system and how they are connected. For instance, the simulated House B model, which was created by previous graduate student [51], can be connected to any HVAC system and the software can estimate the heating and cooling performance of the selected HVAC system in this house under weather condition of a particular city. Moreover, within each component there are inputs, parameters, and outputs that can be linked with other components. The outputs of one component are sent to the inputs of next component. TRNSYS is a powerful modeling software with a comprehensive commercial HVAC component library. Main applications of the software are in solar systems (both thermal and PV), low energy and sustainable buildings, HVAC systems, renewable energy systems, cogeneration, and fuel cells. Capability to add or modify the component code in order to upgrade or change a component is the strength of TRNSYS and the weak point is that by default no assumptions of building and system are made and user needs to have detailed information about the building and the system [68, 69].

5.4.1 Tri-generation Model

In order to model the complete tri-generation system, four essential systems are required to be linked to each other. Which they are listed as followings:

- Calibrated House B TRNSYS model
- ClimateWell chiller type
- Heat rejection system
- Stirling engine based cogeneration system

As mentioned before, the house model was modeled and simulated previously. Since the ClimateWell chiller technology is a registered patent, the TCA TRNSYS model was supplied by the company. The ClimateWell model was validated by Bales and Nordlander [44] and the agreement between the experimental data and simulated result were verified. More detailed description of the model is given by Bales and Ayadi [45]. The heat rejection system was modeled using standard types and components of the TRNSYS program such as tanks and fan-coil. Also the thermal generation of the Stirling engine cogeneration unit was modeled based on the experimental results and actual performance of the engine at the house, using the methodology that was explained in Chapter 4. Figure 5.56 was derived through the polynomial equations, which was defined in Section 4.4.3. This model was the best representative of the experimental data for the installed Whispergen cogeneration system. All the on/off cycling procedures are considered in this model, which named as Type 222. The temperature fluctuation between 67°C and 95°C accurately illustrates the cycling characteristics of the CHP unit.

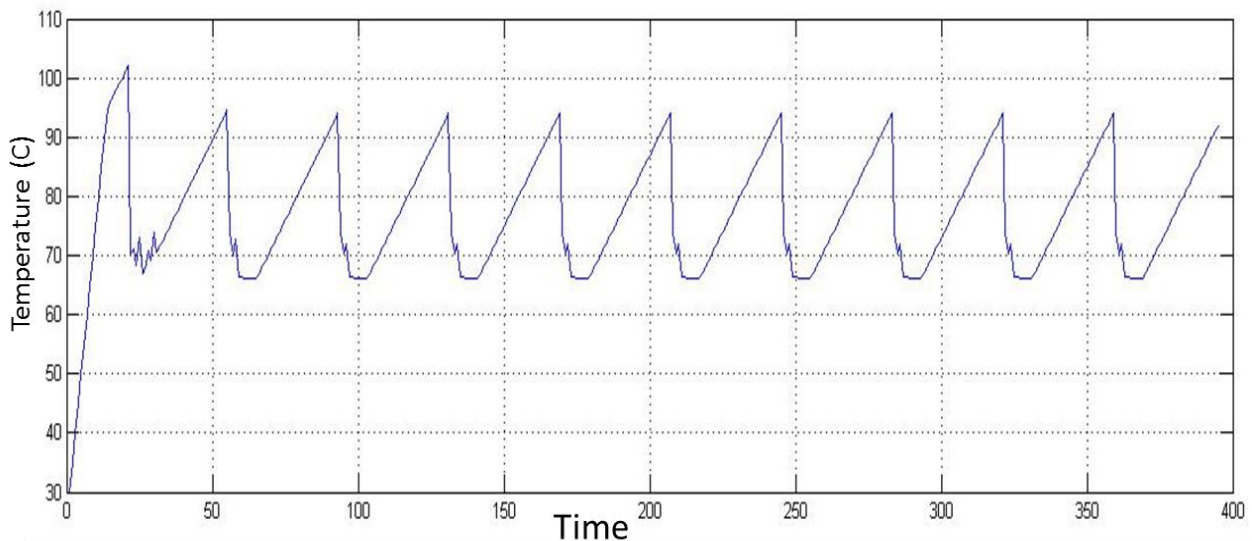


Figure 5.56 - Simulated Behavior of the Stirling Engine Based on the Experimental Result

5.4.2 Charging and Discharging Simulation Result

Understanding the charging process under a realistic condition was the main concern of the project during the preliminary tests and feasibility analysis. Since the heat generation rate of the Stirling engine was at the low end of the minimum charging requirements of the ClimateWell chiller,

the low quality of charging was expected. Although it is experimentally observed that the performance of the tri-generation system at the TRCA house was acceptable, the simulation results show that the state of the charge at each of the barrels is not high enough. Therefore, the ClimateWell chiller is not performing with its highest capacity and at most it is using 60% of its capacity.

Figure 5.57 shows the ideal case (defined by the ClimateWell AB) and the actual case (TRCA systems) together. Since the ClimateWell capacity by default is bigger than a normal single family size, defined ideal condition by the ClimateWell is as follows: The average building cooling demand is 12 kW, which is higher than an average size single family house. The heat generation rate by the heat source must be constantly at 14 kW, while the heat rejection rate at the heat sink must be 30kW. Meeting this defined ideal condition is not possible either at the TRCA house. The TRCA tri-generation condition is as follow and is shown in Table 5.19: The average cooling demand of the ASH is 3.5 kW. The rate of thermal generation by the Stirling engine is 8 kW, which is verified by experiment. And the experimental rate of heat rejection is 6 kW, which can potentially be higher by increasing the domestic main water flow rate and by other means.

Table 5.19 - Details of Ideal Simulated Case by ClimateWell and TRCA Conditions

	IDEAL	TRCA
Average Building Loading Demand (kW)	12	3.5
Rate of Thermal Generation by the Heat Source (kW)	14	8
Rate of Heat Rejection (kW)	30	6

As it is shown in Figure 5.57, state of charge for each barrel in the ideal case is 60 % in the beginning and it increases to 80% after a few cycles. Each charging cycle takes about two hours and each barrel starts discharging when it is full and it continues until the barrel is empty. On the other hand, the upper part of Figure 5.57 shows the state of charge (SOC) of the barrels at TRCA project. In this case each barrel charges up to 50% at the beginning and discharges again, but each time it discharges less than previous cycle, which results in a poor charging/discharging behavior that always stays between 20 and 40%. At first it seems that using a small CHP unit to charge the chiller is the cause of this inefficient performance, but later in this chapter, it will be discussed that a higher heat rejection rate will improve the charging/discharging process.

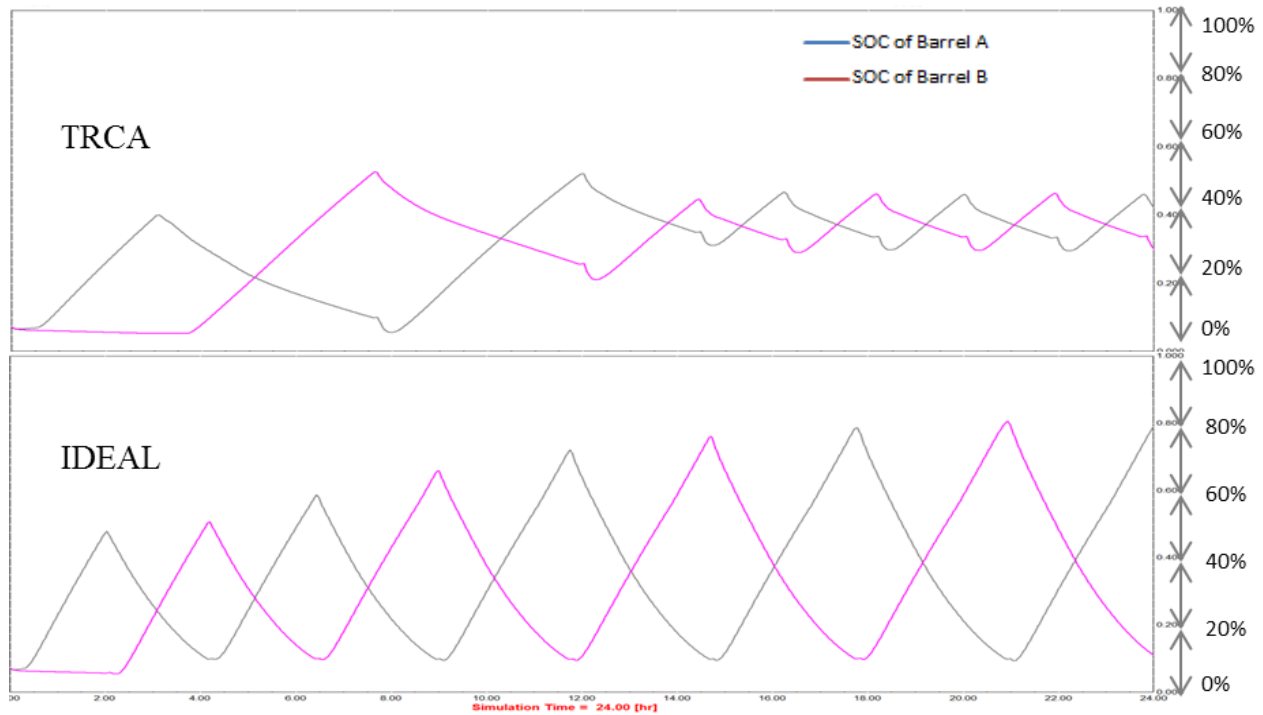


Figure 5.57 – State of Charging of the ClimateWell Barrels for the Ideal Case and TRCA House

Figure 5.58 shows the simulated results for the chilled water supply by the ClimateWell chiller at the TRCA house. Although the SOC of the barrels at the TRCA is not very high, because of the low cooling demand of the building and also high capacity of the chiller it is observed from the Figure 5.58 that temperature of the chilled water supply is very low. Figure 5.58 shows that the temperature of the simulated chilled water supply at the beginning of the discharge process is close to 8°C and it rises to 19°C at the end of each period. The simulated chilled water temperature pattern especially in the beginning has a very good agreement with the experimental results of the chilled water supply sensor (T13), which was discussed in Section 5.3.2.

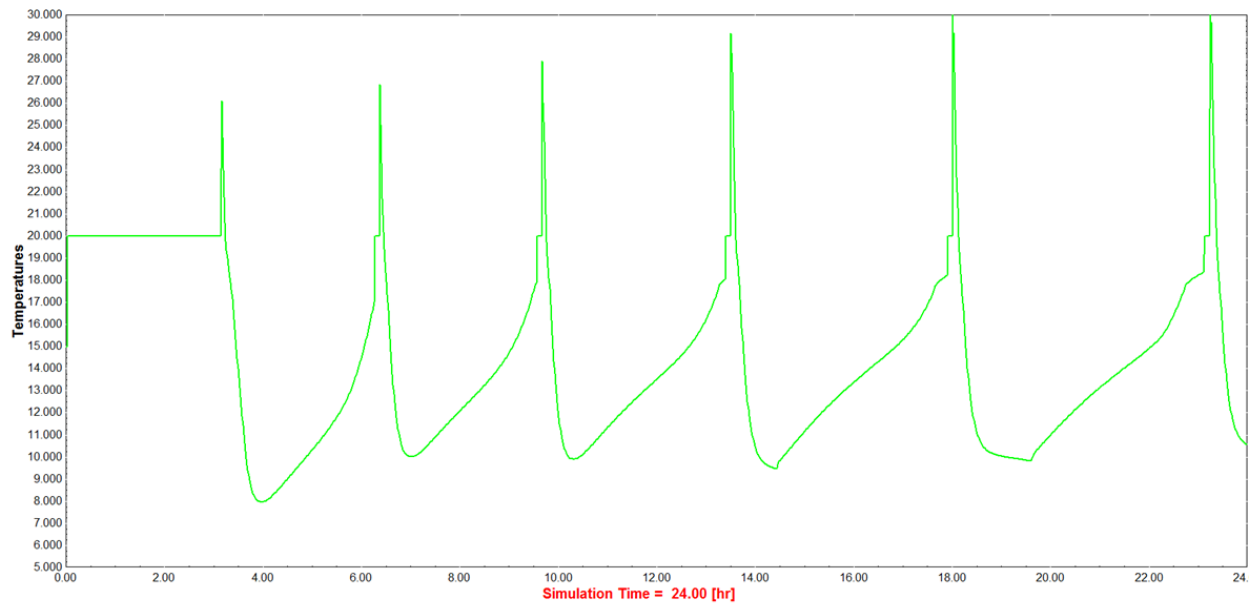


Figure 5.58 - Simulated Chilled Water Supply at TRCA (T13)

5.4.3 Simulation Results of Different CHP and Heat Rejection Systems

Since it was believed that the WhisperGen cogeneration unit is not powerful enough to charge the ClimateWell chiller, a bigger CHP unit was considered in the simulated model to investigate the optimal size of the required heat source.

Figure 5.59 shows the SOC level of the ClimateWell barrels when all the conditions are the same at TRCA and the Stirling engine is replaced by a bigger CHP unit that can generate the thermal energy at the rate of 10 kW. As it is shown in the Figure 5.59 the results are not what it was expected. Unlike the general believe that a bigger CHP unit with a higher thermal generation rate can charge the chiller more effectively, the simulated result shows that the charging process is more dependent on the heat rejection rate rather than heat generation rate. To investigate more, Figure 5.60 was generated, which is the simulated results of the TRCA house with a higher heat rejection rate of 10 kW instead of 6 kW. These results also support the fact that heat rejection rate is more effective in the charging process. As Figure 5.60 shows, the SOC of the barrels are more improved compared to original condition of the TRCA house in Figure 5.57. It should be noted that all these results are based on average cooling demand of 3.5 kW.

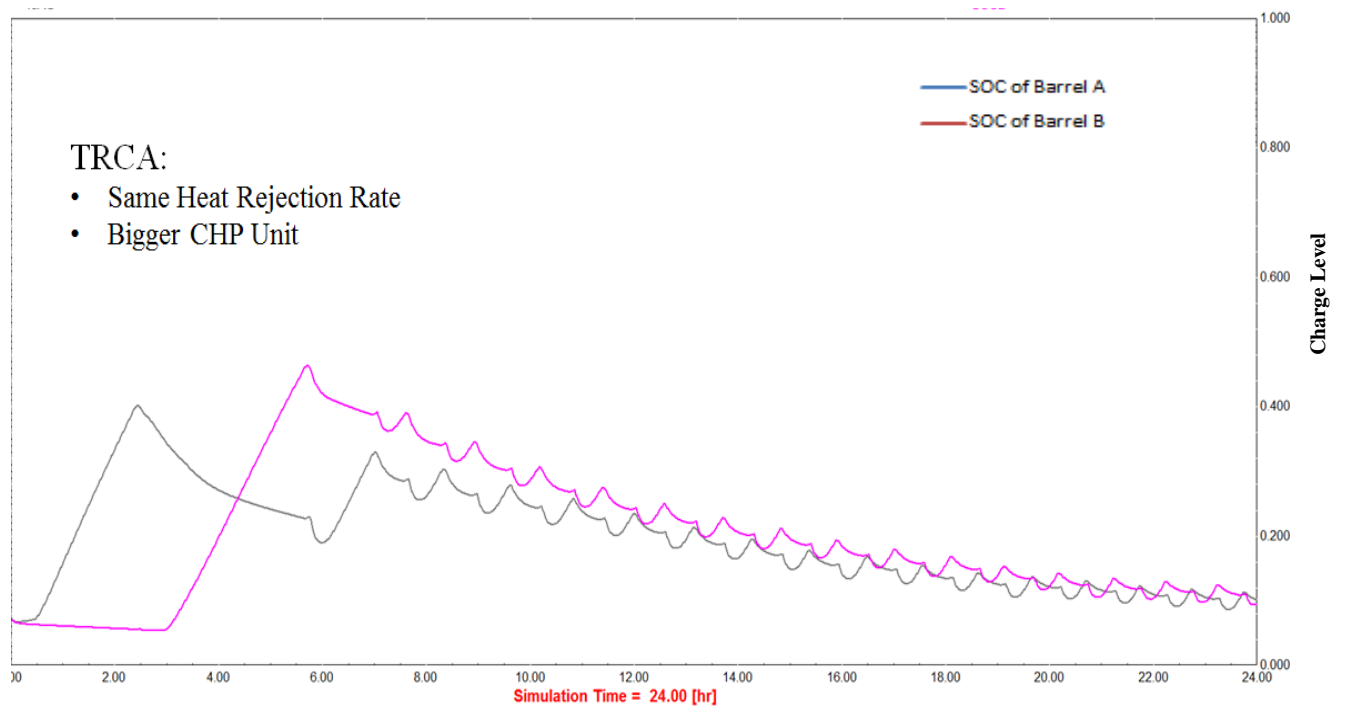


Figure 5.59 - Simulated SOC of the ClimateWell Barrels with a Bigger CHP Unit at TRCA

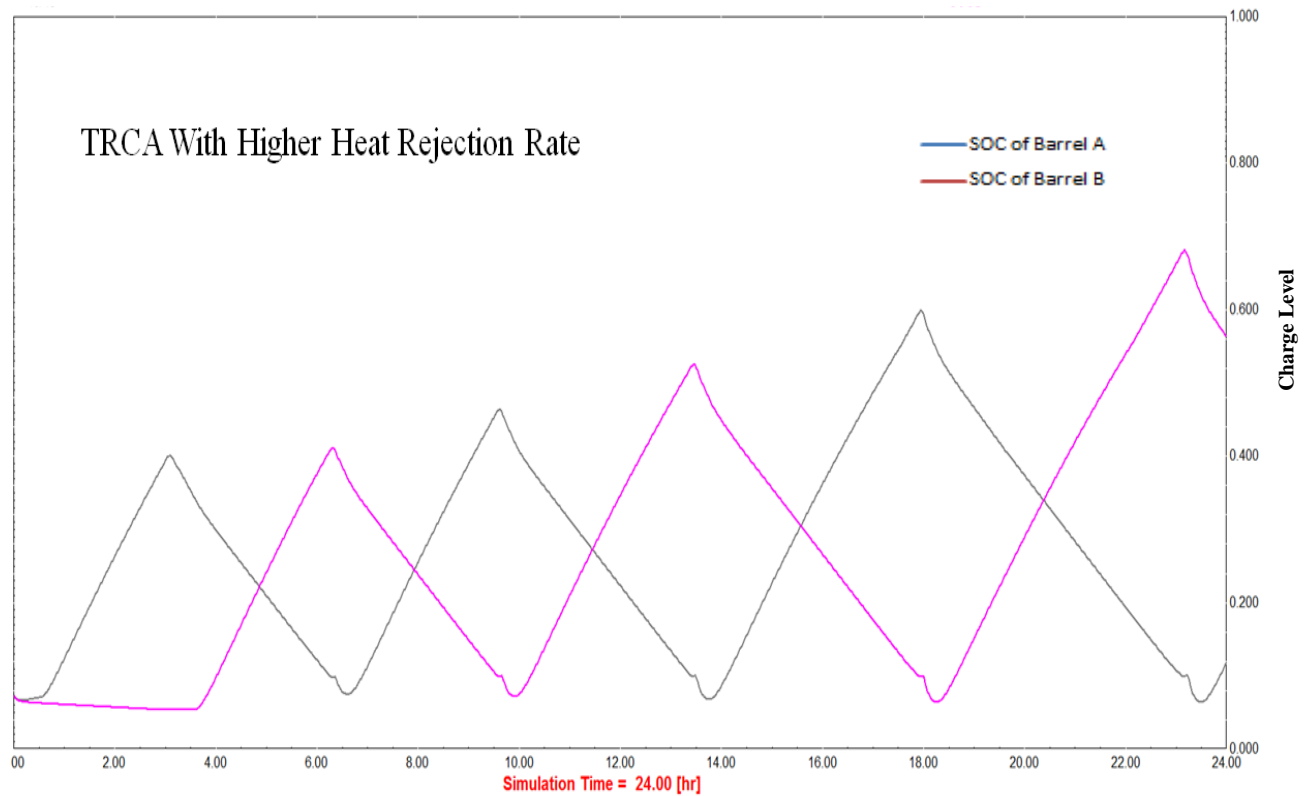


Figure 5.60 - Simulated SOC of the ClimateWell Barrels at TRCA with Higher Heat Rejection Rate

Furthermore, in order to support this fact, another series of simulation test was conducted. This time, a 10 kW heat rejection rate and a smaller CHP unit (4 kW thermal generation rate) were used, this means that the TRCA house is used in a model with higher heat rejection rate and smaller heat source. As Figure 5.61 shows, although the SOC of the barrels are less than 40% and respective charging times are three hours, the charging/discharging periods are in a regular order. Also the green line in Figure 5.61 shows the simulated chilled water supply temperature which is very reasonable with a minimum of 6°C for a few minutes and rising to 20°C during the discharge process.

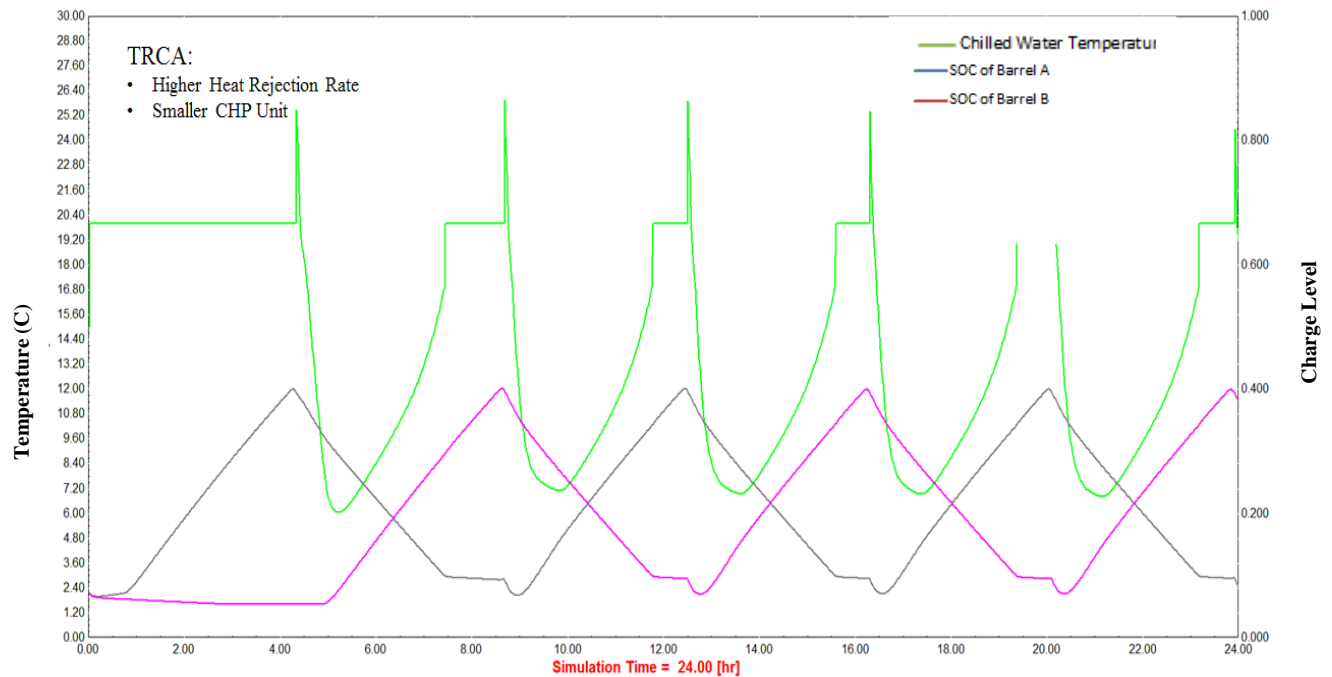


Figure 5.61 - Simulated SOC of the ClimateWell Barrels at TRCA with Smaller CHP Unit and Higher Heat Rejection Rate

As a result, the tri-generation system, because of the low cooling demand at TRCA house is feasible. Although the heat rejection rate during the experiment was 6 kW, the heat rejection circuit at the house is designed in a way that the heat rejection rate can be increased by increasing the flow rate of the domestic main water. Also the existing borehole, which is designed and installed for the ground source heat pump, can be used to increase the heat rejection rate. It is recommended to investigate the effect of heat rejection rate on the charging quality in the future sets of experiment.

Chapter 6 - Summary and Conclusion

A new micro residential tri-generation system was designed and installed at TRCA Archetype Sustainable House. A Stirling engine cogeneration unit was tested to investigate the thermal and electricity generation performance. The potential improvement of the engine was also explored in order to produce continuous high-grade thermal energy. After troubleshooting of the cogeneration unit and modifying the safety shut off control circuit, a comprehensive test series was conducted on the Stirling engine. The TRNSYS simulation model was used to observe the cooling and heating load demands of House B. Accordingly, a feasibility analysis using the extrapolation of the experimental results and the simulated house's thermal demands was carried out based on the daily outdoor average temperature. The same methodology was used for a few other Canadian cities in order to estimate the potential performance of the tri-generation system in different climatic conditions. After commissioning the whole integrated system, the tri-generation system was tested under the artificial cooling demand provided by the GSHP through the in-floor heating system. Data were collected by means of the associated sensors. The ClimateWell chiller was calibrated accordingly. Due to limited experiments, only a few cycles of charging and discharging were performed. The results showed that the Stirling engine cogeneration unit was not able to fully charge the ClimateWell chiller. The chiller was able to produce chilled water down to 8°C. The rate of heat rejection through the heat recovery system was 6 kW, which could be higher by increasing the flow rate of the DHW draw and/or using the borehole. The CHP model in TRNSYS was modified according to the experimental results. The overall tri-generation model in TRNSYS was used to verify the potential improvement in the system.

6.1 Summary of Results

In this section, the summary of results for this study regarding to the CHP performance, feasibility analysis, cost analysis, tri-generation performance, and simulation are provided.

6.1.1 The Stirling Engine Performance

The experimental results for a long-term monitoring of the cogeneration unit, using only the main burner, showed that the average overall efficiency of the system is higher than 89%, which corresponds to the average thermal efficiency of the 78% and average electrical efficiency of 11%.

Employing the auxiliary burner increased the overall efficiency up to 90% and also supplied higher temperature.

6.1.2 Feasibility Analysis

The feasibility analysis was discussed in Section 5.2. The experimental results were extrapolated for the whole heating season; as a result, it is shown that the Stirling engine cogeneration unit is able to provide enough thermal energy for those days that the outdoor daily average temperature is higher than -17°C. Moreover, considering the COP of 0.5 for the chiller, the required thermal energy to charge the chiller in cooling season was estimated. Also, the gas consumption and run time of the engine were assessed. The same methodology was used to estimate the annual gas consumption, electricity generation, and cooling demand of the tri-generation system in other Canadian cities. The house model was used to simulate the cooling and heating demands of the ASH in Halifax, Vancouver, Montreal, Edmonton, and Toronto. Halifax has the lowest cooling demand among all these cities and Montreal has the highest cooling demand.

6.1.3 Cost and GHG Emission Analysis

Cost estimation is based on the 28 ¢/m³ for the natural gas price and \$0.124/kWh for the electricity price. Also the GHG emission factor in Ontario for the electricity was calculated based on 100g CO₂/kWh and 180.3g CO₂/kWh for the natural gas. The annual operation cost of the tri-generation was estimated \$472.56 and annual GHG emission production was calculated to be 4607.35 kg CO₂. Cost and GHG emission of two different conventional systems were compared to the integrated system, which resulted in 42% and 57% higher annual operation cost and lower GHG emission production.

6.1.4 The Tri-generation System Performance

The experimental results of the integrated system showed that during charging process more than 65% of the supplied thermal energy to the ClimateWell chiller was rejected and only 35% of the thermal energy was absorbed by the chiller. It is also observed that the stabilized rate of thermal energy storage in the chiller is almost 3.3 kW and rate of heat rejection is around 5.8 kW. Besides, the average steady heat generation rate was around 9 kW and during the cycling period, the heat generation rate was unstable and it changed from 1 kW to 8.5 kW.

Tank TB-5 is the most effective component of the heat rejection circuit, which rejects more than 43% of the total rejected heat. The outdoor fan coil rejects 36% while TB-4 with 14% and TB-3 with 8% are less effective components. During discharge process, the heat transfer rate for the AC loop started from 3 kW and decreased to 1.5 kW. Besides, the heat rejection rate was lower compared to the charging process as it was expected because of the nature of discharging process. It was also observed that the supply AC loop working fluid temperature was 8.5°C at the beginning of the process and increased to 15°C as the barrel discharged.

6.1.5 TRNSYS Simulation

In previous sections, the house model was modeled and simulated. Validated chiller's model was provided by the ClimateWell AB. The heat rejection system was modeled using standard types and components of the TRNSYS program such as tanks and fan-coil. The thermal generation of the Stirling engine cogeneration unit was also modeled based on the experimental results and actual performance of the engine at the house. Completed model was tested with ideal condition defined by the ClimateWell and the actual condition at TRCA. Correspondingly, the model was tested based on a bigger size CHP system and higher heat rejection rate. As a result, a higher heat rejection rate would improve the quality of charging and discharging process.

6.2 Author's Contribution

This study has contributed a fair amount of results, which are novel regarding to literatures and previous studies. The Archetype Sustainable House has provided the opportunity of testing the tri-generation system in a real residential condition. An accurate data acquisition system has greatly contributed to the precise data collection. The residential tri-generation system based on a gas fired CHP and a TCA was the first of its kind to be tested in Canada. The thesis delivered a detailed feasibility analysis along with experimental data analysis and energy simulation result. Author's contribution can be summarized as follows:

- I. Detailed study about different types of cogeneration system such as: IC engines, Fuel Cells, and Stirling engines
- II. Comprehensive study about different thermally driven chillers such as: absorption, adsorption, and thermo chemical accumulator
- III. Data analysis of the Stirling engine's cogeneration system

- IV. Feasibility analysis of tri-generation system based on the cogeneration performance and extrapolating those results for the whole year and different cities
- V. Designing a heat recovery system to utilize the wasted heat from the chiller for domestic hot water use
- VI. Commissioning the newly integrated system including the chiller, tanks, outdoor fan coil, and sensors
- VII. Data analysis of the tri-generation experiments and performance evaluation of the system.
- VIII. Modifying the CHP type in TRNSYS and using the complete model to verify the experimental results and investigate the potential improvements of the system

6.3. Recommendations and Future Works

The following points are recommended based on the results of the study:

- I. Since the cyclic behavior of the cogeneration unit affects the charging process and heat rejection performance, one or all of the following options are recommended:
 - Installing an electric heater in the supply line of the CHP to reach continuously higher temperature
 - Installing a bigger circulation pump for the charging circuit to increase the heat transfer rate
 - Finding an alternative CHP unit with higher thermal generation capacity at higher supply temperature to replace the existing CHP system
 - Connecting solar thermal collectors to the supply line of the charging circuit to increase the supply temperature. Piping of this solar auxiliary system is predicted and installed during the commissioning process.
- II. Additional ground loop is installed at the TRCA house to test the GSHP system. Using the existing borehole as an independent heat rejection system or as an auxiliary system in series with the existing heat rejection system is recommended to study the effects of higher heat rejection rate on the charging and discharging process.
- III. Due to limited number of experiments on the tri-generation system because of the heating season, it is highly suggested to repeat the experiments in the cooling season. The results in this thesis are generated based on the artificial cooling demand. Another set of experiments in

summer time could explore other aspects of charging, discharging, and heat rejection difficulties.

- IV. Regular temperature sensors calibration is highly recommended. Since the experimental results of the chiller shows lower performance than ClimateWell claimed, it is suggested to check the vacuum of both barrels before future tests.

Bibliography

- [1] Swan, L. G., Ugursal, V. I., "Modeling Of End-Use Energy Consumption In The Residential Sector: A Review Of Modeling Techniques", *Renewable and Sustainable Energy Reviews*, vol. 13, pp.1819–1835, 2009.
- [2] Saidur, R., Masjuki, H., and Jamaluddin, M., "An Application Of Energy And Exergy Analysis In Residential Sector Of Malaysia", *Energy Policy*, vol. 35, pp. 1050-1063, 2007.
- [3] NRCan., "Energy Efficiency Trends in Canada 1990 to 2007", Office of Energy Efficiency Natural Resources Canada, Ottawa, 2009.
- [4] NRCan., "Households and the Environment: Energy Use", authority of the Minister responsible for Statistics Canada - Minister of Industry, Ottawa, 2010.
- [5] Frangopoulos., EDUCOGEN, The European Education Tool on Energy-Efficiency through the Use of Cogeneration, March 2002.
- [6] Knight, I., Ugursal, I., and Beausoleil-Morrison, I., "Residential Cogeneration Systems: A Review of The Current Technologies. A Report of Subtask A of FC+COGEN-SIM. The Simulation of Building-Integrated Fuel Cell and Other Cogeneration Systems", Annex 42 of the International Energy Agency, Energy Conservation in Buildings and Community Systems Programme, Ottawa, 2005.
- [7] Al-Sulaiman, F., Hamdullahpur, F., and Dincer, I., "Trigeneration: A Comprehensive Review Based On Prime Movers", *International Journal Of Energy Research*, vol. 35, pp. 233–258, 2011.
- [8] Zhang, D., Barua, R., and Fung, A., "TRCA-BILD Archetype Sustainable House - Overview Of Monitoring System And Preliminary Results For Mechanical Systems", *ASHRAE Transactions*, vol. 117, no. PART 2, pp. 597-612, 2011.
- [9] Zhang, D., Barua, R., and Fung, A., "Development of Monitoring System for the Sustainable Archetype House at Kortright Centre", *1st International High Performance Buildings Conference*, Purdue, 2010.
- [10] Barua, R., Zhang, D., and Fung, A., "Analysis of Energy Performance of the Sustainable Archetype House at Kortright Centre", *1st International High Performance Buildings Conference*, Purdue, 2010.
- [11] Aussant, C. D., Fung, A. S., and Ugursal, V. I., "The Feasibility Of Internal Combustion Engine Based Cogeneration In Residential Applications", *International Building Performance Simulation Association*, pp. 183-190, 2007.
- [12] "Cogeneration at Small Scale, Simultaneous Production of Electricity and Heat", European Renewable Energy Council, European Biomass Industry Association, RESTMAC.

- [13] I. a. I. C., Energy and Environmental Analysis, "Technology Characterization:Reciprocating Engines", US Environmental Protection Agency,Combined Heat and Power Partnership Program, Washington DC, 2008.
- [14] "Resource Recovery", 20 April 2012. [Online]. Available: www.kingcounty.gov. [Accessed 28 April 2012].
- [15] Onovwiona, H., Ugursal, V., and Fung, A., "Modeling of Internal Combustion Engine based Cogeneration Systems for Residential Applications", *Applied Thermal Engineering (JATE)*, vol. 27, no. 5-6, pp. 848-861, 2007.
- [16] Aussant, C., Fung, A., Ugursal, V., and Taherian, H., "Residential Application of Internal Combustion Engine Based Cogeneration in Cold Climate—Canada", *Energy and Buildings*, vol. 41, no. 12, pp. 1288-1298, 2009.
- [17] I. a. I. C., Energy and Environmental Analysis, "Technology Characterization:Fuel Cell", U.S. Environmental Protection Agency, Combined Heat and Power Partnership Program, Washington DC, 2008.
- [18] "www.nedstack.com", Nedstack PEM Fuel Cells, 2011. [Online]. Available: <http://www.nedstack.com/technology/fuel-cell-types>. [Accessed 8/3/2013].
- [19] Hirschenhofer, J., "Fuel cell status: 1996", *IEEE Aerospace and Electronic Systems Magazine*, vol. 12, no. 3, pp. 23-28, 1997.
- [20] Bowman, L., "Small Modular Power Development At External Power, LLC: Residential And Small Commercial", External Power, LLC., Athens.
- [21] Aliabadi, A., Thompson, M., Wallace, J. S., Tzanetakis, T., Lamont, W., and Carlo, J. D., "Efficiency and Emission Measurement of a Stirling-Engine-Based Residential Microcogeneration System Run on Diesel and Biodiesel", *Energy and Fuels*, vol. 23, pp. 1032-1039, 2009.
- [22] Kongtragool, B., and Wongwises, S., "A Review Of Solar-Powered Stirling Engines And Low Temperature Differential Stirling Engines", *Renewable and Sustainable Energy Reviews*, vol. 7, pp. 131-154, 2003.
- [23] Hsu, S., Lin, F., and Chiou, J., "Heat-Transfer Aspects Of Stirling Powergeneration Using Incinerator Waste Energy", *Renewable Energy*, vol. 28, pp. 59-69, 2003.
- [24] Rix, D., "Some Aspects of the Outline Design Specification of a 0.5 kW Stirling Engine for Domestic Scale Co-generation", *Proceedings of the Institution of Mechanical Engineers, Part A: Journal of Power and Energy*, vol. 25, 1996.
- [25] Angrisani, G., Roselli, C., and Sasso, M., "Distributed Microtrigeneration Systems", *Progress in Energy and Combustion Science*, vol. 1, no. 20, 2012.
- [26] Marianne, M., Frank, S., John, G., Evgueniy Entchev, M. S., and Mark, D., "Integration And Monitoring Of Microchp Systems In Residential Application At The Canadian Centre For Housing Technology", National Resource Council Canada, Ottawa, 2008.

- [27] Ribberink, H., Mottillo, M., and Bourgeois, D., "Performance Assessment Of Prototype Residential Cogeneration Systems In Single Detached Houses In Canada, A Report Of Subtask C Of FC-Cogen-SIM The Simulation Of Building Integrated Fuel Cell And Other Cogeneration Systems", Annex42 of the International energy agency, energy conservation in buildings and community service programme , 2007.
- [28] Aliabadi, A. A., Thomson, M. J., and Wallace, J. S., "Efficiency Analysis of Natural Gas Residential Micro-cogeneration Systems", *Energy Fuels*, vol. 24, pp. 1704-1710, 2010.
- [29] Farra, N., Tzanetakis, T., and Thomsom, M. J., "Experimental Determination of the Efficiency and Emissions of a Residential Microcogeneration System Based on a Stirling Engine and Fueled by Diesel and Ethanol", *Energy and Fuels*, vol. 26, pp. 889-900, 2012.
- [30] Sibilio, S., Sasso, M., Possidente, R., and Roselli, C., "Assessment of Micro-Cogeneration Potential for Domestic Tri-generation", *International Journal of Environmental Technology and Management*, vol. 7, pp. 147-164, 2007.
- [31] Roselli, C., Sasso, M., Sibilio, S., and Tzscheuschler, P., "Experimental Analysis of Microcogenerators based on Different Prime Movers", *Energy and Buildings*, vol. 43, pp. 796-804, 2011.
- [32] "MicroCHP system Model PPS24-ACLG-5", www.whispergen.com, Manual, Whispergen Micro CHP User.
- [33] "European Commission", 7/2/2013. [Online]. Available: <http://ec.europa.eu/europe2020>. [Accessed 20/2/2013].
- [34] Núñez, T., "Technology and Literature", PolySMART, Integrated Project partly funded by the European Union, Cordinated by Fraunhofer Institute for Solar Energy Systems ISE, Germany, 2004.
- [35] Srikuhirin, P., Aphornratana, S., and Chungpaibulpatana, S., "A Review Of Absorption Refrigeration Technologies", *Renewable and Sustainable Energy Reviews*, vol. 5, p. 343–372, 2001.
- [36] Iyer, P., Murthy, S., and Murthey, M., "Analysis Of Three Pressure Vapor Absorption Refrigeration Systems", *Renewable Energy*, vol. 1, no. 1, pp. 55-58, 1991.
- [37] Liu, Y., Wang, R., and Xia, Z., "Experimental Performance Of A Silica Gel–Water Adsorption Chiller", *Applied Thermal Engineering*, vol. 25, p. 359–375, 2005.
- [38] Saravanan, R., and Maiya, M. P., "Thermodynamic Comparison Of Water-Based Working Fluid Combinations For A Vapour Absorption Refrigeration System", *Applied Thermal Engineering* , vol. 18, no. 7, pp. 553-568, 1998.
- [39] "The Basics of R718: the Adsorption cycle", 10/08/2012. [Online]. Available: <http://www.r718.com/news/viewprintable/3432>. [Accessed 21/02/2013].
- [40] Tangkongsirisin, V., Kanzawa, A., and Watanabe, T., "A Solar-Powered Adsorption Cooling System Using A Silica Gel–Water Mixture", *Energy*, vol. 23, no. 5, p. 347–353, 1998.

- [41] Aprile, M., "The Market Potential Of Micro-CHCP", Integrated Project partly funded by the European Union coordinated by Fraunhofer Institute for Solar Energy Systems ISE, Germany, 2004.
- [42] Sanjuan, C., Soutullo, S., and Heras, M., "Optimization Of A Solar Cooling System With Interior Energy Storage", *Solar Energy*, vol. 84, p. 1244–1254, 2010.
- [43] "www.Climatewell.com", Climate-Well Chiller/Product Description. [Online]. [Accessed 12 April 2012].
- [44] Bales, C., and Nordlander, S., "TCA Evaluation Lab Measurements, Modelling and System Simulations", Master Thesis in Högskolan Dalarna, December 2005.
- [45] Bales, C., and Ayadi, O., "Modelling Of Commercial Absorption Heat Pump With Integral Storage", *Effstock 2009 - The 11th International Conference on Energy Storage*, Stockholm, Sweden, 2009.
- [46] Zhang, D., Barua, R., and Fung, A., "TRCA-BILD Archetype Sustainable House – Overview of Monitoring System and Preliminary Results for Mechanical Systems", *ASHRAE Transactions*, vol. 117, no. 2, pp. 597-612, 2011.
- [47] "The Archetype Sustainable House", 2009. [Online]. Available: <http://www.sustainablehouse.ca/>. [Accessed 27/2/2013].
- [48] Dembo, A., Fung, A., NG, K. R., and Pyrka, A., "The Archetype Sustainable House: Investigating Its Potentials To Achieving The Net-Zero Energy Status Based On The Results Of A Detailed Energy Audit", *1st International High Performance buildings confrence purdue university*, Purdue, 2010.
- [49] Barua, R., "Assessment And Energy Benchmarking For Two Archetype Sustainable Houses Through Comprehensive Long Term Monitoring", Master of Applied Science Thesis, Ryerson University, Toronto, 2010.
- [50] The California Public Utilities Commission (CPUC), "California Solar Initiative Program Handbook", California Solar Initiative, California, 2009.
- [51] Safa, A., "Performance Analysis Of A Two-Stage Variable Capacity Air Source Heat Pump And A Horizontal Loop Coupled Ground Source Heat Pump System", Ryerson University, Master of Applied Science Thesis, Toronto, Ontario, Canada, 2012.
- [52] "Control System Manual of ClimateWell SolarChiller", ClimateWell AB, Article no: 700021 Version: v9:33.3 EN, 2010.
- [53] "DATA SHEET; Temperature Sensors and Pockets", Kamstrup, 2009.
- [54] Kuphaldt, T. R., "Instrumentation, Lessons In Industrial", in *13.9.2 Temperature Standards*, San Francisco, Creative Commons, California, 94105, USA, 2009, pp. 353-355.
- [55] "www.proteusind.com", Proteus Industries Inc., 2011. [Online]. Available:

- http://www.proteusind.com/800_flow_meter/800flow1.html. [Accessed 9/3/2013].
- [56] NIST., "National Institute of Standards and Technology", 02 July 2009. [Online]. Available: <http://ts.nist.gov/MeasurementServices/Calibrations/flow.cfm#18020C>. [Accessed 02 July 2009].
- [57] Cengel, Y., and Ghajar, A., Heat and Mass Transfer: Fundamentals and Applications, 4th Edition, McGraw-Hill, 2010.
- [58] D. C. Company., "Engineering and Operating Guide", DOWTHERM, 2008.
- [59] Ekrami, N., Hasib, Z., Dworkin, S., Fung, A., and Naylor, D., "Feasibility Study of Residential Tri-generation System Based on LiCl-H₂O Absorption Chiller", *The Canadian Society of Mechanical Engineering (CSME) Conference*, Winnipeg, Manitoba, 2012.
- [60] Ren, H., Gao, W., and Ruan, Y., "Optimal Sizing For Residential CHP System", *Applied Thermal Engineering*, vol. 28, no. 5-6, pp. 514-523, 2008.
- [61] "Statistics Canada", Households and the Environment Survey, 19/12/2012. [Online]. Available: <http://www.statcan.gc.ca/pub/11-526-s/2010001/t004-eng.htm>. [Accessed 24/03/2013].
- [62] Ghajarkhosravi, M., "Utility Benchmarking and Potential Savings of Multi-Unit Residential Buildings (MURBs) in Toronto", Ryerson University, Master Thesis, Toronto, 2013.
- [63] "Enbridge Gas," [Online]. Available: <https://www.enbridgegas.com/homes/accounts-billing/residential-gas-rates/purchasing-gas-from-enbridge.aspx>. [Accessed 28/03/2013].
- [64] "Toronto Hydro," [Online]. Available: <http://www.torontohydro.com/sites/electricsystem/business/yourbilloverview/Pages/ElectricityRates.aspx>. [Accessed 28/03/2013].
- [65] "GHG Emission Quantification Guidance", Environment Canada, [Online]. Available: www.ec.gc.ca/ges-ghg/default.asp?lang=En&n=EAF0E96A-1#footnote2. [Accessed 28/03/2013].
- [66] www.whispergen.com, "Whispergen User manual, Applies to WhisperGe microCHP system Model PPS24-ACLG-5".
- [67] ClimateWell, vol. ver 09/03 EN1, ClomateWell, 2008.
- [68] "Building Energy Software Tools Directory", U.S. Department of Energy, Energy Efficiency and Renewable Energy, 14/09/2011. [Online]. Available: http://apps1.eere.energy.gov/buildings/tools_directory/software.cfm/ID=58/pagename=alpha_list. [Accessed 28/03/2013].
- [69] "A TRaNsient SYstems Simulation Program", University of Wisconsin Madison, 02 2013. [Online]. Available: <http://sel.me.wisc.edu/trnsys/index.html>. [Accessed 28 03 2013].

- [70] Safa, A., Fung, A., and Leong, W., "Part Load Performance of a Two Stage Variable Capacity Air Source Heat Pump System in Cooling Mode", *ASHRAE Transactions*, vol. 117, no. 2, pp. 158-165, 2011.
- [71] "The Engineering ToolBox", 2005. [Online]. Available: http://www.engineeringtoolbox.com/propylene-glycol-d_363.html. [Accessed December 2008].
- [72] "engineeringtoolbox", [Online]. Available: http://www.engineeringtoolbox.com/propylene-glycol-d_363.html. [Accessed 1/03/2013].

Appendices:

Appendix A – Sensors List

Sensor address, list, type and location

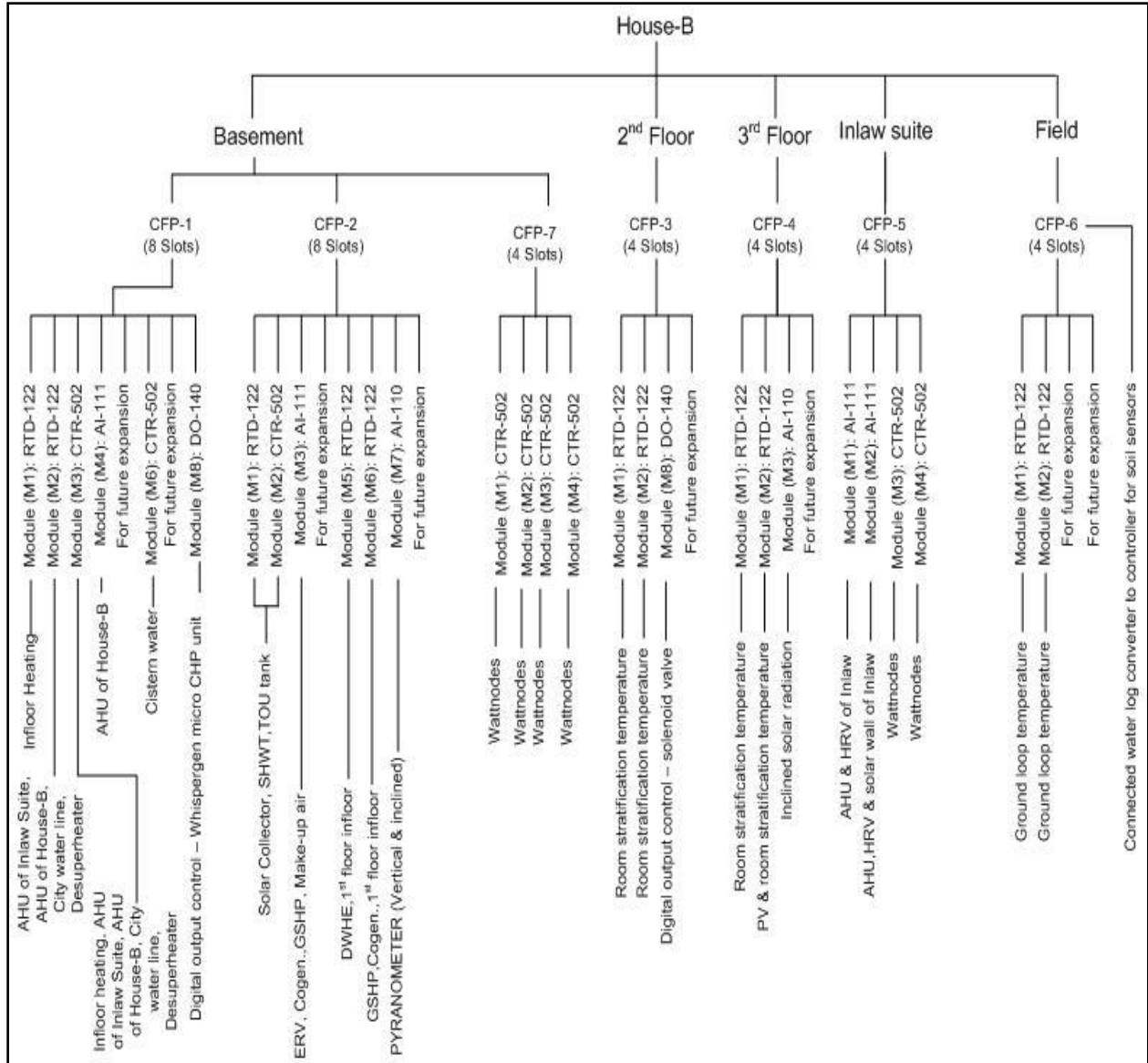


Figure A.1 - DAQ infrastructure in House-B

Module: RTD-122 (Output signal: RTD)				
Address	Sensors	Sensors type	Location	Status
B-CFP1-M1-CH1	T20	Pt. 500	Supply to ground loop (Before Pump)	Getting signal (GS)
B-CFP1-M1-CH2	T21	Pt. 500	Return from ground loop (Before Pump)	GS
B-CFP1-M1-CH3	T10	Pt. 500	Radiant 1 st floor supply	GS
B-CFP1-M1-CH4	T9	Pt. 500	Radiant 1 st floor return	GS
B-CFP1-M1-CH5	T8	Pt. 500	Radiant 2 nd floor supply	GS
B-CFP1-M1-CH6	T7	Pt. 500	Radiant 2 nd return	GS
B-CFP1-M1-CH7	T6	Pt. 500	Radiant 3 rd supply	GS
B-CFP1-M1-CH8	T5	Pt. 500	Radiant 3 rd return	GS
Module: RTD-122 (Output signal: RTD)				
Address	Sensors	Sensors type	Location	Status
B-CFP1-M2-CH1	T4	Pt. 500	Buffer tank to Inlaw AHU supply	GS
B-CFP1-M2-CH2	T3	Pt. 500	Buffer tank to Inlaw AHU return	GS
B-CFP1-M2-CH3	T13	Pt. 500	CW to B-AHU S.	GS
B-CFP1-M2-CH4	T14	Pt. 500	B-AHU R. to CW	GS
B-CFP1-M2-CH5	T18	Pt. 500	Desuperheater return	GS
B-CFP1-M2-CH6	T19	Pt. 500	Desuperheater supply	GS
B-CFP1-M2-CH7	T27	Pt. 100	City water	GS
Module: CTR-502 (Output signal: Pulse)				
Address	Sensors	Sensors type	Location	Status
B-CFP1-M3-CH1	FL15	Flow rate	Radiant Basement	GS
B-CFP1-M3-CH2	FL14	Flow rate	Radiant 1 st floor	GS
B-CFP1-M3-CH3	FL13	Flow rate	Radiant 2 nd floor	GS
B-CFP1-M3-CH4	FL12	Flow rate	Radiant 3 rd floor	GS
B-CFP1-M3-CH5	FL9	Flow rate	Buffer tank to Inlaw AHU	GS
B-CFP1-M3-CH6	FL8	Flow rate	Buffer tank to B-AHU	GS
B-CFP1-M3-CH7	FL5	Flow rate	Desuperheater	GS
B-CFP1-M3-CH8	FL4	Flow rate	City water	GS
Module: AI-111 (Output signal: mA)				
Address	Sensors	Sensors type	Location	Status
B-CFP1-M4-CH1	RH13	RH	Supply air duct to 1 st floor of B-AHU	GS
B-CFP1-M4-CH2	AT13	Air Temp.		
B-CFP1-M4-CH3	RH14	RH	Supply air duct to 2 nd floor of B-AHU	GS
B-CFP1-M4-CH4	AT14	Air Temp.		
B-CFP1-M4-CH5	RH15	RH	Supply air duct to 3 rd floor of B-AHU	GS
B-CFP1-M4-CH6	AT15	Air Temp.		
B-CFP1-M4-CH7	RH11	RH	Return air duct of 1 st floor of B-AHU	GS
B-CFP1-M4-CH8	AT11	Air Temp.		
B-CFP1-M4-CH9	RH9	RH	Return air duct of 2 nd & 3 rd floor of B-AHU	GS
B-CFP1-M4-CH10	AT9	Air Temp.		
B-CFP1-M4-CH11	AF13	Air Flow	Supply air duct to 1 st floor of B-AHU	GS
B-CFP1-M4-CH12	AF12	Air Flow	Supply air duct to 2 nd floor of B-AHU	GS
B-CFP1-M4-CH13	AF11	Air Flow	Supply air duct to 3 rd floor of B-AHU	GS
B-CFP1-M4-CH14	AF7	Air Flow	Return air duct of 1 st floor of B-AHU	GS
B-CFP1-M4-CH15	AF5	Air Flow	Return air duct of 2 nd & 3 rd floor of B-	GS

			AHU	
B-CFP1-M5-CH0	0/1		CW SP signal	
Module:				
Address	Sensors	Sensors type	Location	Status
B-CFP1-M7-CH1	T35	Pt. 500	HS from TB3 to TB4	
B-CFP1-M7-CH2	T40	Pt. 500	City water from TB4 to TB3	
B-CFP1-M7-CH3	T36	Pt. 500	HS from TB4 to TB5	
B-CFP1-M7-CH4	T34	Pt. 500	HS from CW to TB3 before DVB2	
B-CFP1-M7-CH5	T37	Pt. 500	HS to outdoor fan	
B-CFP1-M7-CH6	T39	Pt. 500	City water from TB5 to TB4	
B-CFP1-M7-CH7	T38	Pt. 500	HS outlet from outdoor fan	
Module: DO-410 (Digital control)				
Address	Sensors	Sensors type	Location	Status
B-CFP1-M8-CH1		Pt. 100	Whispergen micro CHP unit Main Burner	GS
B-CFP1-M8-CH2		Pt. 100	Whispergen micro CHP unit Aux. Burner	GS
B-CFP1-M8-CH3		Pt. 100	Whispergen micro CHP unit	GS
Module: RTD-122 (Output signal: RTD)				
Address	Sensors	Sensors type	Location	Status
B-CFP2-M1-CH1	T24	Pt. 500	Solar collector supply	GS
B-CFP2-M1-CH2	T25	Pt. 500	Solar collector return	GS
B-CFP2-M1-CH3	T23	Pt. 100	Solar pre-heat tank supply to TOU tank	GS
B-CFP2-M1-CH4	T1	Pt. 100	Cold water to solar pre-heat tank	GS
B-CFP2-M1-CH5	T40	Pt. 100	Recirculation water to solar pre-heat tank	GS
B-CFP2-M1-CH6	T22	Pt. 100	Tempered water from TOU tank	GS
B-CFP2-M1-CH7	T2	Pt. 100	Un-tempered water from TOU tank	GS
B-CFP2-M1-CH8	T33	*Pt. 100 (SM)	Flue gas from CHP unit	GS
Module: CTR-502 (Output signal: Pulse)				
Address	Sensors	Sensors type	Location	Status
B-CFP2-M2-CH1	FL1	Flow rate	Solar collector supply	GS
B-CFP2-M2-CH2	FL2	Flow rate	Cold water to Solar pre-heat tank	GS
B-CFP2-M2-CH3	FL40	Flow rate	Recirculation water to Solar pre-heat tank	Damaged
B-CFP2-M2-CH4	FL3	Flow rate	Tempered water from TOU tank	GS
B-CFP2-M2-CH5	FL10	Flow rate	Un-tempered water from TOU tank	GS
B-CFP2-M2-CH6	FL19	Flow rate	Omega CHP unit	
Module: AI-111 (Output signal: mA)				
Address	Sensors	Sensors type	Location	Status
B-CFP2-M3-CH1	RH18	RH	Supply air from ERV to AHU	GS
B-CFP2-M3-CH2	AT18	Air Temp.		
B-CFP2-M3-CH3	RH19	RH	Return air from zone to ERV	GS
B-CFP2-M3-CH4	AT19	Air Temp.		
B-CFP2-M3-CH5	RH20	RH	Fresh air from outdoor to ERV	GS
B-CFP2-M3-CH6	AT20	Air Temp.		
B-CFP2-M3-CH7	RH21	RH	Exhaust air from ERV to	GS

B-CFP2-M3-CH8	AT21	Air Temp.	outdoor	
B-CFP2-M3-CH9	AF16	Air Flow	Supply air from ERV to B-AHU	GS
B-CFP2-M3-CH10	AF15	Air Flow	Return air from zone to ERV	GS
B-CFP2-M3-CH11				
B-CFP2-M3-CH12	FL18	Flow rate (SPARLING)	CHP unit (NRCan)	GS
B-CFP2-M3-CH13	RH25	RH	Outdoor air RH (South side)	Not installed
B-CFP2-M3-CH14	AT25	Air Temp.	Outdoor air temperature (South side)	Not installed
B-CFP2-M3-CH15	RH24	RH	Outdoor air RH (North side)	GS
B-CFP2-M3-CH16	AT24	Air Temp.	Outdoor air temperature (North side)	GS

Module: RTD-122 (Output signal: RTD)

Address	Sensors	Sensors type	Location	Status
B-CFP2-M5-CH1	T30	Pt. 500	Pre-heat water to GWHE	GS
B-CFP2-M5-CH2	T26	Pt. 500	Warm water from GWHE	GS
B-CFP2-M5-CH3	T28	Pt. 100 (SM)	Drain water to GWHE	GS
B-CFP2-M5-CH4	T29	Pt. 100 (SM)	Drain water from GWHE	GS
B-CFP2-M5-CH5	T _{B1_3b_TOP}	Pt. 100 (SM)	1 st floor infloor top (North end)	Not installed
B-CFP2-M5-CH6	T _{B1_3b_BOT}	Pt. 100 (SM)	1 st floor infloor bottom (North end)	installed
B-CFP2-M5-CH7	T _{B1_2b_TOP}	Pt. 100 (SM)	1 st floor infloor top (Middle)	Damaged
B-CFP2-M5-CH8	T _{B1_2b_BOT}	Pt. 100 (SM)	1 st floor infloor bottom (Middle)	installed

Module: RTD-122 (Output signal: RTD)

Address	Sensors	Sensors type	Location	Status
B-CFP2-M6-CH1	NRCan1	Pt. 100	Solar tank CHP control	GS
B-CFP2-M6-CH2	NRCan2	Pt. 100	Buffer tank CHP control	GS
B-CFP2-M6-CH3	T16	Pt. 500	Supply from GSHP to Buffer tank	GS
B-CFP2-M6-CH4	T17	Pt. 500	Return to GSHP from Buffer tank	GS
B-CFP2-M6-CH5	T32	Pt. 500	Supply from CHP to Buffer tank	GS
B-CFP2-M6-CH6	T31	Pt. 500	Return to CHP from Buffer tank	GS
B-CFP2-M6-CH7	T _{B1_1b_TOP}	Pt. 100 (SM)	1 st infloor top (South end)	Damaged
B-CFP2-M6-CH8	T _{B1_1b_BOT}	Pt. 100 (SM)	1 st floor infloor bottom (South end)	GS

Module: AI-110 (Output signal: mA or mV)

Address	Sensors	Sensors type	Location	Status
B-CFP2-M7-CH1	PY_V	Pyranometer	Vertical position	GS
B-CFP2-M7-CH2	PY_H	Pyranometer	Horizontal position	GS
B-CFP2-M7-CH3	NG2	Gas meter (SIERRA)	CHP unit	GS
B-CFP2-M7-CH4	FL16	Flow rate (Proteus)	GSHP ground loop	GS
B-CFP2-M7-CH5				
B-CFP2-M7-CH6	FL19	Water flow rate (Omega)	CHP unit (NRCan)	GS
B-CFP2-M7-CH8	FL6	Water flow rate (Proteus)	GSHP to Buffer tank	GS
B-CFP2-M7-CH7	FL17	Water flow rate (Proteus)	CHP unit	GS

Module: RTD-122 (Output signal: RTD)

Address	Sensors type	Location	Status
B-CFP2-M8-CH1	Pt. 100 (SM)	Ground loop supply temperature (After pump)	GS
B-CFP2-M8-CH2	Pt. 100 (SM)	Ground loop return temperature (After pump)	GS

Module: RTD-122 (Output signal: RTD)

Address	Sensors	Sensors type	Location	Status
B-CFP3-M1-CH1	T _{B2_1b_TOP}	Pt. 100 (SM)	2 nd floor infloor top (South end)	installed
B-CFP3-M1-CH2	T _{B2_1b_BOT}	Pt. 100 (SM)	2 nd floor infloor bottom (South end)	installed
B-CFP3-M1-CH3	T _{B2_2b_TOP}	Pt. 100 (SM)	2 nd floor infloor top (Middle)	installed
B-CFP3-M1-CH4	T _{B2_2b_BOT}	Pt. 100 (SM)	2 nd floor infloor bottom (Middle)	installed
B-CFP3-M1-CH5	T _{B2_3b_TOP}	Pt. 100 (SM)	2 nd floor infloor top (North end)	installed
B-CFP3-M1-CH6	T _{B2_3b_BOT}	Pt. 100 (SM)	2 nd floor infloor bottom (North end)	installed
B-CFP3-M1-CH7	T _{2'}	Pt. 100 (SM)	2 nd floor room temperature at 2' height	Not installed
B-CFP3-M1-CH8	T _{4'}	Pt. 100 (SM)	2 nd floor room temperature at 4' height	Not installed

Module: RTD-122 (Output signal: RTD)

Address	Sensors	Sensors type	Location	Status
B-CFP3-M2-CH1	T _{6'}	Pt. 100 (SM)	2 nd floor room temperature at 6' height	Not installed
B-CFP3-M2-CH2	T _{8'}	Pt. 100 (SM)	2 nd floor room temperature at 8' height	Not installed

Module: DO-410 (Digital control)

Address	Sensors	Sensors type	Location	Status
B-CFP3-M3-CH1	C1	Solenoid valve	Simulated water draw profile	GS
B-CFP3-M3-CH2	C2	Solenoid valve	Simulated water draw profile	GS
B-CFP3-M3-CH3	C3	Solenoid valve	Simulated water draw profile	GS
B-CFP3-M3-CH4	H1	Solenoid valve	Simulated water draw profile	GS
B-CFP3-M3-CH5	H2	Solenoid valve	Simulated water draw profile	GS
B-CFP3-M3-CH6	H3	Solenoid valve	Simulated water draw profile	GS

Module: RTD-122 (Output signal: RTD)

Address	Sensors	Sensors type	Location	Status
B-CFP4-M1-CH1	T _{B3_1b_TOP}	Pt. 100 (SM)	3 rd floor infloor top (South end)	installed
B-CFP4-M1-CH2	T _{B3_1b_BOT}	Pt. 100 (SM)	3 rd floor infloor bottom (South end)	installed
B-CFP4-M1-CH3	T _{B3_2b_TOP}	Pt. 100 (SM)	3 rd floor infloor top (Middle)	installed
B-CFP4-M1-CH4	T _{B3_2b_BOT}	Pt. 100 (SM)	3 rd floor infloor bottom (Middle)	installed
B-CFP4-M1-CH5	T _{B3_3b_TOP}	Pt. 100 (SM)	3 rd floor infloor top (North end)	installed
B-CFP4-M1-CH6	T _{B3_3b_BOT}	Pt. 100 (SM)	3 rd floor infloor bottom (North end)	installed
B-CFP4-M1-CH7	T _{2'}	Pt. 100 (SM)	3 rd floor room temperature at 2' height	Not installed
B-CFP4-M1-CH8	T _{4'}	Pt. 100 (SM)	3 rd floor room temperature at 4' height	Not installed

Module: RTD-122 (Output signal: RTD)

Address	Sensors	Sensors type	Location	Status
B-CFP4-M2-CH1	T _{6'}	Pt. 100 (SM)	3 rd floor room temperature at 6' height	Not installed

B-CFP4-M2-CH2	T ₈	Pt. 100 (SM)	3 rd floor room temperature at 8' height	Not installed
B-CFP4-M2-CH3	T40	Pt. 100 (SM)	PV array temperature	GS
B-CFP4-M2-CH4	T41	Pt. 100 (SM)	Outlet air temperature under PV array	GS
B-CFP4-M2-CH5	T42	Pt. 100 (SM)	Inlet air temperature under PV array	GS

Module: AI-111 (Output signal: mA)

Address	Sensors	Sensors type	Location	Status
B-CFP5-M1-CH1	RH1	RH	Fresh air from outdoor to Inlaw-HRV	Installed
B-CFP5-M1-CH2	AT1	Air Temp.		
B-CFP5-M1-CH3	RH2	RH	Exhaust air from Inlaw-HRV	Installed
B-CFP5-M1-CH4	AT2	Air Temp.		
B-CFP5-M1-CH5	RH3	RH	Supply air from Inlaw-HRV to AHU	Not installed
B-CFP5-M1-CH6	AT3	Air Temp.		
B-CFP5-M1-CH7	RH4	RH	Supply air from Inlaw-AHU to zone	Installed
B-CFP5-M1-CH8	AT4	Air Temp.		
B-CFP5-M1-CH9	RH5	RH	Exhaust air from zone to Inlaw-HRV	Not installed
B-CFP5-M1-CH10	AT5	Air Temp.		
B-CFP5-M1-CH11	RH6	RH	Return air from zone to Inlaw-AHU	Installed
B-CFP5-M1-CH12	AT6	Air Temp.		
B-CFP5-M1-CH13	RH7	RH	Supply air from solar wall	Not installed
B-CFP5-M1-CH14	AT7	Air Temp.		
B-CFP5-M1-CH15	RH8	RH	Return air to solar wall	Not installed
B-CFP5-M1-CH16	AT8	Air Temp.		

Module: AI-111 (Output signal: mA)

Address	Sensors	Sensors type	Location	Status
B-CFP5-M2-CH1	AF1	Air Flow station	Return air from zone to Inlaw-AHU	Installed
B-CFP5-M2-CH2	AF2	Air Flow station	Exhaust air from HRV to outdoor	Installed
B-CFP5-M2-CH3	AF3	Air Flow station	Fresh air from outdoor to Inlaw-HRV	Installed
B-CFP5-M2-CH4	AF4	Air Flow station	Return air to solar wall	Not installed
B-CFP5-M2-CH5	AF18	Air Flow station	Return air from room to HRV	Not installed
B-CFP5-M2-CH6		DC CT	Solar air heater fan	
B-CFP5-M2-CH7		DC CT	PV inverter DC amps	
B-CFP5-M2-CH8		Voltage transducer	Solar air heater fan	
B-CFP5-M2-CH9		Voltage transducer	PV inverter DC amps	

Module: CTR-502 (Output signal: Pulse), Sensors type: Watt-node

Address	Sensors	Location and CT size	Status
B-CFP5-M3-CH1	1-PV-1	PV cell forward: 30 Amps	
B-CFP5-M3-CH2	1-PV-2	PV cell reverse: 30 Amps	
B-CFP5-M3-CH3	2-PV-1	Wind turbine forward: 15 Amps	

B-CFP5-M3-CH4	2-PV-2	Wind turbine reverse: 15 Amps	
B-CFP5-M3-CH5	4-P3-1 4-P3-2	Emergency EXIT lights and instrumentation: total = 5 Amps	
B-CFP5-M3-CH6	4-P3-3	Inlaw-AHU: 15 Amps	
B-CFP5-M3-CH7	3-P3-3	Inlaw interior lights: 5 Amps	
B-CFP5-M3-CH8	3-P3-2	Inlaw interior receptacles: 15, 15 Amps = 30 Amps	

Module: CTR-502 (Output signal: Pulse), Sensors type: Watt-node

Address	Sensors	Location and CT size	Status
B-CFP5-M4-CH1	2-PV-3	Garage receptacles and exhaust fan: 15 Amps	
B-CFP5-M4-CH2	1-PV-3	Garage interior and exterior lights: total = 15 Amps	
B-CFP5-M4-CH3	3-P3-1	Garage exterior GFI receptacles: 15, 15 Amps = 30 Amps	

Module: RTD-122 (Output signal: RTD)

Address	Sensors	Sensors type	Location	Status
B-CFP6-M1-CH1	RTD-2	Pt. 100 (SM)	Supply flow pipe at the beginning of 1 st earth loop	installed
B-CFP6-M1-CH2	RTD-1	Pt. 100 (SM)	Return flow pipe at the beginning of 1 st earth loop	installed
B-CFP6-M1-CH3	RTD-12	Pt. 100 (SM)	Supply flow pipe at the beginning of 2 nd earth loop	installed
B-CFP6-M1-CH4	RTD-11	Pt. 100 (SM)	Return flow pipe at the beginning of 2 nd earth loop	installed
B-CFP6-M1-CH5	RTD-9	Pt. 100 (SM)	Return flow pipe at the middle of 2 nd earth loop	installed
B-CFP6-M1-CH6	RTD-10	Pt. 100 (SM)	Supply flow pipe at the middle of 2 nd earth loop	installed
B-CFP6-M1-CH7	RTD-4	Pt. 100 (SM)	Supply flow pipe at the middle of 1 st earth loop	installed
B-CFP6-M1-CH8	RTD-3	Pt. 100 (SM)	Return flow pipe at the middle of 1 st earth loop	installed

Module: RTD-122 (Output signal: RTD)

Address	Sensors	Sensors type	Location	Status
B-CFP6-M2-CH1	RTD-7	Pt. 100 (SM)	Return flow pipe at the end of 2 nd earth loop	installed
B-CFP6-M2-CH2	RTD-5	Pt. 100 (SM)	Return flow pipe at the end of 1 st earth loop	installed

Module: CTR-502 (Output signal: Pulse), Sensor type: Wattnode

Address	Sensors	Location and CT size	Status
B-CFP7-M2-CH1	5-P3-1	GSHP to Buffer tank: 5 Amps	GS
B-CFP7-M2-CH2	5-P3-2	Desuperheater pump: 5 Amps	GS
B-CFP7-M2-CH3	5-P3-3	Earth loop of GSHP: 5 Amps	GS
B-CFP7-M2-CH4	6-P3-1	Buffer tank to B-AHU pump: 5 Amps	GS

B-CFP7-M2-CH5	6-P3-2	Buffer tank to Infloor radiant heating pump: 5 Amps	GS
B-CFP7-M2-CH6	6-P3-3	Buffer tank to Inlaw-AHU pump: 5 Amps	GS
B-CFP7-M2-CH7	10-P-1	Cook top and oven: total= 30 Amps	GS
B-CFP7-M2-CH8	11-P-1	Dryer: 30 Amps	GS

Module: CTR-502 (Output signal: Pulse), Sensor type: Wattnode

Address	Sensors	Location and CT size	Status
B-CFP7-M3-CH1	7-PV-1	CHP unit @ Panel: 15 Amps	GS
B-CFP7-M3-CH2	7-PV-2	CHP unit @ Machine: 15 Amps	GS
B-CFP7-M3-CH3	12-P3-1	Basement drain pump: 15 Amps	GS
B-CFP7-M3-CH4	8-P3-1	Basement, kitchen, great room, bathroom, 2 nd floor, 2 nd floor washroom hallway and 3 rd floor receptacles: total= 60Amps	GS
B-CFP7-M3-CH5	8-P3-2	Hot water circulation pump: 5 Amps	GS
B-CFP7-M3-CH6	8-P3-3	Basement lights: 5 Amps	GS
B-CFP7-M3-CH7	9-P3-1	Fridge: 15 Amps	GS
B-CFP7-M3-CH8	9-P3-2	Kitchen fan with lights (Shared)	GS

Module: CTR-502 (Output signal: Pulse), Sensor type: Wattnode

Address	Sensors	Location and CT size	Status
B-CFP7-M4-CH1	9-P3-3	Washing machine: 15 Amps	GS
B-CFP7-M4-CH2	7-PV-3	CHP unit circulator pump after X-FMR: 5 Amps	GS
B-CFP7-M4-CH3	12-P3-2	Kitchen, great room, 1 st floor bath, dining room lights: total = 5Amps	GS
B-CFP7-M4-CH4	12-P3-3	Solar collector glycol loop: 5 Amps	GS
B-CFP7-M4-CH5	13-P3-1	Upstairs lights and 2 nd floor lights: total = 5 Amps	GS
B-CFP7-M4-CH6	13-P3-2	3 rd floor lights: 5Amps	GS
B-CFP7-M4-CH7	13-P3-3	Outdoor lighting and receptacles: total= 15 Amps	GS
B-CFP7-M4-CH8			GS

GS- Getting signal in the NI interface.

Installed – Sensors already installed but not connected to the DAQ systems.

Not installed – Sensors yet to be installed.

Damage – Sensors installed but damaged.

Not getting any signal – Connected with DAQ but not getting any signal.

Appendix B – PG-Water Solution Specifications

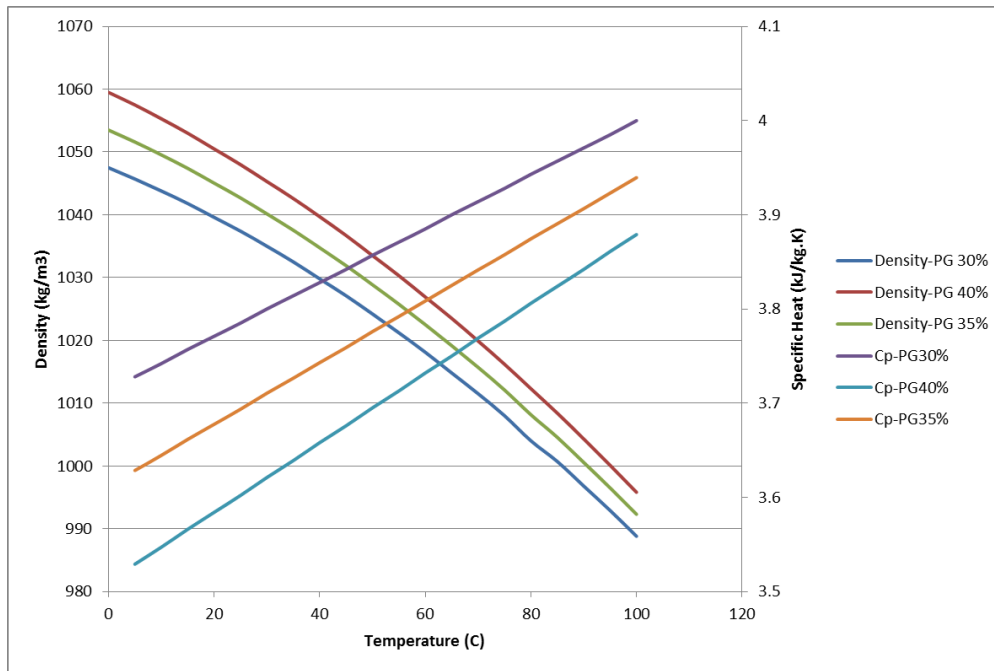


Figure B.62 - Density and Specific Heat Change of Water-PG Solution Versus Temperature [1]

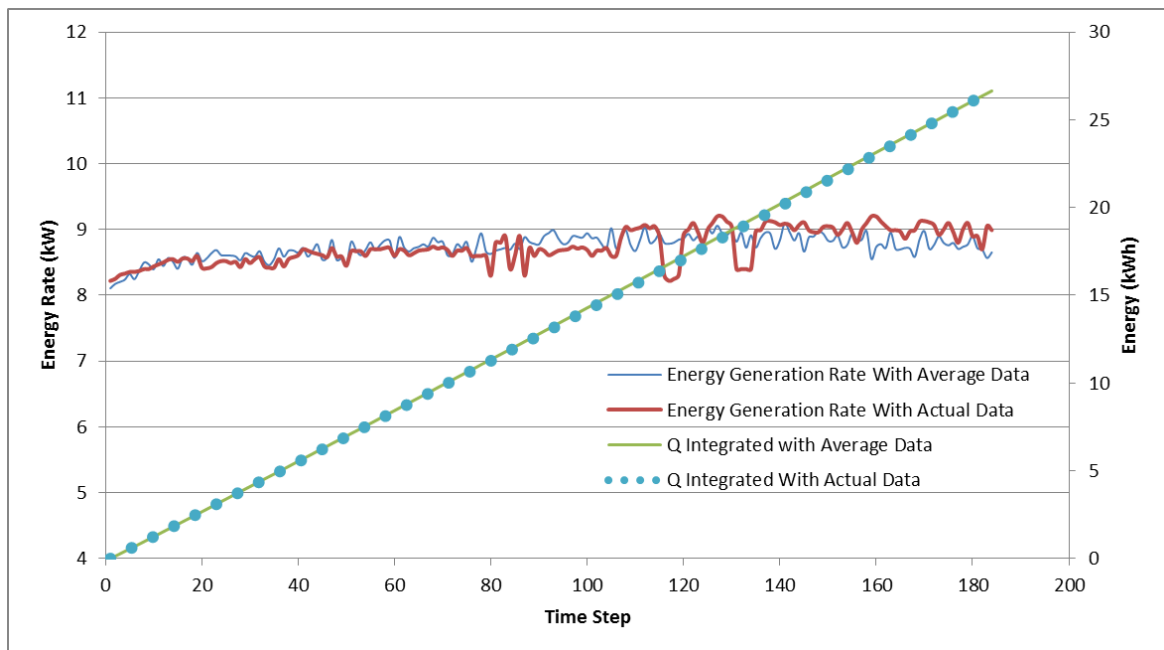


Figure B.63 - Error of Considering Average Values of Density and Specific Heat

Table B.20 - Densities of Water-PG Solutions⁹ (kg/m³)

Temp. °C	Volume Percent Propylene Glycol							
	0%	10%	20%	30%	40%	50%	60%	70%
-35							1094.7	1104.7
-30						1081.9	1092.8	1102.5
-25						1080.2	1090.8	1100.2
-20					1066.6	1078.4	1088.7	1097.8
-15					1065.0	1076.5	1086.5	1095.3
-10				1050.7	1063.3	1074.5	1084.2	1092.7
-5			1035.1	1049.2	1061.5	1072.4	1081.8	1089.9
0		1018.2	1033.8	1047.5	1059.5	1070.1	1079.3	1087.1
5	1006.7	1017.0	1032.3	1045.7	1057.5	1067.8	1076.6	1084.2
10	1004.3	1015.7	1030.6	1043.8	1055.3	1065.3	1073.9	1081.2
15	1001.9	1014.2	1028.9	1041.8	1053.0	1062.7	1071.1	1078.1
20	999.4	1012.6	1027.0	1039.6	1050.5	1060.0	1068.1	1074.9
25	996.9	1010.9	1025.0	1037.4	1048.0	1057.2	1065.0	1071.5
30	994.3	1009.1	1022.9	1035.0	1045.3	1054.3	1061.9	1068.1
35	991.7	1007.2	1020.7	1032.5	1042.6	1051.3	1058.6	1064.6
40	989.0	1005.1	1018.3	1029.8	1039.7	1048.1	1055.2	1061.0
45	986.3	1002.9	1015.8	1027.1	1036.7	1044.9	1051.7	1057.3
50	983.5	1000.6	1013.2	1024.2	1033.5	1041.5	1048.1	1053.4
55	980.7	998.1	1010.5	1021.2	1030.3	1038.0	1044.4	1049.5
60	977.8	995.5	1007.6	1018.1	1026.9	1034.5	1040.6	1045.5
65	974.9	992.8	1004.6	1014.8	1023.5	1030.8	1036.7	1041.4
70	971.9	990.0	1001.5	1011.5	1019.9	1026.9	1032.7	1037.2
75	968.8	987.0	998.3	1008.0	1016.2	1023.0	1028.5	1032.8
80	965.7	984.0	995.0	1004.4	1012.3	1019.0	1024.3	1028.4
85	962.6	980.7	991.5	1000.7	1008.4	1014.8	1020.0	1023.9
90	959.3	977.4	987.9	996.8	1004.3	1010.5	1015.5	1019.3
95	956.0	974.0	984.2	992.9	1000.1	1006.2	1010.9	1014.6
100	952.6	970.4	980.3	988.8	995.8	1001.7	1006.3	1009.7
105	949.2	966.7	976.3	984.6	991.4	997.1	1001.5	1004.8
110	945.7	962.8	972.3	980.2	986.9	992.3	996.6	999.8
115	942.1	958.9	968.0	975.8	982.2	987.5	991.6	994.7
120	938.5	954.8	963.7	971.2	977.5	982.6	986.5	989.4
125	934.7	950.6	959.2	966.5	972.6	977.5	981.3	984.1
130	930.9	946.3	954.7	961.7	967.6	972.3	976.0	978.7
135	927.1	941.8	949.9	956.8	962.5	967.1	970.6	973.1
140	923.1	937.2	945.1	951.8	957.2	961.7	965.1	967.5
145	919.1	932.5	940.2	946.6	951.9	956.2	959.5	961.8
150	914.9	927.7	935.1	941.3	946.4	950.5	953.7	956.0
155	910.7	922.7	929.9	935.9	940.8	944.8	947.9	950.0
160	906.4	917.7	924.5	930.3	935.1	939.0	941.9	944.0

⁹ The blue color in the table means at or above the atmospheric boiling point

Table B.21 - Specific Heat of Water-PG Solution¹⁰ (kJ/kg.K)

Temp. °C	Volume Percent Propylene Glycol							
	0%	10%	20%	30%	40%	50%	60%	70%
-35							2.860	2.542
-30						3.166	2.887	2.573
-25						3.189	2.913	2.604
-20					3.455	3.211	2.940	2.635
-15					3.473	3.234	2.967	2.666
-10				3.699	3.492	3.256	2.994	2.697
-5			3.893	3.714	3.510	3.279	3.021	2.728
0		4.057	3.903	3.728	3.529	3.302	3.047	2.760
5	4.229	4.063	3.913	3.742	3.547	3.324	3.074	2.791
10	4.195	4.069	3.923	3.757	3.566	3.347	3.101	2.822
15	4.168	4.074	3.933	3.771	3.584	3.370	3.128	2.853
20	4.147	4.080	3.944	3.785	3.602	3.392	3.155	2.884
25	4.132	4.085	3.954	3.800	3.621	3.415	3.181	2.915
30	4.121	4.091	3.964	3.814	3.639	3.437	3.208	2.946
35	4.115	4.096	3.974	3.828	3.658	3.460	3.235	2.977
40	4.114	4.102	3.984	3.842	3.676	3.483	3.262	3.008
45	4.115	4.107	3.994	3.857	3.695	3.505	3.288	3.039
50	4.120	4.113	4.004	3.871	3.713	3.528	3.315	3.070
55	4.128	4.119	4.014	3.885	3.732	3.551	3.342	3.101
60	4.138	4.124	4.024	3.900	3.750	3.573	3.369	3.132
65	4.150	4.130	4.034	3.914	3.769	3.596	3.396	3.163
70	4.164	4.135	4.044	3.928	3.787	3.618	3.422	3.194
75	4.179	4.141	4.054	3.943	3.806	3.641	3.449	3.225
80	4.196	4.146	4.064	3.957	3.824	3.664	3.476	3.256
85	4.213	4.152	4.074	3.971	3.842	3.686	3.503	3.287
90	4.231	4.157	4.084	3.985	3.861	3.709	3.530	3.318
95	4.249	4.163	4.094	4.000	3.879	3.732	3.556	3.349
100	4.267	4.169	4.104	4.014	3.898	3.754	3.583	3.380
105	4.285	4.174	4.114	4.028	3.916	3.777	3.610	3.411
110	4.303	4.180	4.124	4.043	3.935	3.800	3.637	3.442
115	4.321	4.185	4.134	4.057	3.953	3.822	3.664	3.474
120	4.338	4.191	4.145	4.071	3.972	3.845	3.690	3.505
125	4.355	4.196	4.155	4.086	3.990	3.867	3.717	3.536
130	4.371	4.202	4.165	4.100	4.009	3.890	3.744	3.567
135	4.387	4.208	4.175	4.114	4.027	3.913	3.771	3.598
140	4.402	4.213	4.185	4.128	4.046	3.935	3.798	3.629
145	4.416	4.219	4.195	4.143	4.064	3.958	3.824	3.660
150	4.430	4.224	4.205	4.157	4.083	3.981	3.851	3.691
155	4.443	4.230	4.215	4.171	4.101	4.003	3.878	3.722
160	4.456	4.235	4.225	4.186	4.119	4.026	3.905	3.753

¹⁰ The blue color in the table means at or above the atmospheric boiling point

Appendix C – Cooling Demand Prediction Based on Different COPs

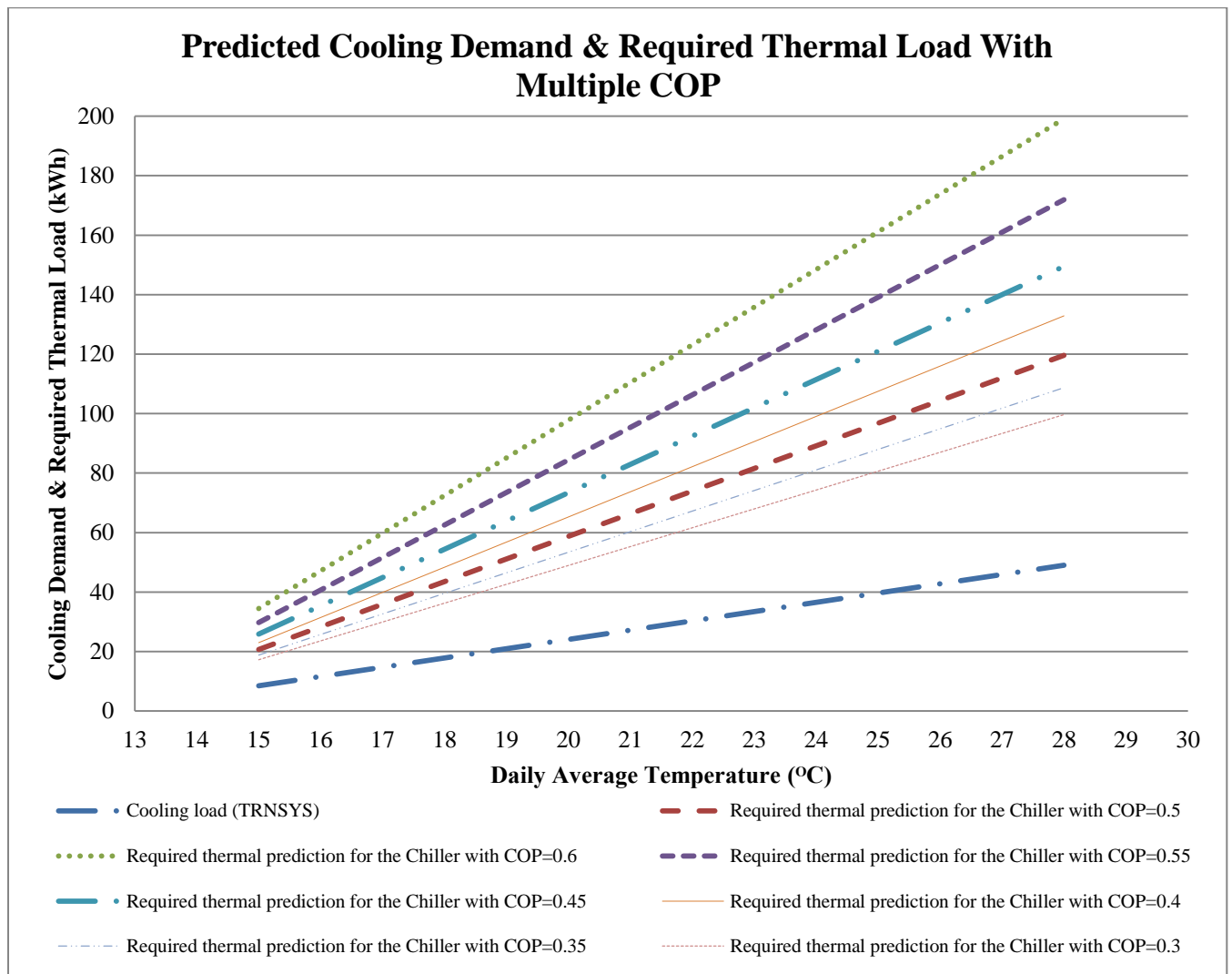


Figure C64 - Predicted Cooling Demand & Required Thermal Load With Multiple COP

Appendix E – Valves Positions for the Heat Rejection Circuit

The following Table shows the valve position for different heat rejection options

Table E.1 - Valve Positions for different Heat Rejection Options

Combinations	Valve position					
	DV-B1	DV-B2	DV-B3	VH5	VH6	VH7
Heat is rejected to three tanks first and then to the outdoor fan coil	2	1	1	open	closed	open
Heat is rejected to fan coil first and then to the three tanks	1	2	2	open	closed	open
Heat is rejected to three tanks only	1	1	closed	open	closed	open
Heat is rejected to fan coil only	closed	2	1	open	closed	open
Heat is rejected to tank TB-3 only	1	1	closed	closed	open	closed
Heat is rejected to tank TB-3 and then to fan coil	2	1	1	closed	open	closed
Heat is rejected to fan coil first and then to tank TB-3	2	2	2	closed	open	closed

Appendix F – HOUSE B Pictures



Figure F.65 - TRCA House B



Figure F.66 - Air Handling Unit

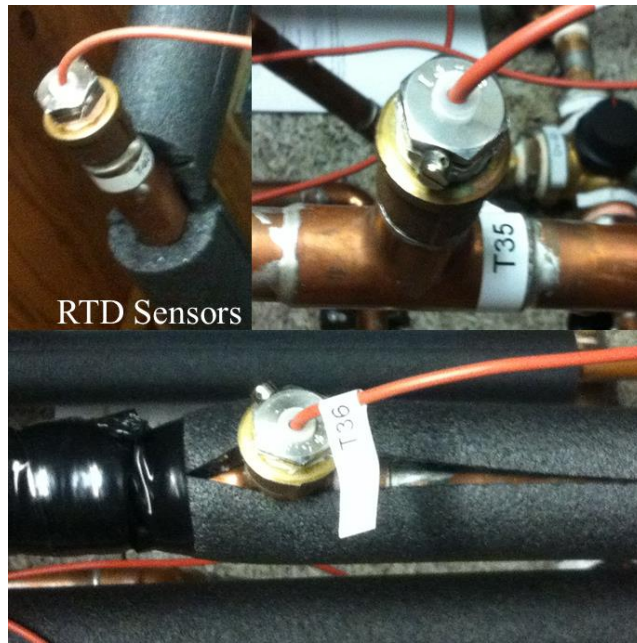


Figure F.67 - RTD Sensors



Figure F.68 - Stirling Engine Cogeneration Unit



Figure F.69 - Flow Meter and Pump



Figure F.70 - Heat Rejection Tanks



Figure F.71 - ClimateWell Chiller